Stereoelectroencephalography (SEEG)

Pramote Laoprasert, M.D.
Director, Comprehensive Pediatric Epilepsy Program
Beaumont Health
OUWB School of Medicine

ECoG
1950's

SEEG
1960's

SDE
1990's

2015

Primary Localization
Secondary Localization
Tertiary Localization

Ictal onset
Zone of primary organization

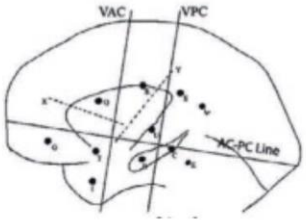

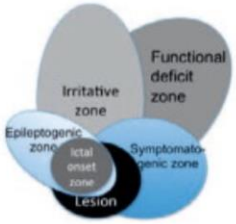

Spatiotemporal zones of ictal dynamics

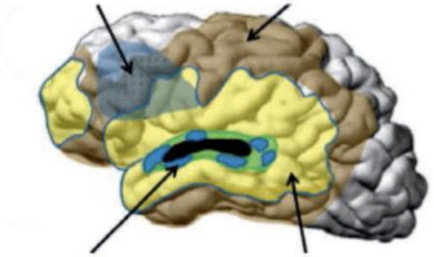

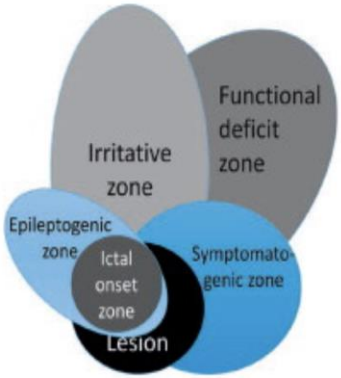

Implications:

1)- No single zone is equivalent to the EZ

2)- No single TEST allows measurement of the EZ

3)- Specifically, defining the IOZ is not the same as defining the EZ.

Zone	Tests Used to Define It
Irritative zone: area of cortex that generates interictal spikes	EEG, MEG, EEG-fMRI
Seizure-onset zone: area of cortex that initiates clinical seizures	EEG, ictal SPECT and, to a lesser degree, f-MRI and MEG
Symptomatogenic zone: area of cortex that, when activated, produces the initial ictal symptoms or signs	Initial seizure symptomatology
Epileptogenic lesion: macroscopic lesion that is causative of the epileptic seizures because the lesion itself is epileptogenic (e.g., cortical dysplasia) or by secondary hyperexcitability of adjacent cortex)	MRI
Functional deficit zone: area of cortex that is not functioning normally in the interictal period	Neurological examination, neuropsychological examination and functional imaging (interictal SPECT and PET)

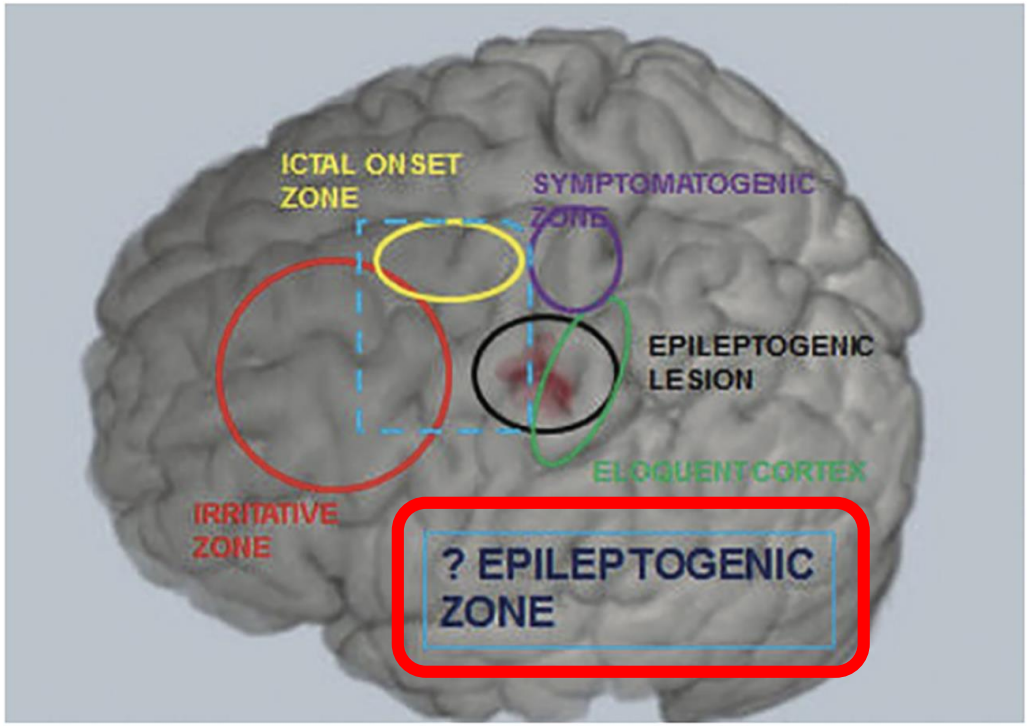

Figure 1: Illustration of discordant cortical zones and lesions

Epileptogenic zone	Region of cortex that can generate epileptic seizures. By definition, total removal or disconnection is necessary for seizure freedom
Irritative zone	Region of cortex that generates interictal epileptiform discharges, evident in the EEG or magnetoencephalography (MEG)
Seizure onset zone	Region where the clinical seizures originate
Epileptogenic lesion	Structural lesion that is causally related to the epilepsy
Ictal symptomatogenic zone	Region of cortex that generates the initial seizure symptoms
Functional deficit zone	Region of cortex that in the interictal period is functionally abnormal, as indicated by neurological examination, neuropsychological testing and functional imaging or non-epileptiform EEG or MEG abnormalities
Eloquent cortex	Region of cortex that is indispensable for defined cortical functions

Epileptogenic zone

- The definition of the epileptogenic zone, as proposed by *Talairach and Bancaud*, is an ictal electro-clinical definition based on the results of SEEG recordings. It takes into account not only the anatomical location of the **site of the beginning and of the primary organization" of the epileptic discharge**, but also **how this discharge gives rise to the accompanying clinical symptoms**.
- This definition is different from the North American view since, for the French authors, the epileptogenic zone is not synonymous with what can be called the "what-to-remove area". In fact, it is above all a conceptual definition which emphasizes the importance of studying the spatio-temporal dynamics of seizure discharges, and not only their starting point (Kahane et al 2006).

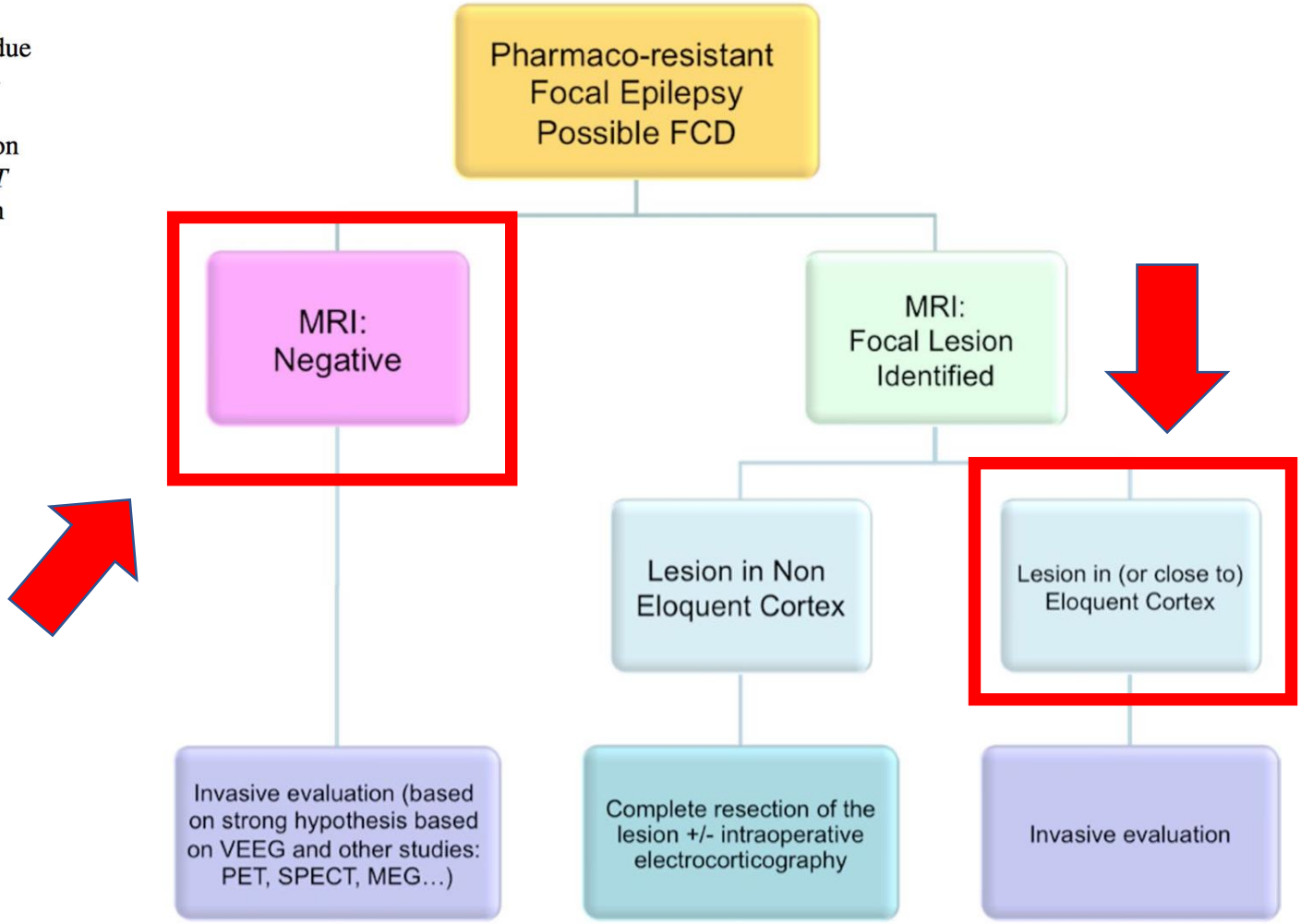

Fig. 3 Surgical approach to pharmaco-resistant epilepsy due to FCDs. *MRI* magnetic resonance imaging, *VEEG* video EEG monitoring, *PET* positron emission tomography, *SPECT* (Ictal) single photon emission computed tomography, *MEG* magnetoencephalography

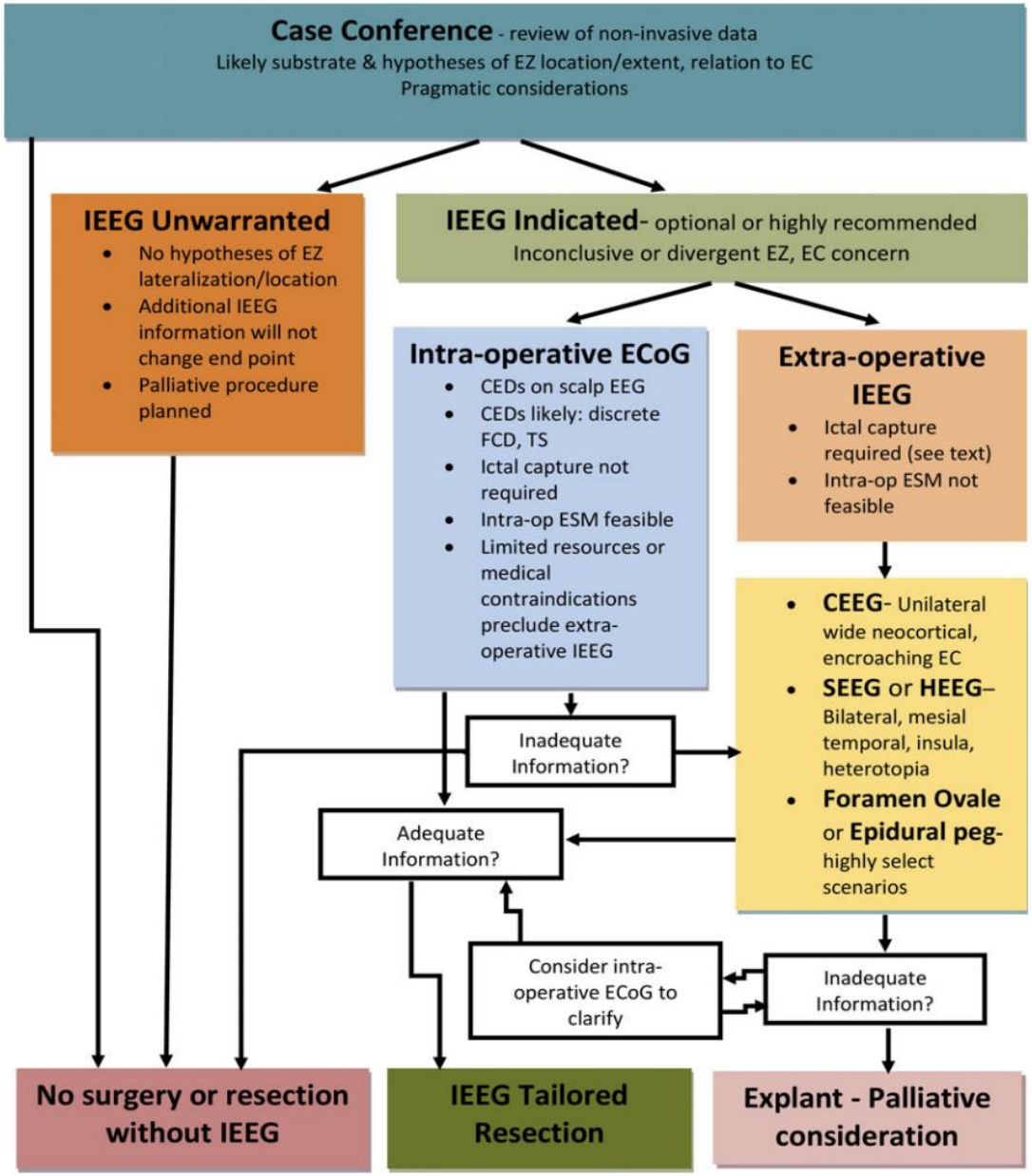

Epilepsia, 57(11):1735–1747, 2016
doi: 10.1111/epi.13515

Diagnostic utility of invasive EEG for epilepsy surgery: Indications, modalities, and techniques

*Prasanna Jayakar, †Jean Gotman, ‡A. Simon Harvey, §André Palmini, ¶Laura Tassi, #Donald Schomer, †Francois Dubeau, **Fabrice Bartolomei, ††Alice Yu, ‡‡Pavel Kršek, §§Demetrios Velis, and ¶¶Philippe Kahane

Epilepsia, 57(11):1735–1747, 2016
doi: 10.1111/epi.13515

Figure 1.
Protocol guiding IEEG strategies.
Epilepsia © ILAE

Table 1 Advantages and drawbacks of the different types of invasive explorations.

	Strips	Grids	Combination of subdural electrodes and depth electrodes	SEEG
Craniotomy bone flap	No	Yes	Yes if grids are used	No
Exploration of the deep cortex	No	No	Yes	Yes
Explorations of regions at a distance from one another	Yes	No	Yes	Yes
Exploration of the inner surface of the hemispheres	Yes	No	Yes	Yes
Exploration of the inner surface of the temporal lobe	Difficult	No	Yes	Yes
Topographic accuracy	No	Yes	No	Yes
Good regional sampling	No	Yes	Yes if grids are used	No
Most frequent complications	Hemorrhages Infections	Hemorrhages Edema Infections	Hemorrhages, edema (grids) Infection	Hemorrhages

Annals of Neurology
Volume 37, Issue 4, pages 476–487, April 1995

Intrinsic Epileptogenicity of Human Dysplastic Cortex as Suggested by Corticography and Surgical Results

André Palmini, MD,* Antonio Gambardella, MD,†§ Frederick Andermann, MD, FRCP(C),† Francois Dubeau, MD, FRCP(C),† Jaderson C. da Costa, MD, PhD,* André Olivier, MD, PhD, FRCS(C),† Donatella Tampieri, MD,† Pierre Gloor, MD, PhD,† Felipe Quesney, MD, PhD,† Eva Andermann, MD, PhD,† Eduardo Paglioli, MD,* Eliseu Paglioli-Neto, MD,* Ligia Coutinho, MD, PhD,* Richard Leblanc, MD, FRCS(C),† and Hyoung-Ihl Kim, MD, PhD‡

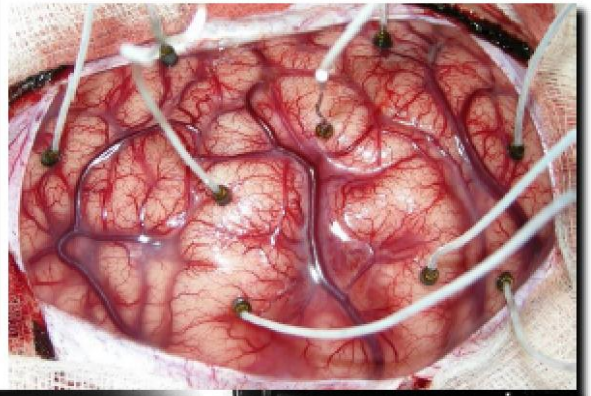

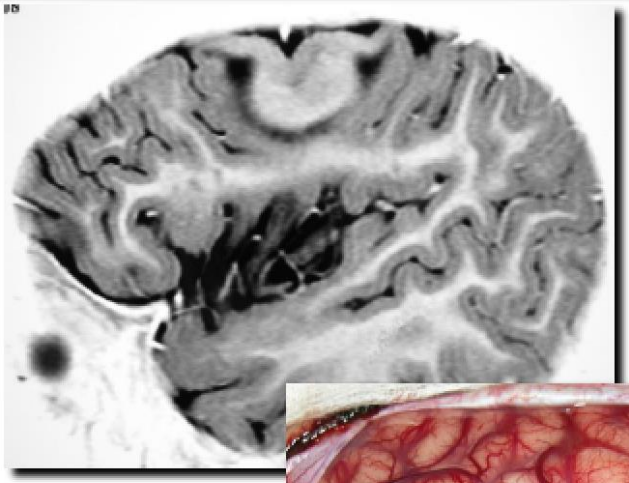

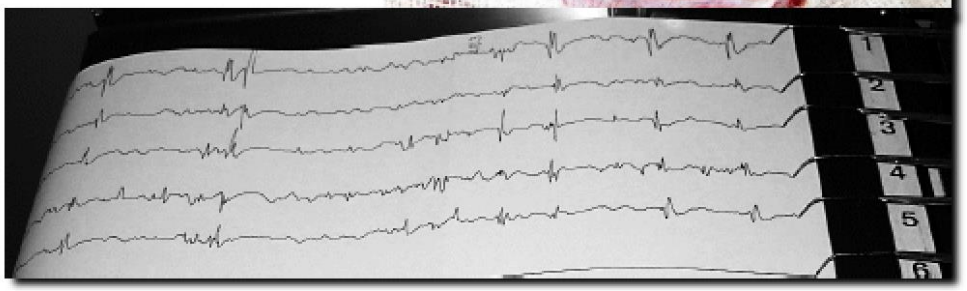

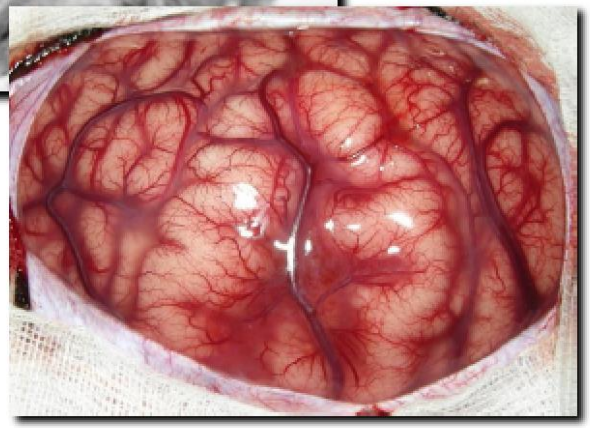

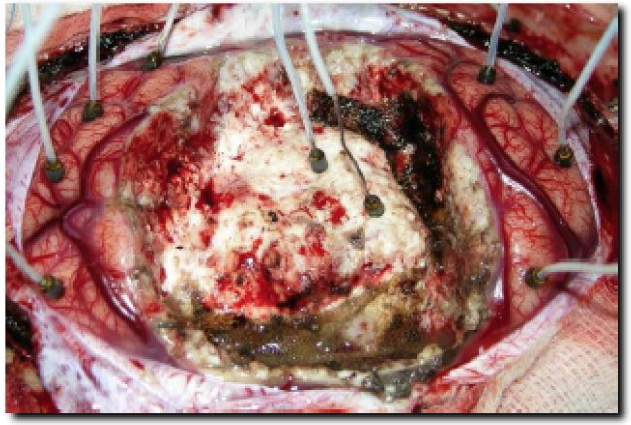

Disadvantage of Intraoperative ECoG

- MRI negative epilepsy
  - Against the principal of resective epilepsy surgery ---→ Resection of "epileptogenic zone", not "irritative zone (interictal epileptiform discharges)"
- Effect of general anesthesia
- Short duration of observation
- Rare capturing of ictal EEG activity
- Deep-seated epileptogenic zone
- "Bottom-of-the-sulcus" FCD

Precision of localization with 'surface' electrodes ***according to lesion location***

Precise localization w/ECoG

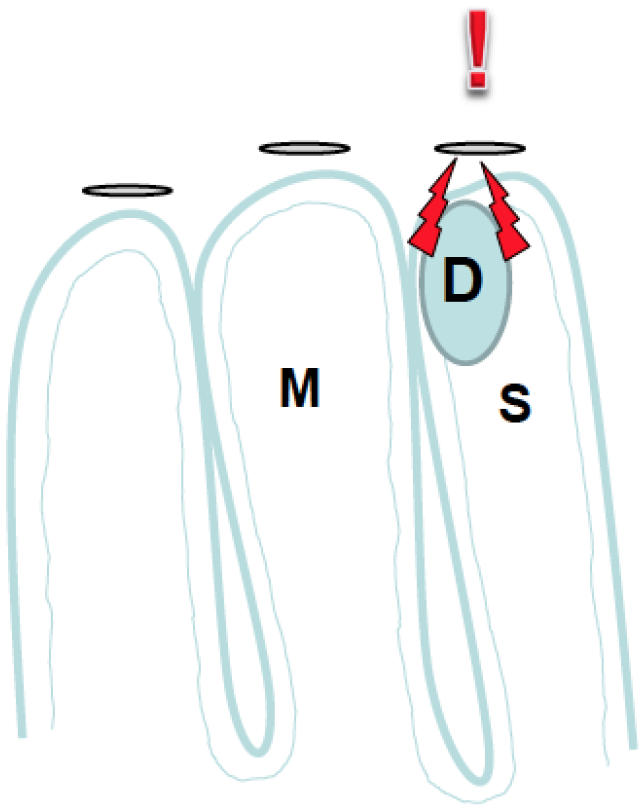

Superficial "gyral" lesion

ECoG mislocalization

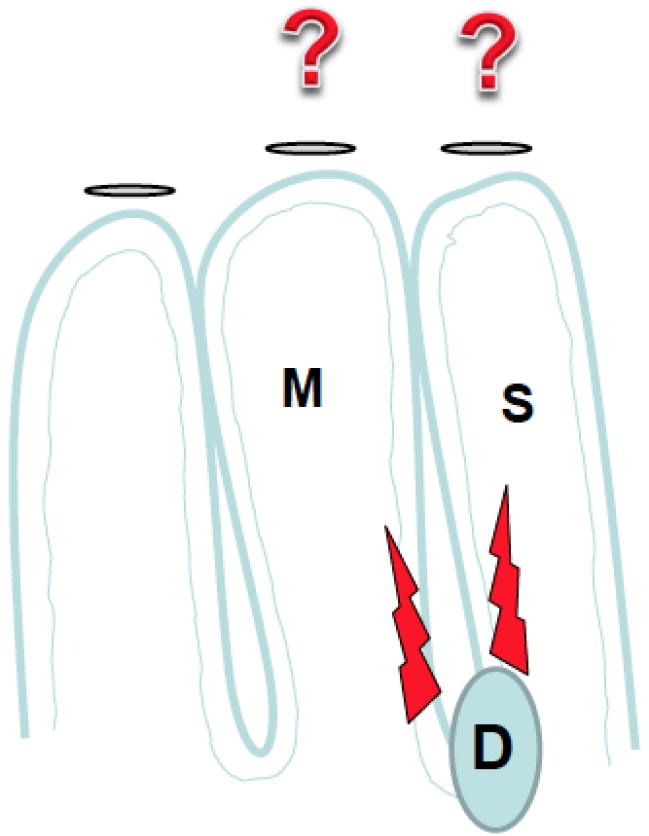

Lesion at depth of sulcus

Figure 3 **Coregistered PET and MRI of a right frontal BOSD**

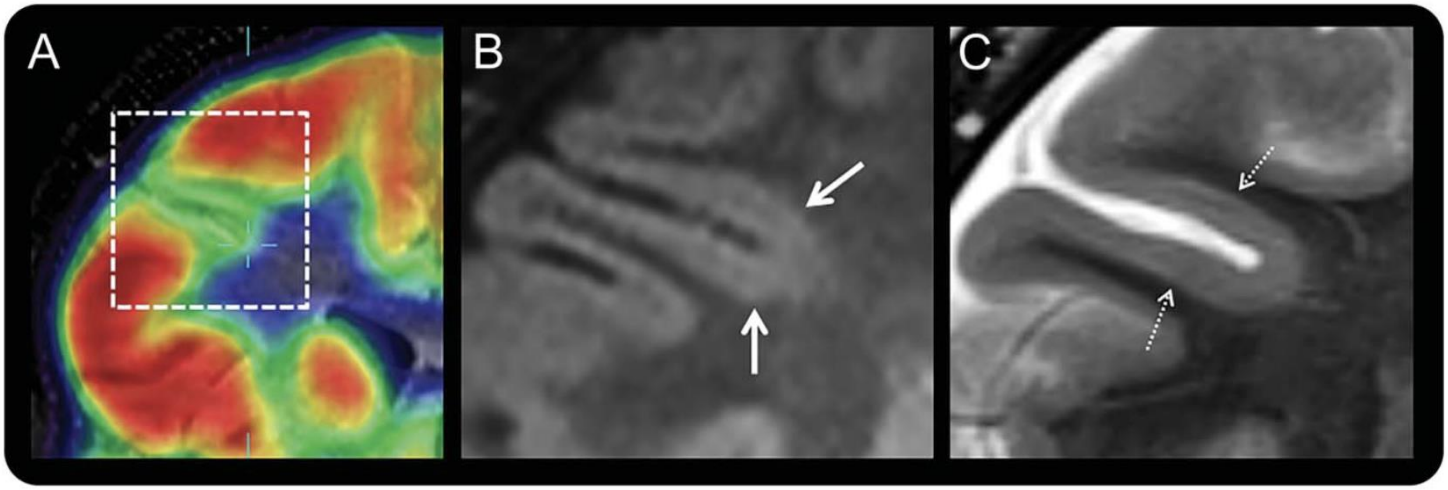

Coregistered coronal FDG-PET and T1-weighted MRI scans (A) through the right frontal lobe in a 10-year-old boy with versive seizures and right frontal epileptiform activity on scalp EEG showing localized cortical hypometabolism in the right inferior frontal sulcus. Magnified coronal FLAIR (B) and T2-weighted (C) MRI scans at 3.0 tesla with a 32-channel head coil showing subtle thickening of cortex with blurring of gray–white junction (thick arrow) and faint subcortical signal hyperintensity (hatched arrow) in the bottom of the hypometabolic sulcus, but no "transmantle sign." The BOSD was not detected on this MRI scan until after coregistration with the PET scan and recognition that there was thickened gray matter deeper than the apparent depth of the hypometabolic sulcus on the PET scan, being more hypometabolic than the sulcal banks. Focal cortical dysplasia type 2B pathology was identified at the depth of the resected sulcus. BOSD = bottom-of-sulcus dysplasia; FDG = fluorodeoxyglucose; FLAIR = fluid-attenuated inversion recovery.

Disadvantage of Intraoperative ECoG

- MRI negative epilepsy
  - Against the principal of resective epilepsy surgery ---→ Resection of "epileptogenic zone", not "irritative zone (interictal epileptiform discharges)"
- Effect of general anesthesia
- Short duration of observation
- Rare capturing of ictal EEG activity
- Deep-seated epileptogenic zone
  - **Mesial temporal lobe (hippocampus, amygdala, entorhinal)**
  - **Operculo-insular cortex**
  - **Cingulate cortex**
  - **Interhemispheric regions**
  - **Orbitofrontal cortex (especially posterior portion)**
- "Bottom-of-the-sulcus" FCD
- Network epilepsy

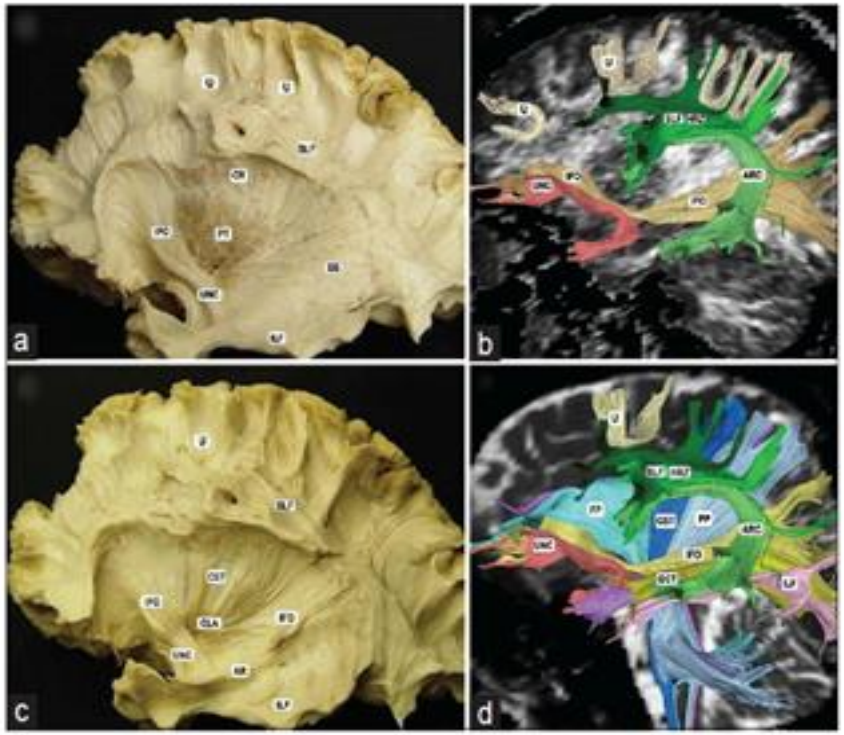

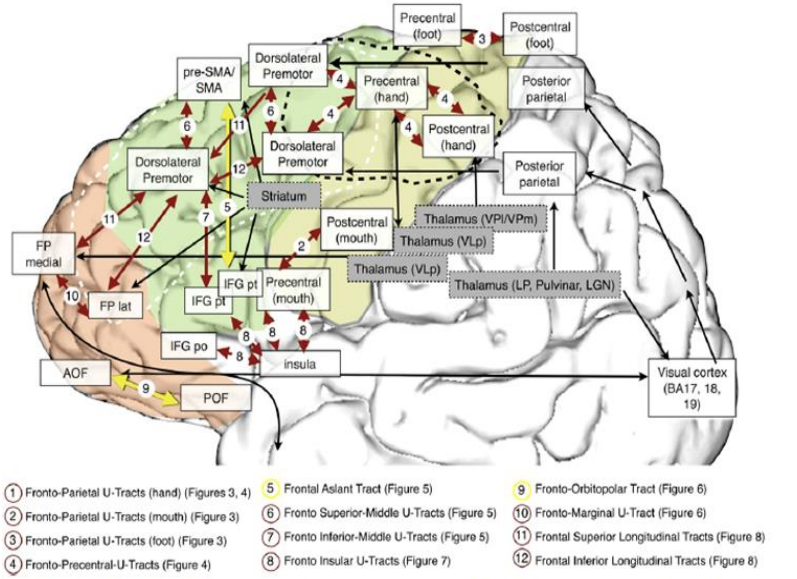

Fig. 13 – Diagram of the frontal lobe connections. U-tracts are in red, intralobar frontal tracts are in yellow and the long-range association and projection connections are in black. The different areas outlined correspond to the different functional divisions as following: central sulcus connections (yellow area), hand-knob connections (dashed black line area), premotor connections (green area), prefrontal and orbito-polar (light red area), dorsolateral longitudinal connections (dashed white line area).

Extraoperative Intracranial EEG Monitoring: Indications

- **MRI – negative epilepsy**
- **Discordance of anatomical location (MRI lesion** or **definite PET hypometabolism, SPECT hyperperfusion, MEG) with the electro-clinical features**
  - **Deep-seated lesions** such as **"Bottom of-a-sulcus" FCD, insula**
  - The spatial distribution *of IEDs is usually more extensive than the structural abnormality*
- **Two or more anatomical lesions**
  - Location of at least one of them being **discordant with the electro-clinical hypothesis**
  - **Both lesions** are **located within the same functional network** and it is **unclear if one (or both) of them is (are) epileptic.**
- The generated anatomo-electro-clinical hypothesis involves a **potentially highly functional cortex**.

  (Najm et al., 2014)

Subdural EEG vs SEEG

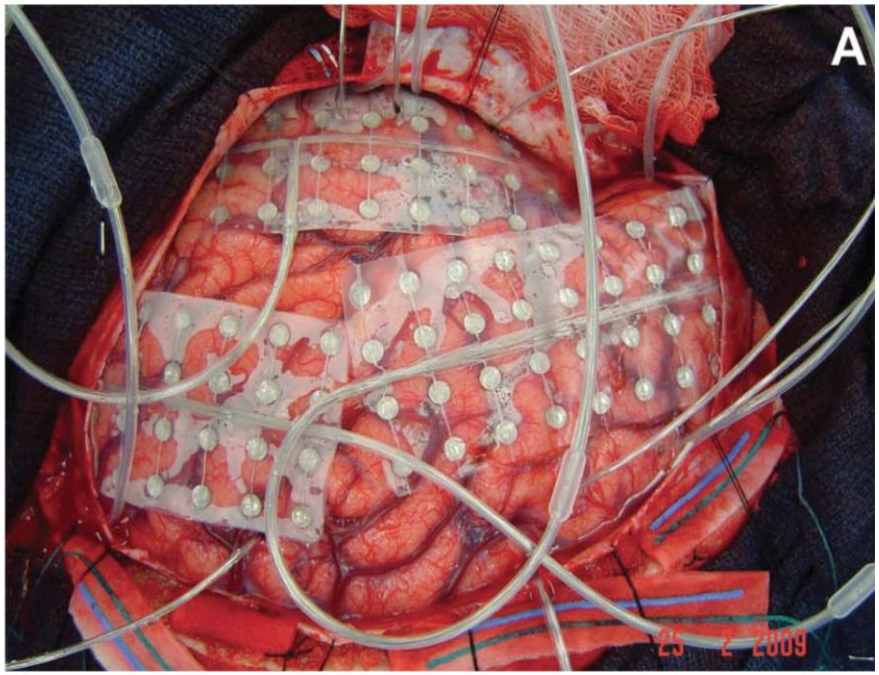

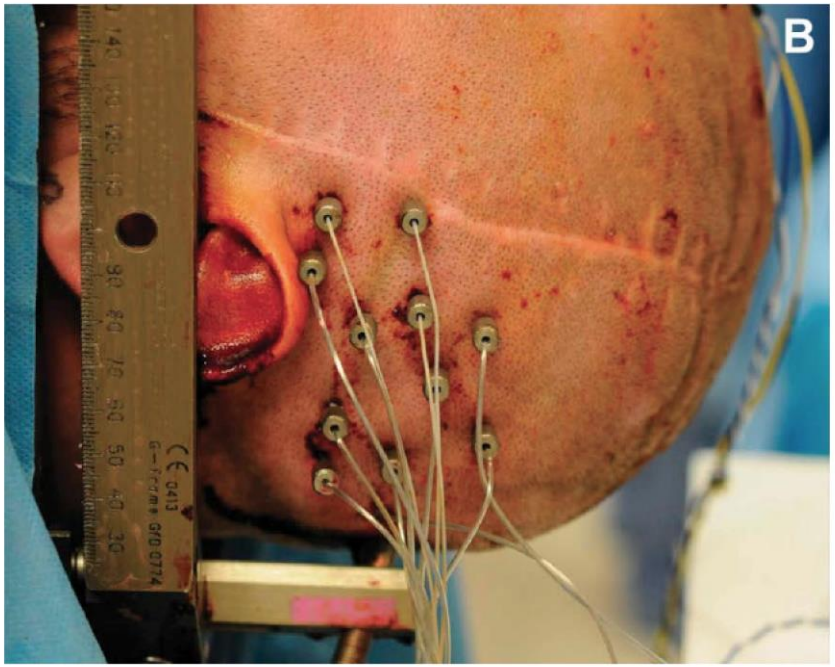

Subdural EEG

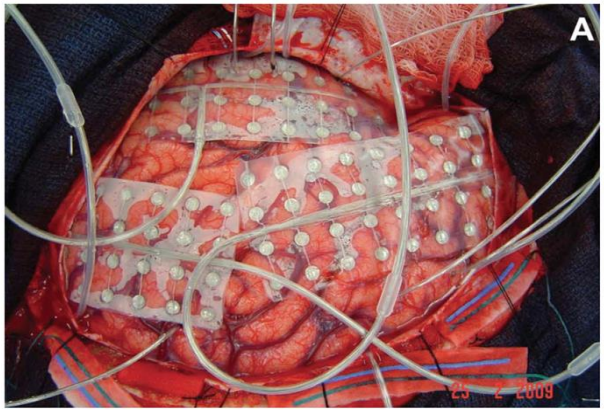

- For >30 years, subdural EEG was a gold standard of extraoperative invasive monitoring techniques in the US (Engel et al., 1990; Silberbusch et al., 1998; Najm et al., 2002; Widdess-Walsh et al., 2007).
- Despite its efficacy and spatial accuracy in mapping the superficial cortex, invasive monitoring using the subdural methodology has limitations.
- **Disadvantages:**
  - Relatively high surgical morbidity
  - Limitations in accessing deep or bilateral cortical structures
  - MRI-negative epilepsy
  - Electroclinical features suggestive of **functional network involvement** such as temporal-perisylvian-insular regions (Hamer et al., 2002; Onal et al., 2003; Simon et al., 2003; Johnston et al., 2006; Widdess-Walsh et al., 2007).

SEEG

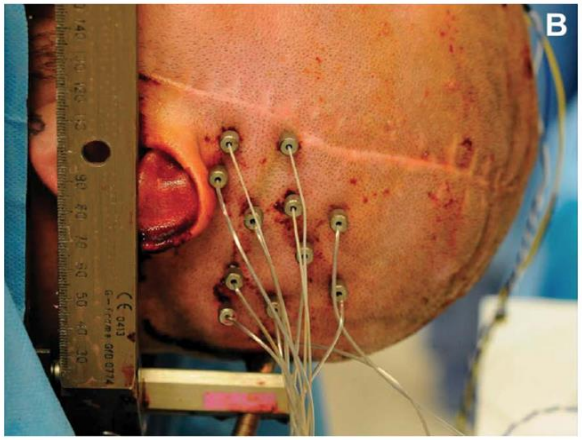

- **MRI-negative epilepsy**
- **Deep-seated or Difficult to cover region(s) by SDG:**
  - **Bottom-of-a-sulcus FCD**
  - **Mesial temporal lobe (hippocampus, amygdala, entorhinal)**
  - **Operculo-insular cortex**
  - **Cingulate cortex**
  - **Interhemispheric regions**
  - **Posterior orbitofrontal cortex**
- **Failure of a previous subdural EEG monitoring**
- **Bi-hemispheric exploration in**
  - **Bi-temporal lesions or SOZ**
  - Multilobar, bi-hemispheric lesions or SOZ
- **Anatomo- functional network involvement** (e.g., limbic system) **in the setting of a normal MRI.**

(Gonzalez-Martinez et al., 2013)

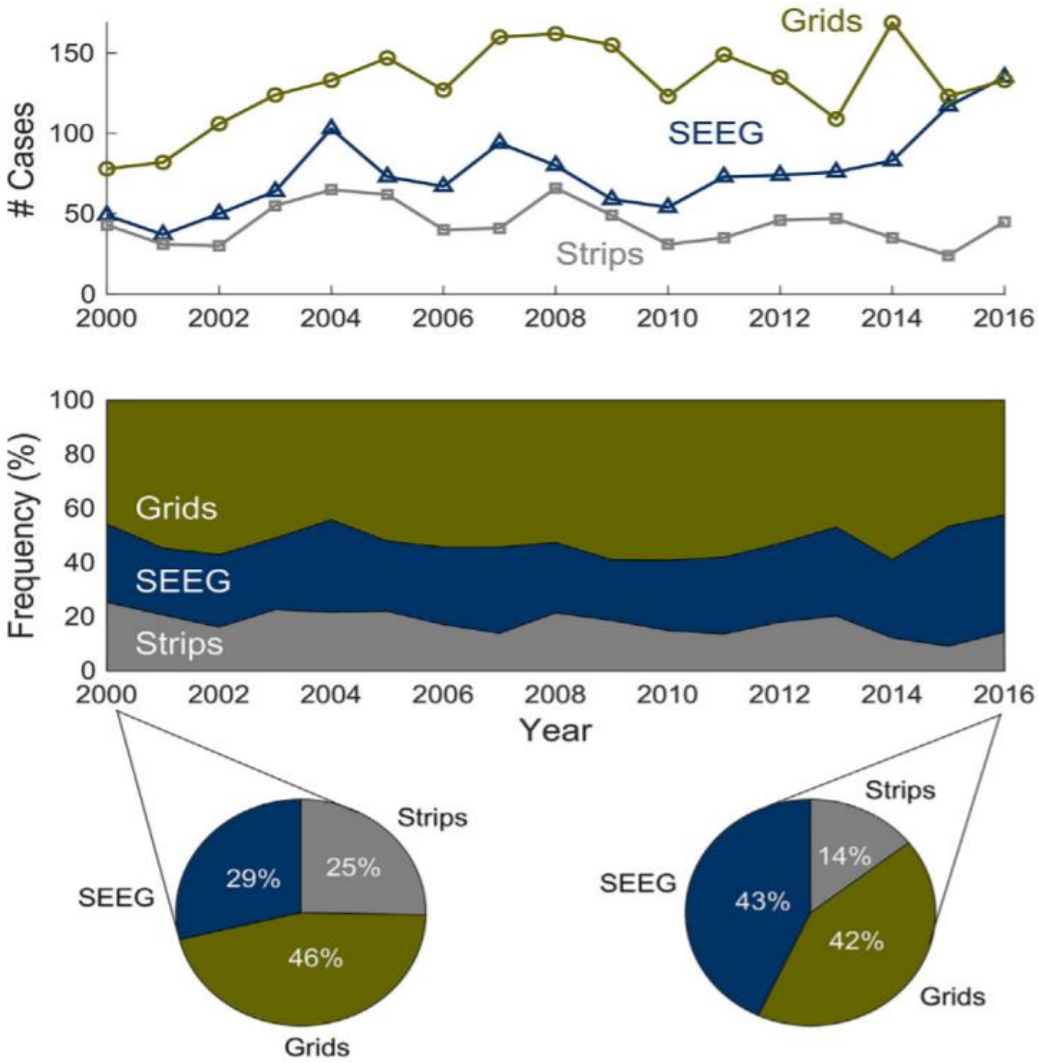

Fig. 1. Trends in iEEG recordings techniques in the United States using national data from CMS. The top panel shows the number of cases per year and the middle panel shows the frequency of cases per year, both demonstrating that SEEG cases significantly increased from 2000 to 2016, while subdural implantation of only strip electrodes through burr holes declined and craniotomy with subdural implantation of electrode arrays, grids, strips, and/or depth electrodes remained stable. The pie charts depict the proportions of iEEG recordings techniques for the first and last year of the study (2000 and 2016).

Commentary: Understanding Stereoelectroencephalography: What's Next?

SEEG is distinct in that its appropriate application inextricably depends on that establishment of an individualized anatomo-electro-clinical hypothesis. Thus, SEEG is not only the technique of percutaneous intracerebral electrode implantation, but also a comprehensive methodology that depends on the multidisciplinary effort of specialized epileptologists and neurosurgeons to craft an anatomo-electro-clinical hypothesis and plan a concomitant SEEG exploration strategy that enables the seizure onset and propagation to be analyzed in 4 dimensions (spatially and temporally).

The purpose of SEEG is to test an anatomoelectroclinical hypothesis that is individualized based on clinical history, semiology, preoperative imaging, and video EEG data for each specific patient.

In this paradigm, the goal of intracerebral recording is to understand the spatial and temporal dynamics of the seizure itself (ie, where the seizure starts and when and where it spreads). (Chabardes et al., 2017)

Commentary: Understanding Stereoelectroencephalography: What's Next?

"In conclusion, the next mandatory step is to understand that SEEG is not only a surgical technique for the implantation of percutaneous intracerebral electrodes, but rather part of a comprehensive methodology for the identification of the EZ. SEEG-like implantation of intracerebral electrodes, without a proper anatamo-electro-clinical hypothesis (ie, the true SEEG methodology), is not enough, and may result in inadequate characterization of the epileptic network and, more importantly, lower rates of postresection seizure freedom. Therefore, we encourage centers adopting SEEG to apply their implantation strategies based on rigorously established anatomo-electro-clinical hypotheses to ensure that SEEG is as efficacious as possible for identifying the EZ" (Chabardes et al., 2017)

Francesco Cardinale, MD, PhD*
Massimo Cossu, MD*
Laura Castana, MD*
Giuseppe Casaceli, MD*‡
Marco Paolo Schiariti, MD*
Anna Miserocchi, MD*
Dalila Fuschillo, MD*‡
Alessio Moscato, MSc*§
Chiara Caborni, MSc¶
Gabriele Arnulfo, PhD||#
Giorgio Lo Russo, MD*

*"Claudio Munari" Centre for Epilepsy and Parkinson Surgery, Niguarda Ca' Granda Hospital, Milano, Italy; ‡Department of Neurological Sciences, Università degli Studi di Milano, Milano, Italy; §Unit of Medical Physics, Niguarda Ca' Granda Hospital, Milano, Italy; ¶Politecnico di Milano, Bioengineering Department, Nearlab, Milano, Italy; ||Department of Informatics, Bioengineering, Robotics and System Engineering (DIBRIS), Università di Genova, Genova, Italy; #Neuroscience Center, University of Helsinki, Helsinki, Finland

Dr Schiariti is now at the Department of Neurosurgery, Fondazione IRCCS Istituto Neurologico Carlo Besta, Milano, Italy. Dr Miserocchi is now at the Institute of Neurology, National Hospital for Neurology and Neurosurgery, London, United Kingdom.

Correspondence:
Francesco Cardinale, MD, PhD,
Centro per la Chirurgia dell'Epilessia e del Parkinson "Claudio Munari," Ospedale Niguarda Ca' Granda, Piazza Ospedale Maggiore, 3, 20162, Milano, Italia.
E-mail: francesco.cardinale@ospedaleniguarda.it

Received, August 11, 2012.
Accepted, October 23, 2012.
Published Online, November 19, 2012.

Stereoelectroencephalography: Surgical Methodology, Safety, and Stereotactic Application Accuracy in 500 Procedures

BACKGROUND: Stereoelectroencephalography (SEEG) methodology, originally developed by Talairach and Bancaud, is progressively gaining popularity for the presurgical invasive evaluation of drug-resistant epilepsies.

OBJECTIVE: To describe recent SEEG methodological implementations carried out in our center, to evaluate safety, and to analyze in vivo application accuracy in a consecutive series of 500 procedures with a total of 6496 implanted electrodes.

METHODS: Four hundred nineteen procedures were performed with the traditional 2-step surgical workflow, which was modified for the subsequent 81 procedures. The new workflow entailed acquisition of brain 3-dimensional angiography and magnetic resonance imaging in frameless and markerless conditions, advanced multimodal planning, and robot-assisted implantation. Quantitative analysis for in vivo entry point and target point localization error was performed on a sub–data set of 118 procedures (1567 electrodes).

RESULTS: The methodology allowed successful implantation in all cases. Major complication rate was 12 of 500 (2.4%), including 1 death for indirect morbidity. Median entry point localization error was 1.43 mm (interquartile range, 0.91-2.21 mm) with the traditional workflow and 0.78 mm (interquartile range, 0.49-1.08 mm) with the new one ($P < 2.2 \times 10^{-16}$). Median target point localization errors were 2.69 mm (interquartile range, 1.89-3.67 mm) and 1.77 mm (interquartile range, 1.25-2.51 mm; $P < 2.2 \times 10^{-16}$), respectively.

CONCLUSION: SEEG is a safe and accurate procedure for the invasive assessment of the epileptogenic zone. Traditional Talairach methodology, implemented by multimodal planning and robot-assisted surgery, allows direct electrical recording from superficial and deep-seated brain structures, providing essential information in the most complex cases of drug-resistant epilepsy.

KEY WORDS: Complications, Epilepsy surgery, In vivo application accuracy, Intraoperative imaging, Invasive EEG, Stereoelectroencephalography, Stereotaxy

SEEG helps looking beyond the cortical surface

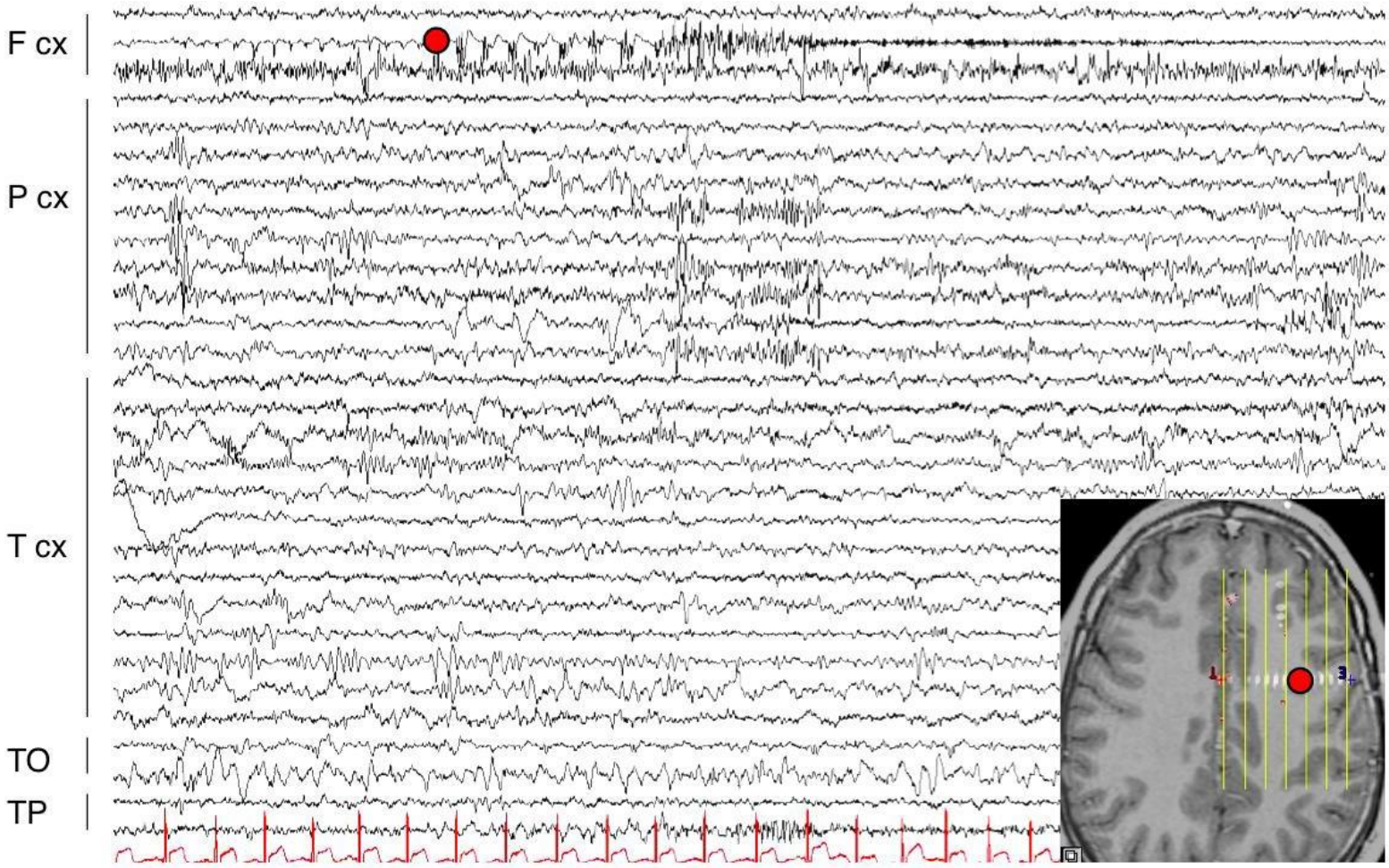

Misconception regarding spatial sampling of SEEG

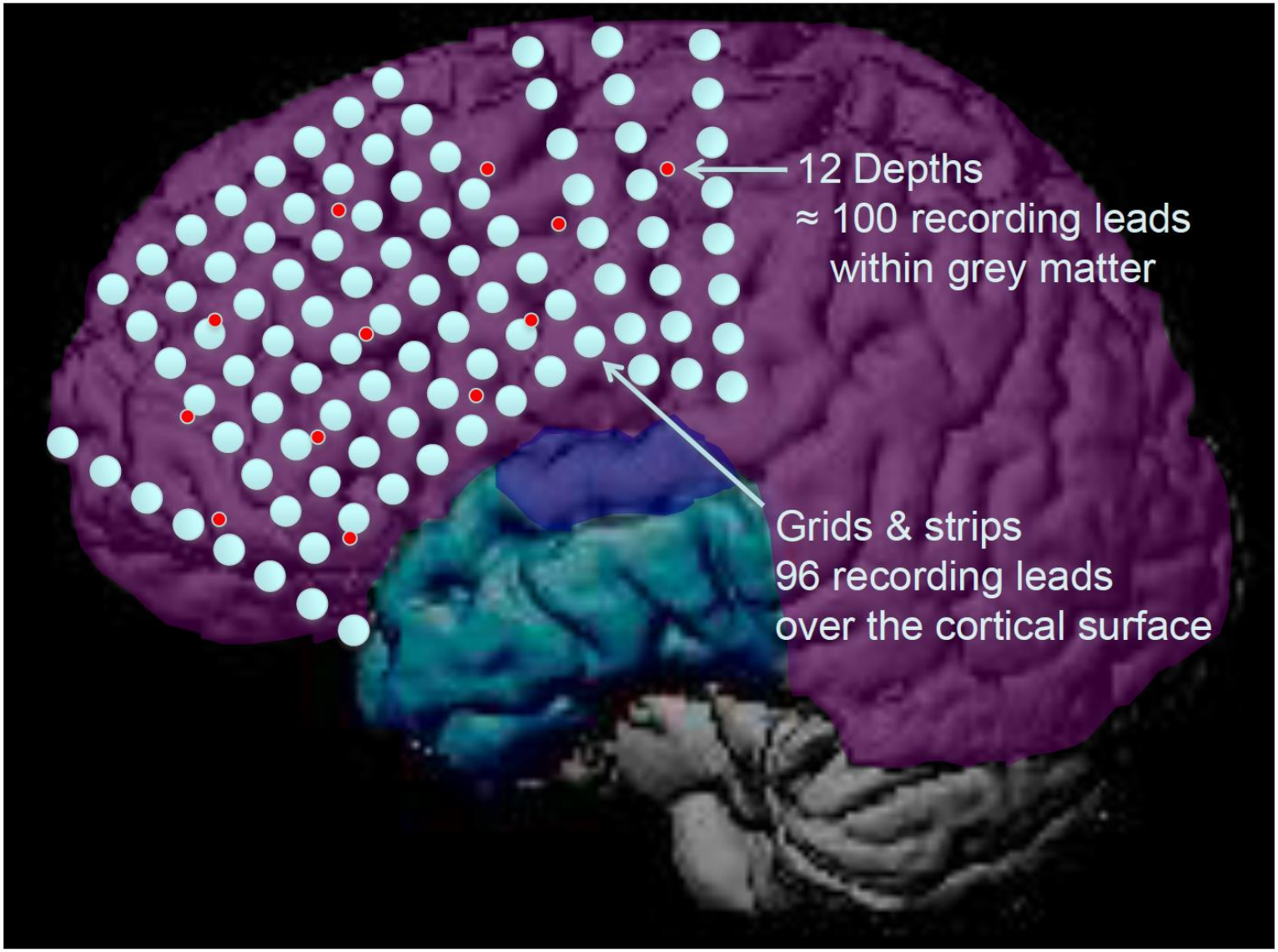

Conc.

Why to implant

Who to implant

How to implant

How to interpret

Misconception regarding spatial sampling of SEEG

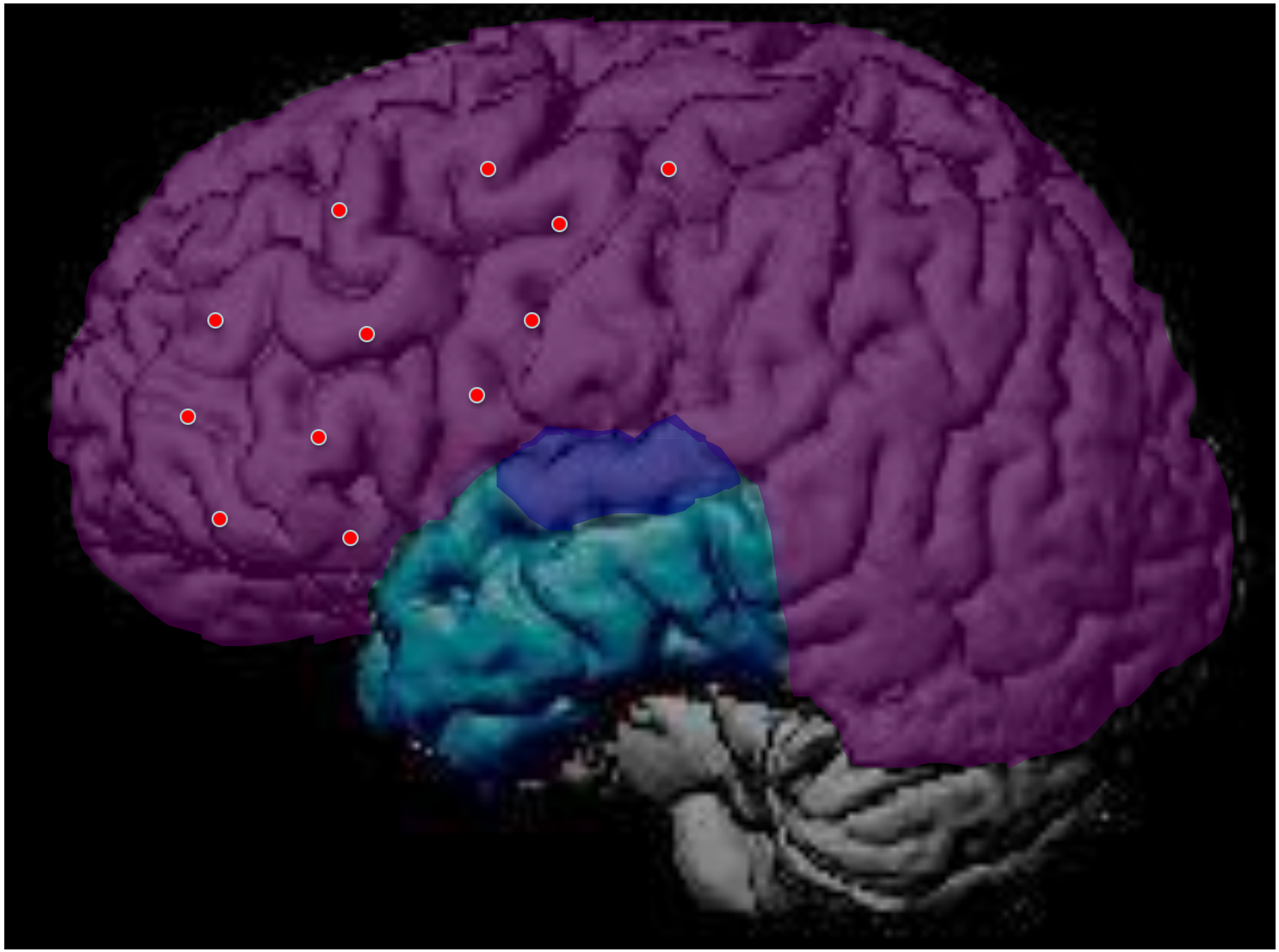

Have a strong hypothesis with a clear objective

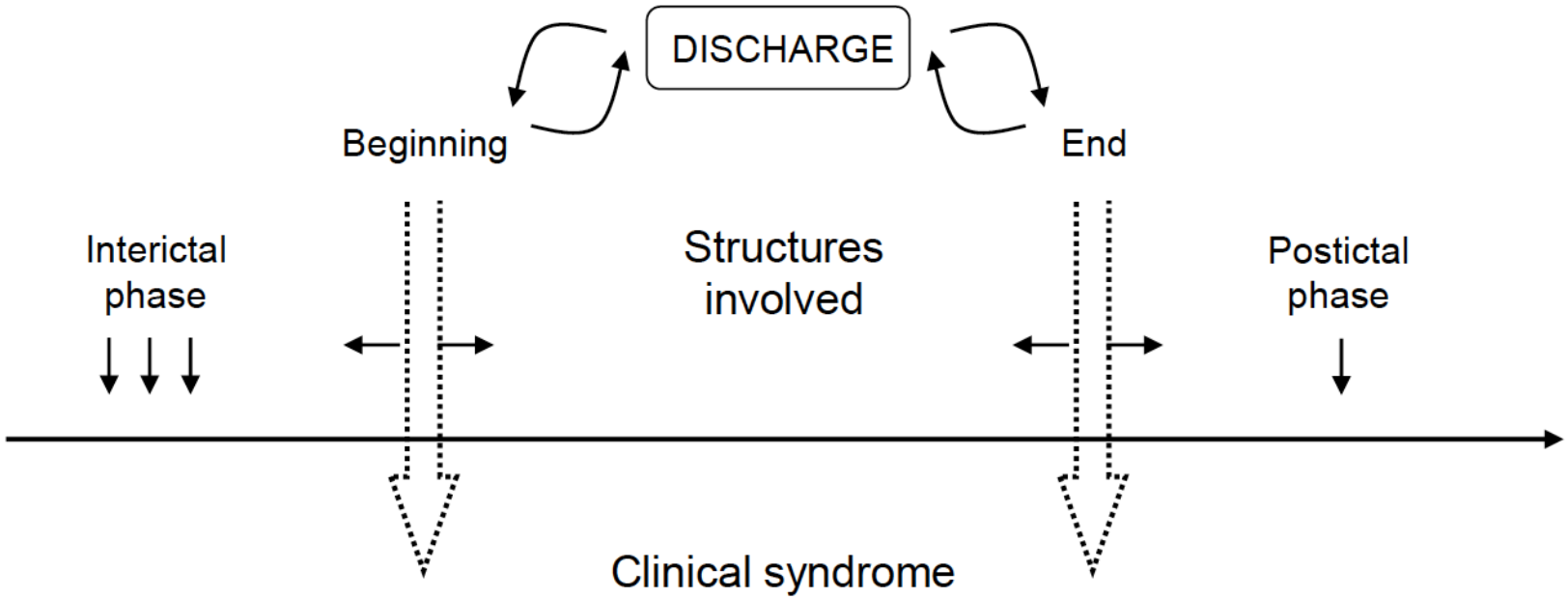

Bancaud & Talairach 1992, modified

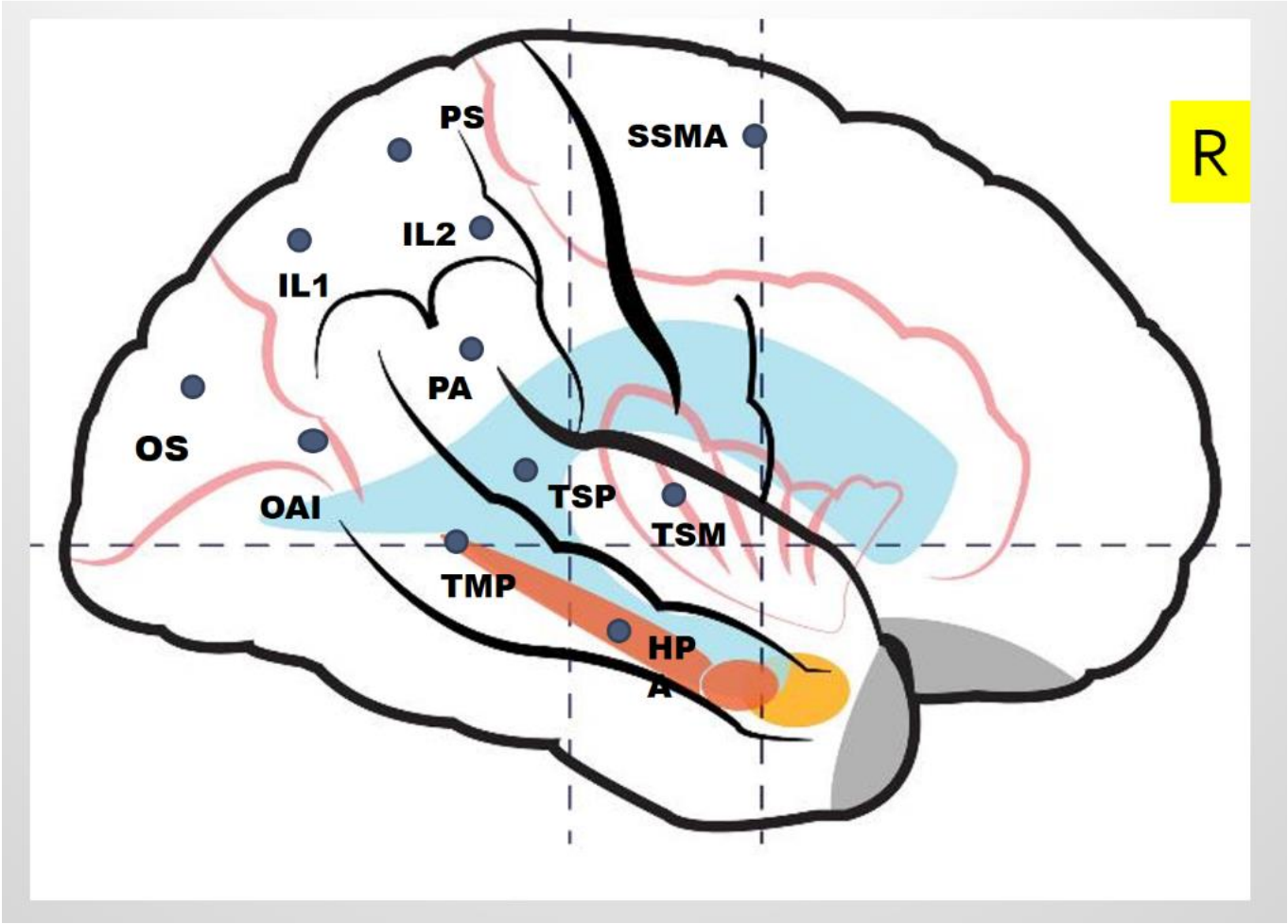

The preimplantation **“anatomo-electro-clinical” hypotheses** formulation is the single most important element in the process of planning the placement of SEEG electrodes. If the preimplantation hypotheses are incorrect, the placement of the depth electrodes will be inadequate and the interpretation of the SEEG recordings will not give access to the definition of the Epileptogenic Zone.

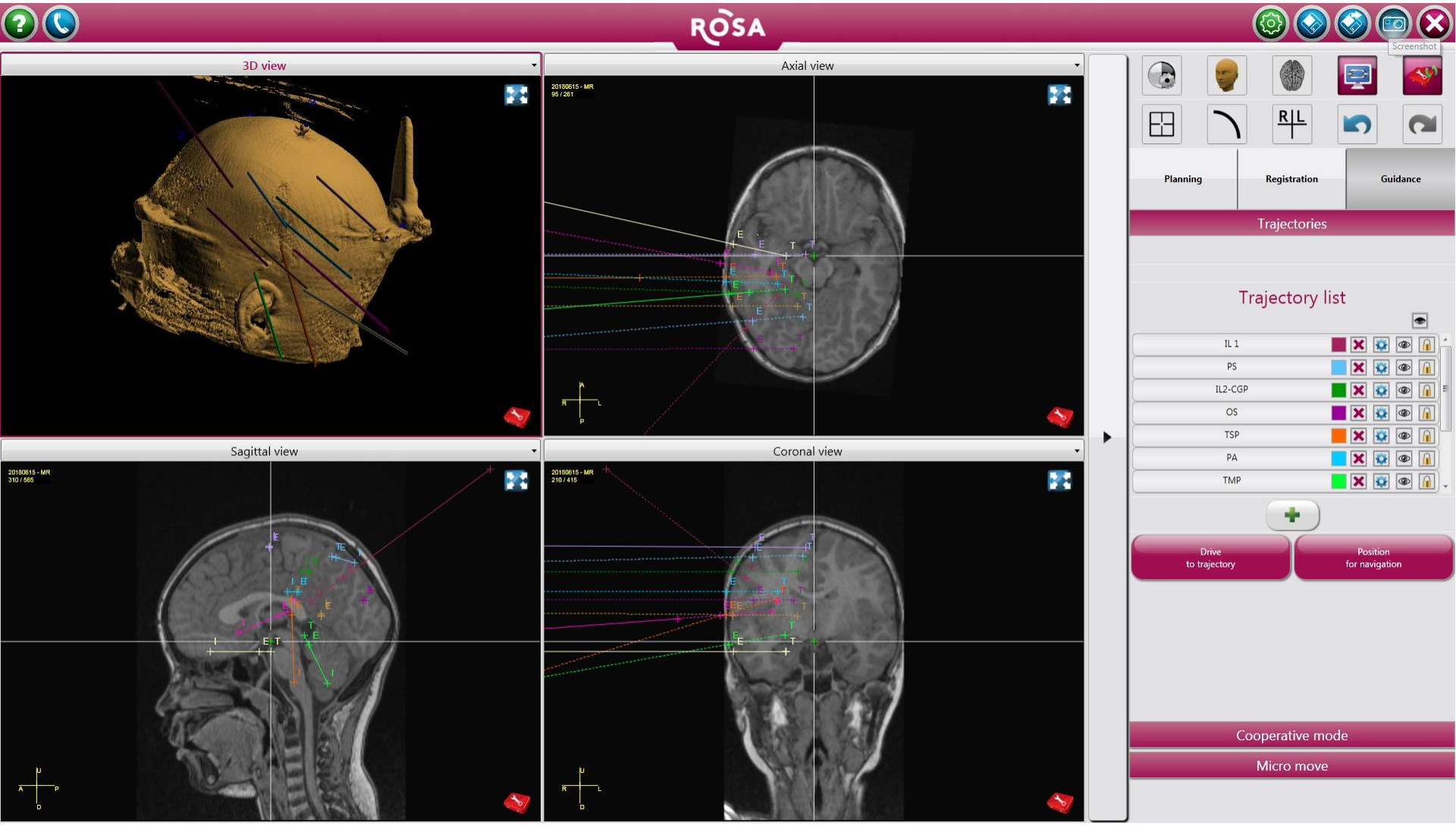
ROSA
Screenshot
3D view
Axial view
Sagittal view
Coronal view
20180615 - MR
95 / 261
20180615 - MR
310 / 565
20180615 - MR
210 / 415
Planning
Registration
Guidance
Trajectories
Trajectory list
IL 1
PS
IL2-CGP
OS
TSP
PA
TMP
Drive
to trajectory
Position
for navigation
Cooperative mode
Micro move

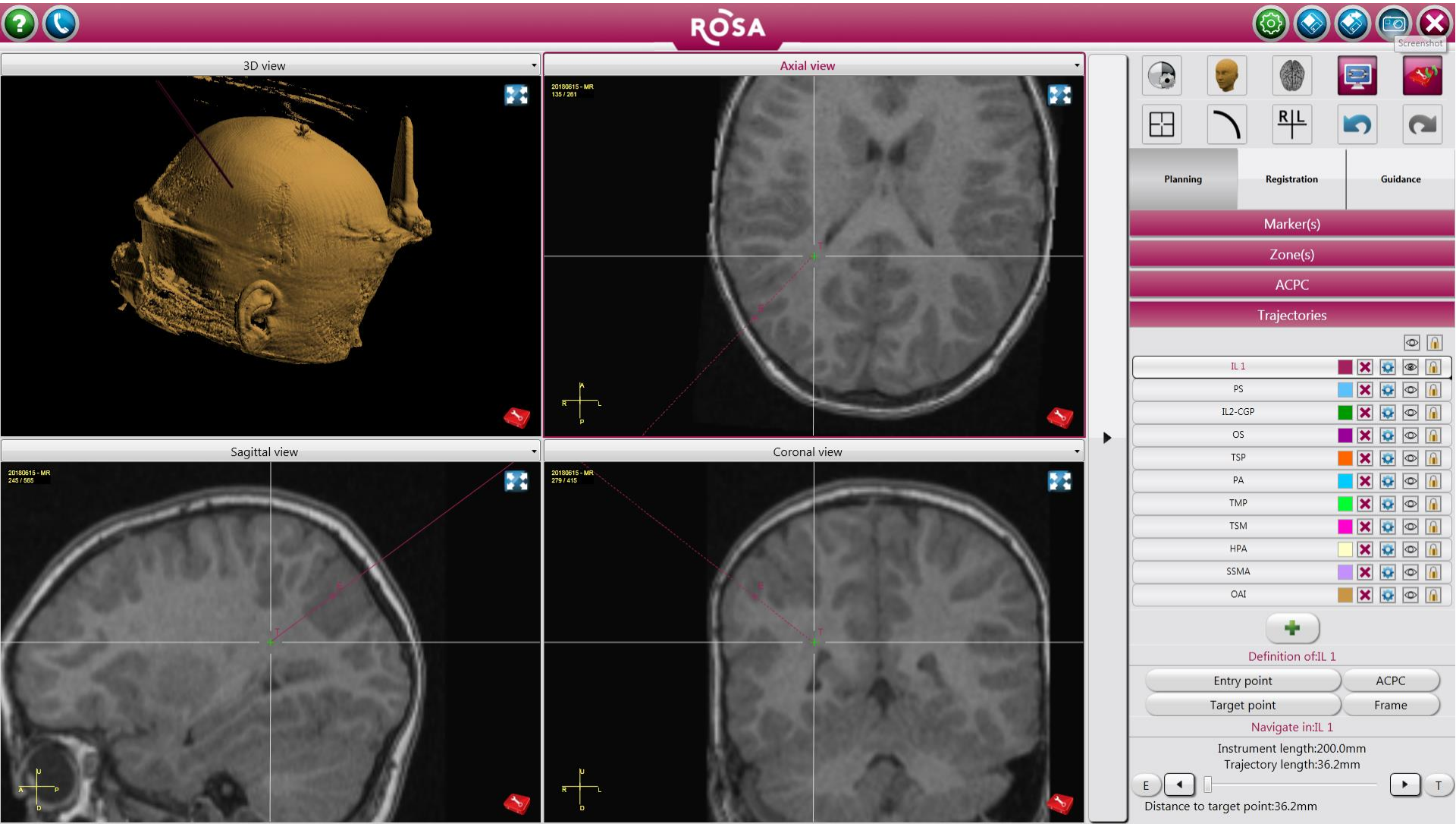
ROSA
Screenshot
3D view
Axial view
20180615 - MR
135 / 261
Sagittal view
20180615 - MR
245 / 565
Coronal view
20180615 - MR
279 / 415
Planning
Registration
Guidance
Marker(s)
Zone(s)
ACPC
Trajectories
IL 1
PS
IL2-CGP
OS
TSP
PA
TMP
TSM
HPA
SSMA
OAI
Definition of:IL 1
Entry point
ACPC
Target point
Frame
Navigate in:IL 1
Instrument length:200.0mm
Trajectory length:36.2mm
E
T
Distance to target point:36.2mm

MT-02-157
ATI-IA.COM

MAYFIELD
MAYFIELD®
UNLOCK


ROSA
INCORRECT COUNT: STOP


SURG-W378429 T-BAR ONLY

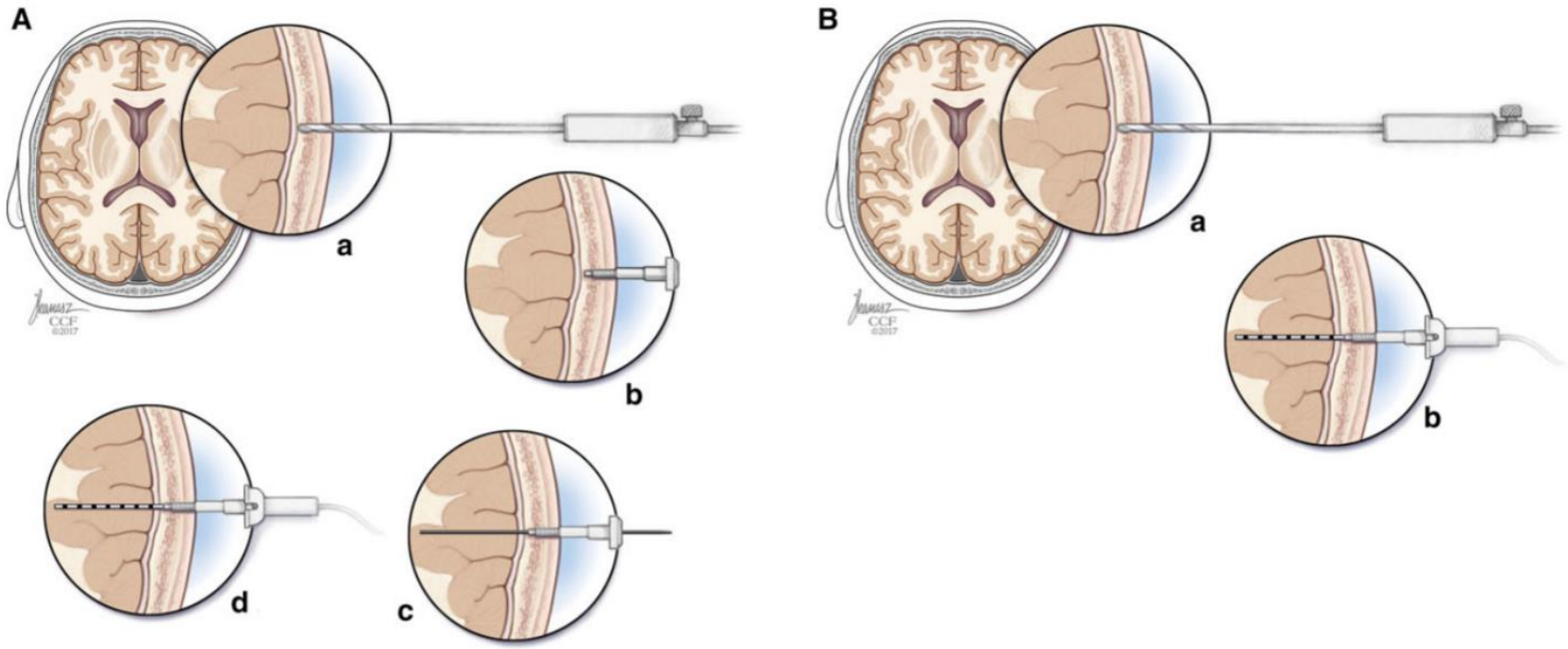

FIGURE 1 Implantation techniques. A, Technique 1: (a) The stereotactic robot is used to drill the initial burr hole in the skull (b) followed by fixation of a guide to the skull. (c) The stylet is then passed through the cranially fixed guide and removed without use of the stereotactic robot (d) followed by the implantation of the electrode through and fixation to the cranially fixed guide. B, Technique 2: (a) The stereotactic robot is used to drill the initial burr hole in the skull and then is used as the guide for implantation of the stylet/electrode complex. (b) The stylet is manually removed and the electrode is manually fixed in place via skin suture without the aid of the stereotactic robot

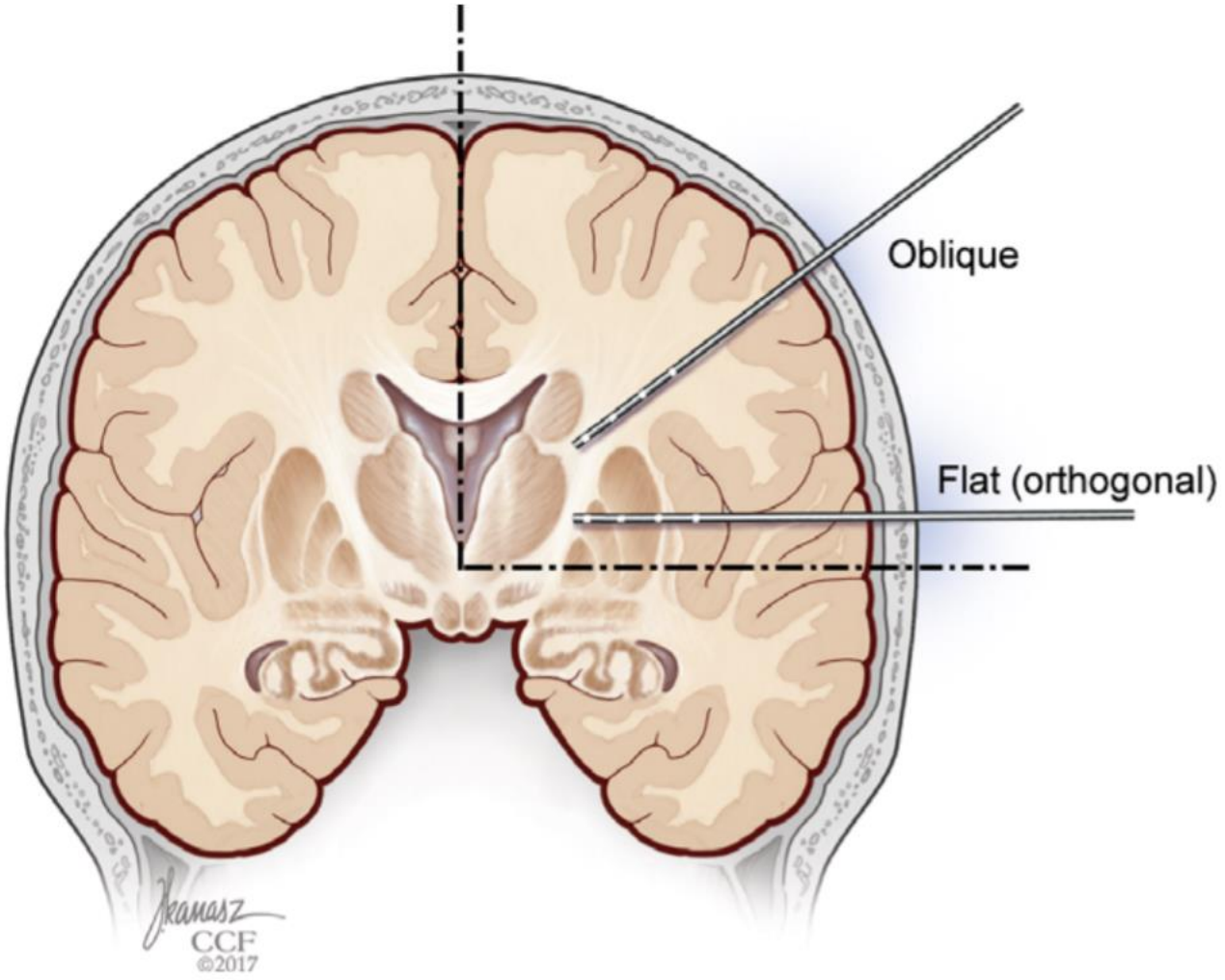

FIGURE 2 Oblique and orthogonal trajectories are defined in relation to the midsagittal line

MRI-Negative Epilepsy

- Current practice in epilepsy resective surgery generally relies heavily on the identification of radiologically visible lesions considered likely to be responsible for the epilepsy (Polkey, 2004).
- **The absence of a lesion visualized by MRI has been previously shown to relate to poorer prognosis in resective epilepsy surgery**, both for temporal (Berkovich et al., 1995) and extratemporal cases (Zentner et al., 1996; Smith et al., 1997; Mosewich et al., 2000; Jeha et al., 2007).
- Despite major advances in neuroimaging, MRI-negative cases still account for up to a quarter of all those presenting for presurgical evaluation (Berg et al., 2003).
- It is increasingly recognized that **certain MRI-negative cases**, while among the most challenging in terms of presurgical assessment, **are indeed surgically treatable with satisfactory and sometimes excellent outcomes** (Alarcon et al., 2006). This has been highlighted in a number of recent series (Cukiert et al., 2001; Siegel et al., 2001; Hong et al., 2002; Chapman et al., 2005; Cohen-Gadol et al., 2005; Lee et al., 2005; Alarcon et al., 2006).

doi:10.1093/brain/awm218 *Brain* (2007), **130**, 3169–3183

Stereoelectroencephalography in presurgical assessment of MRI-negative epilepsy

Aileen McGonigal,[1,2,3] Fabrice Bartolomei,[1,2,3] Jean Régis,[1,2,5] Maxime Guye,[1,2,3] Martine Gavaret,[1,2,3] Agnès Trébuchon-Da Fonseca,[1,2,3] Henry Dufour,[1,2,5] Dominique Figarella-Branger,[2,4] Nadine Girard,[2,6] Jean-Claude Péragut[1,2,5] and Patrick Chauvel[1,2,3]

[1]INSERM, U 751, Laboratoire de Neurophysiologie et Neuropsychologie, Marseille, F-13000, [2]Aix Marseille Université, Faculté de Médecine, Marseille, F-13000, [3]Assistance Publique Hôpitaux de Marseille, Hôpital La Timone, Service de Neurophysiologie Clinique, Marseille, F-13005, [4]Assistance Publique Hôpitaux de Marseille, Hôpital La Timone, Service d'Anatomie Pathologique, Marseille, F-13005, [5]Assistance Publique Hôpitaux de Marseille, Hôpital La Timone, Service de Neurochirurgie, Marseille, F-13005 and [6]Assistance Publique Hôpitaux de Marseille, Hôpital La Timone, Service de Neuroradiologie, Marseille, F-13005, France

Correspondence to: Dr Aileen McGonigal, Laboratoire de Neurophysiologie et Neuropsychologie, INSERM U 751 & Service de Neurophysiologie Clinique, CHU Timone, Marseille, France, 27 boulevard Jean Moulin 13005 Marseille France
E-mail: aileenmcg@hotmail.com

According to most existing literature, the absence of an MRI lesion is generally associated with poorer prognosis in resective epilepsy surgery. Delineation of the epileptogenic zone (EZ) by intracranial recording is usually required but is perceived to be more difficult in 'MRI negative' cases. Most previous studies have used subdural recording and there is relatively less published data on stereoelectroencephalography (SEEG). The objective of this study was to report the experience of our group in using SEEG in presurgical evaluation, comparing its effectiveness in normal and lesional MRI cases. One hundred consecutive patients undergoing SEEG for presurgical assessment were studied. Forty-three patients out of one hundred (43%) had normal MRI and 57 (57%) had lesional MRI. Successful localization was achieved with no difference between these two groups, in 41/43 (95%) normal MRI and in 55/57 (96%) lesional MRI cases ($P = 1.00$). Surgery was proposed in 84/100 patients and contra-indicated in 16/100 with no significant difference between lesional and MRI-negative groups ($P > 0.05$). At 1 year follow-up, 11/20 (55%) of those having undergone cortectomy in the MRI-negative group and 21/40 (53%) in the lesional MRI group were entirely seizure free ($P > 0.05$) and these proportions were maintained at 2 years follow-up. Significant improvement in seizure control (ILAE outcome groups 1–4) was achieved in >90% cases with no difference between groups ($P > 0.05$). Of MRI-negative cases that underwent surgery, 10/23 (43%) had focal cortical dysplasia. This series showed that SEEG was equally effective in the presurgical evaluation of MRI-negative and lesional epilepsies.

Epilepsy surgery of NLE is not rare and tends to increase

Diagnosis	N° (%)
Hippocampal sclerosis	3463 (36.4)
Ganglioglioma	986 (10.4)
Focal cortical dysplasia type II	859 (9.0)
No lesion	738 (7.7)
Dysembryoplastic neuroepithelial tumor	565 (5.9)
Glial scar	461 (4.8)
Cavernous angioma	431 (4.5)
Mild malformation of cortical development	279 (2.9)
Focal cortical dysplasia type I	268 (2.8)
Focal cortical dysplasia not otherwise specified	206 (2.2)
Total	8256 (86.7)

Blumcke et al. 2017

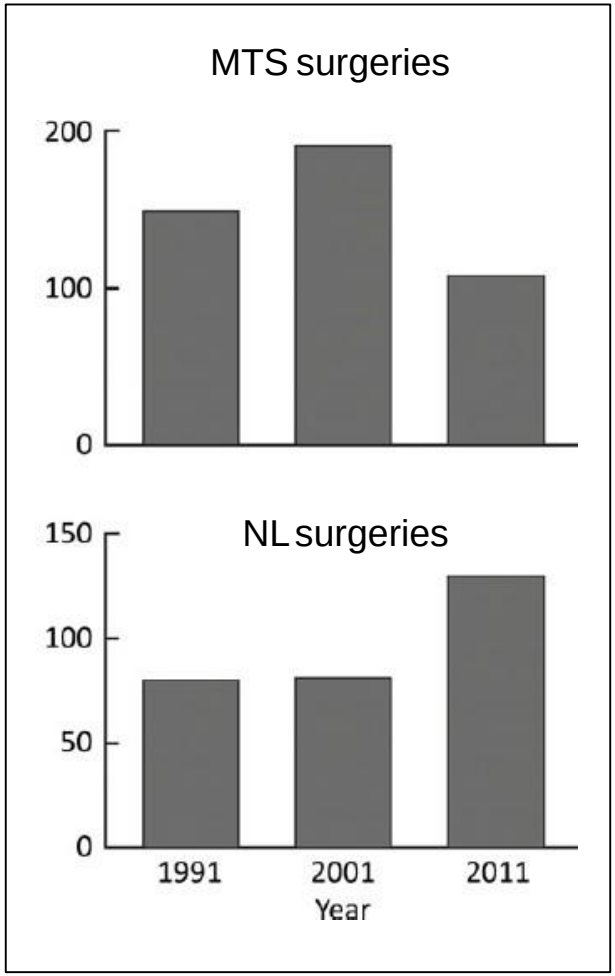

Jehi et al. 2015

Surgery is less efficient than for MRI+ cases

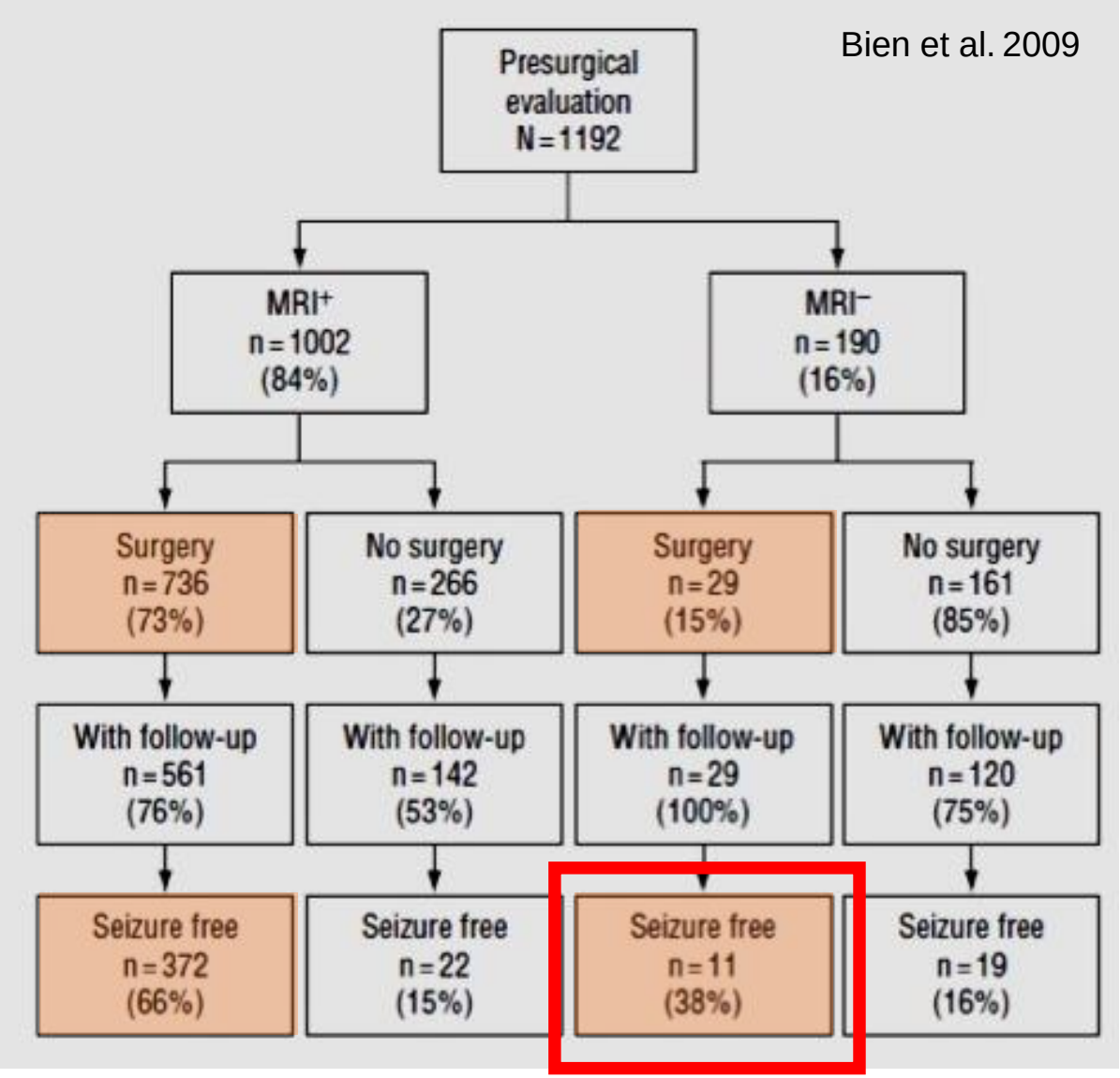

A number of NLE cases need an invasive EEG

Series	EEG	iSPECT	PET	iEEG
Siegel et al. 2001	100%	+ (?%)	-	100%
Hong et al. 2002	100%	83%	83%	100%
Worrel et al. 2002	100%	-	-	+ (?%)
Sylaja et al. 2003	100%	-	-	-
Blume et al. 2004	100%	-	-	62%?
Chapman et al. 2005	100%	+ (?%)	100%	63%
Lee et al. 2005	100%	63%	89%	100%
Bien et al. 2009	100%	58%	58%	?

DECISIONAL TREE IN NLE

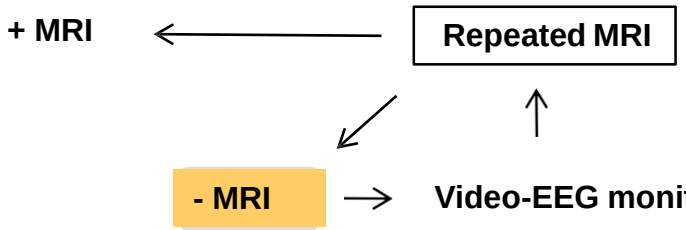

- Ictal EEG better localize than PET or SPECT [1, 2]

- Ictal patterns predictive of favourable outcome
  - TL cases : anterior T rythmic theta [3]
  - FL cases : focal beta discharge [4]
- FDG-PET has a greater localizing value in neocxTLE [5, 6] Helps to identify surgery candidates in catastrophic Epi [7] Helps for the placement of intracranial electrodes [8] Helps to avoid IEEG in MRI- FCD [9]
- Ictal SPECT has a lower localizing value than PET [1, 2]
- Is better in TLE than in extraTL cases [1]

(1) Hong 2002; (2) Lee 2005; (3) Sylaja 2004; (4) Worrel 2002; (5) Carnel 2004; (6) Lee 2005; (7) Chugani 2010; (8)Asano 2001; (9) Chassoux 2010;

DECISIONAL TREE IN NLE

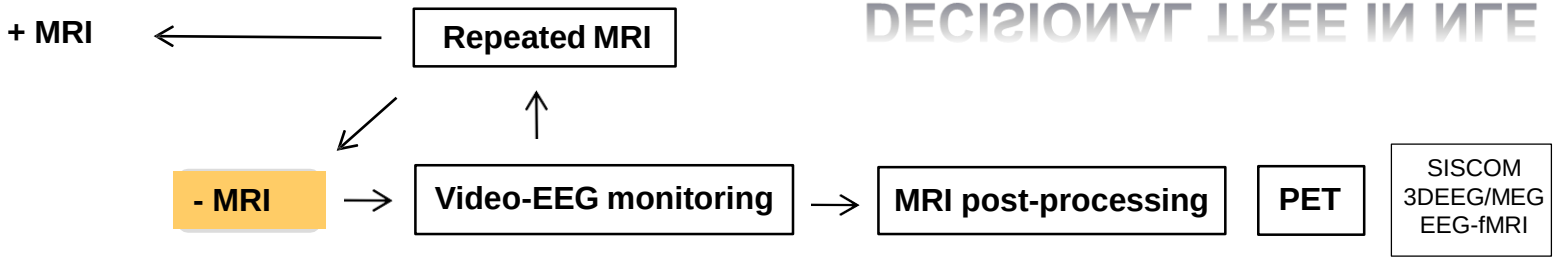

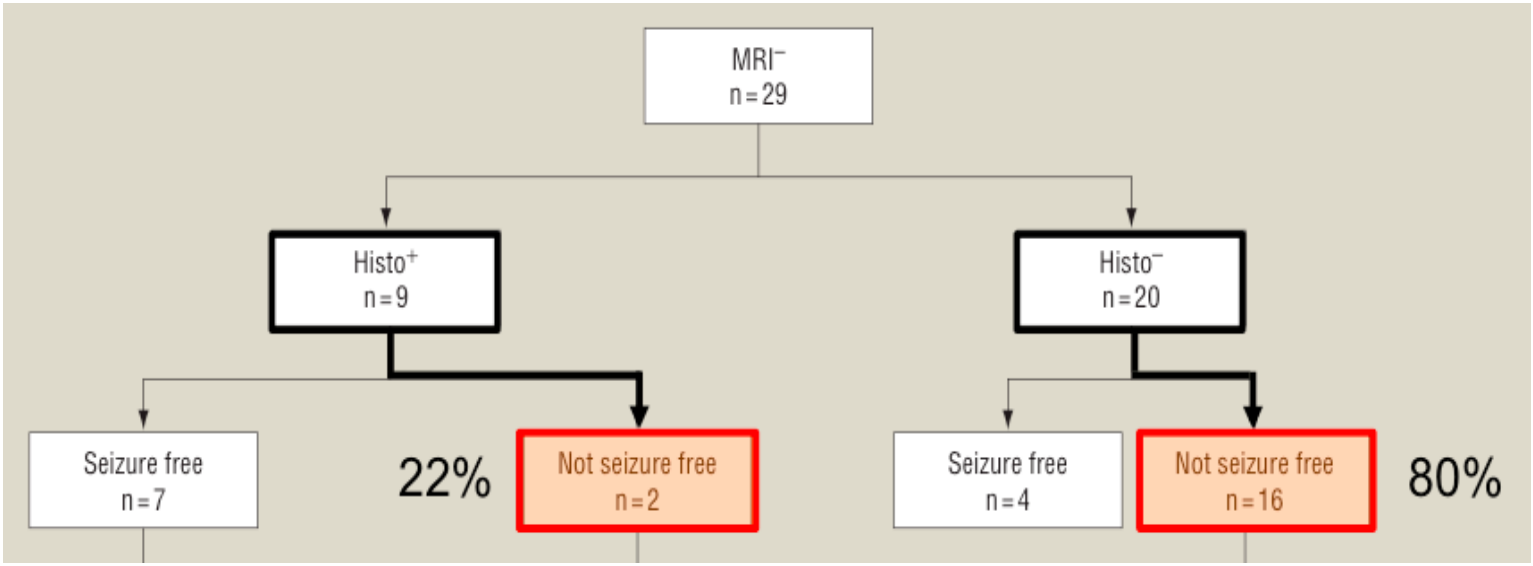

Bien et al. 2009

DECISIONAL TREE IN NLE

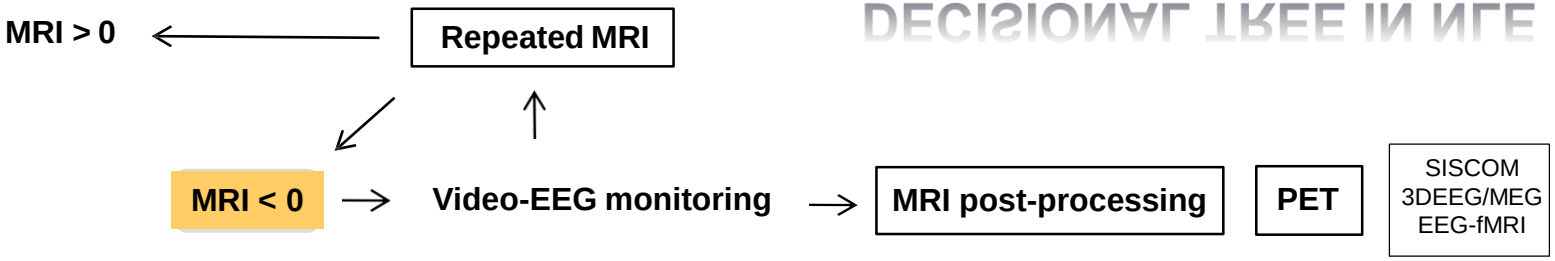

Good outcome when

1) Concordance of

Bien et al. 2009

semiology
interictal EEG
postproc. MRI

2) Concordance of 2 or more modalities

Lee et al. 2005

interictal EEG
ictal EEG
ictal SPECT
interictal PET

Poor outcome when discordance of

Bien et al. 2009

semiology
interictal EEG
postproc. MRI
SISCOM

DECISIONAL TREE IN NLE

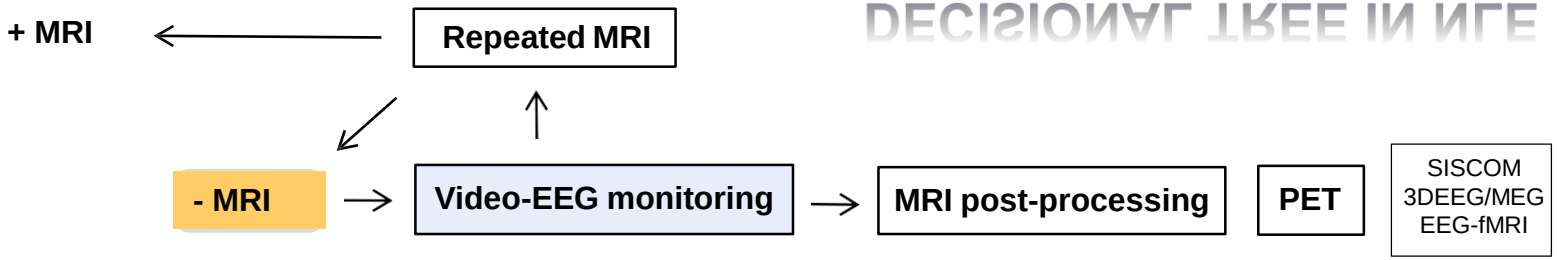

Usefulness of focal rhythmic discharges on scalp EEG of patients with focal cortical dysplasia and intractable epilepsy [1]

Antonio Gambardella [a,2], André Palmini [b], Frederick Andermann [a,*], François Dubeau [a], Jaderson C. Da Costa [b], L. Felipe Quesney [a], Eva Andermann [a], André Olivier [a]

Table 2
Comparison of the spatial distribution of interictal epileptiform abnormalities on scalp EEGs with the location of the structural lesion

	Rhythmic epileptiform discharges (REDs)			Interictal spiking		
	Focal/regional	Multiregional	Absent	Focal/regional	Multiregional	Absent
FCDLs [a]						
Focal/lobar	7	0	9	3	12	1
Multilobar	3	5	10	7	11	0
Non-FCDLs [b]						
Focal/lobar	0	0	36	10	7	19
Multilobar	0	0	4	0	4	0

FCDLs = focal cortical dysplastic lesions.
[a] Patients with cortical dysplasia (n = 34).
[b] Patients with other structural cortical lesions (n = 40).

Electroenceph clin Neurophysiol 1996; 98: 243-249

Perisylvian-Temporal Lobe Epilepsy

SEEG investigations may be needed in patients in whom the epileptogenic area, though probably involving the temporal lobe, is suspected to extend also to extratemporal areas. In these cases, the main implantation patterns point to disclose a preferential spread of the discharge to:

- Insulo-opercular complex
- Temporo-parieto-occipital junction
- Anterior frontal cortex

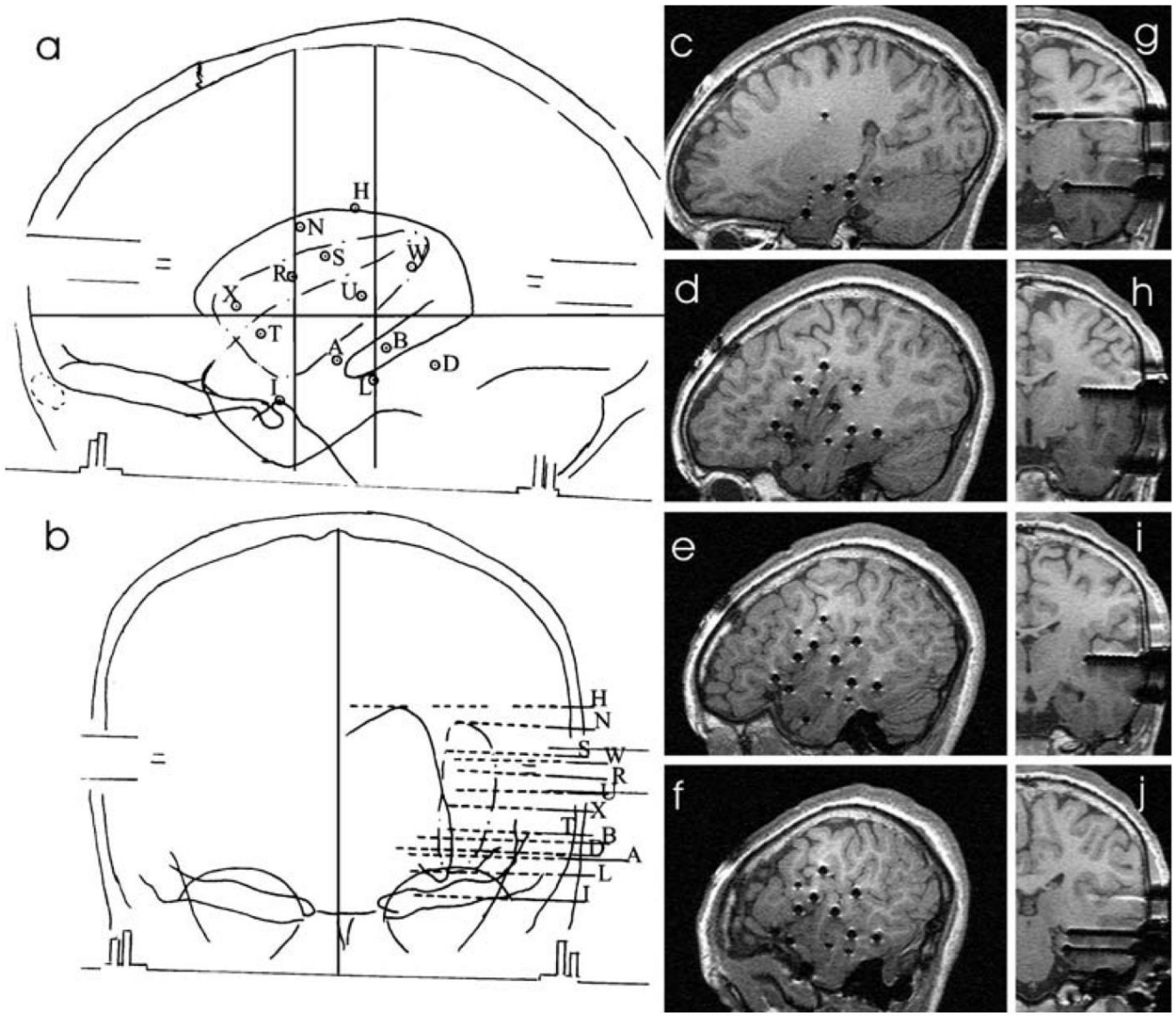

Fig. 2 Lateral (**a**) and antero-posterior (**b**) views of the stereotactic sketch, according to the bicommissural reference system, of a left temporal, perisylvian, and insular exploration. Electrodes are indicated either with *circled dots* or *dashed lines* labeled by *uppercase letters*. **c**–**j** T1-weighted 3-D postimplantation MRI. The electrode arrangement is shown in four sagittal and four coronal slices. Note (**h** and **i**) the two electrodes "S" and "U" sampling the insular cortex with their internal contacts. The SEEG exploration was indicated to evaluate a possible spread of a temporal discharge to the insular and opercular regions, as suggested by some clinical features of the patient's seizures

SEEG in Mesial Temporal Lobe Epilepsy Network

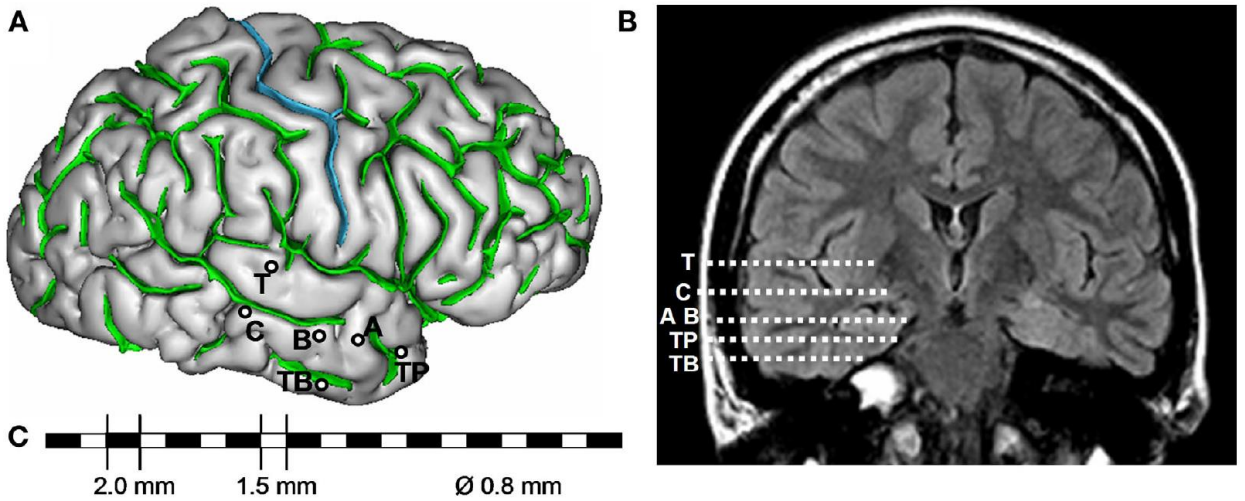

FIGURE 2 | Example of SEEG exploration in patient with mesial temporal lobe epilepsy. (A) Intracerebral implantation scheme. Electrodes are identified by one or two capital letters: A, B and C (medial contacts: amygdala, anterior part of hippocampus, posterior part of hippocampus; lateral contacts: middle temporal gyrus from anterior to posterior part), T (medial contacts, insula; lateral contacts, superior temporal gyrus), TB (medial contacts, entorhinal cortex; lateral contacts, temporo-basal cortex), TP (temporal pole). **(B)** Electrode trajectories reported on MRI data (coronal view). **(C)** Each intracerebral electrode is composed of 10–15 cylindrical contacts (length: 2 mm, diameter: 0.8 mm, 1.5 mm apart).

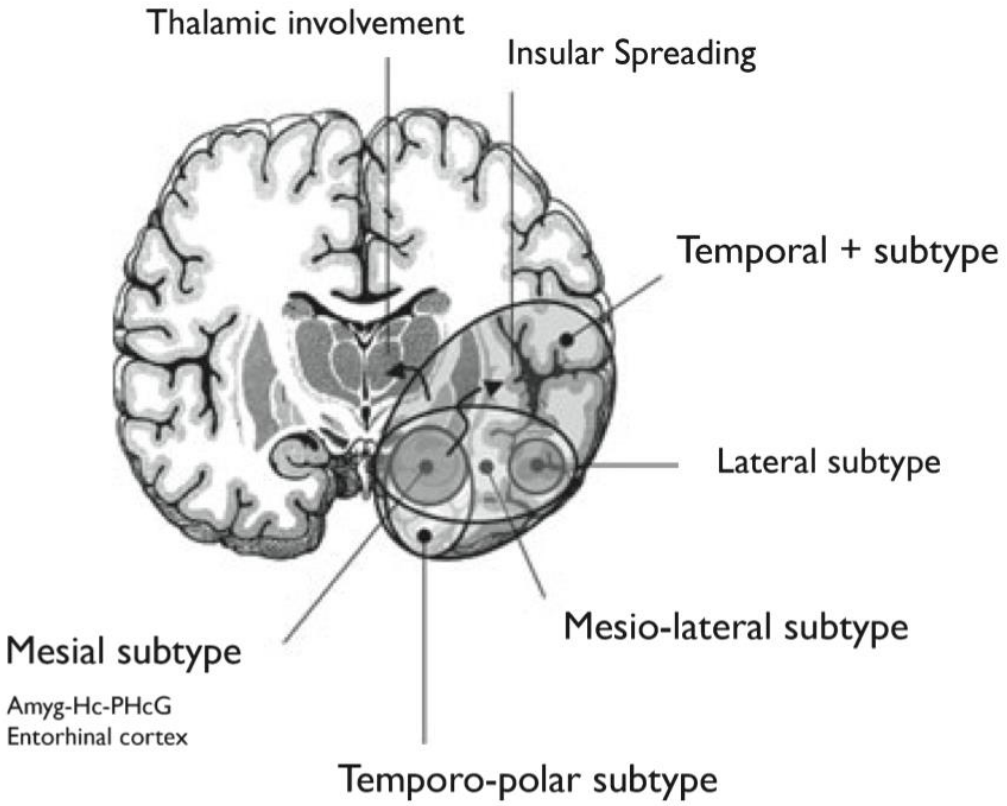

Figure 1.

The spectrum of temporal lobe epilepsy associated with hippocampal sclerosis. There might be a continuum from a focal network centered over mesiotemporal lobe structures to a widely extended network that goes beyond the limit of the temporal lobe. Amyg, amygdala; Hc, hippocampus; PHcG, parahippocampal gyrus; Temporal+, Temporal "plus."

Insular Epilepsy

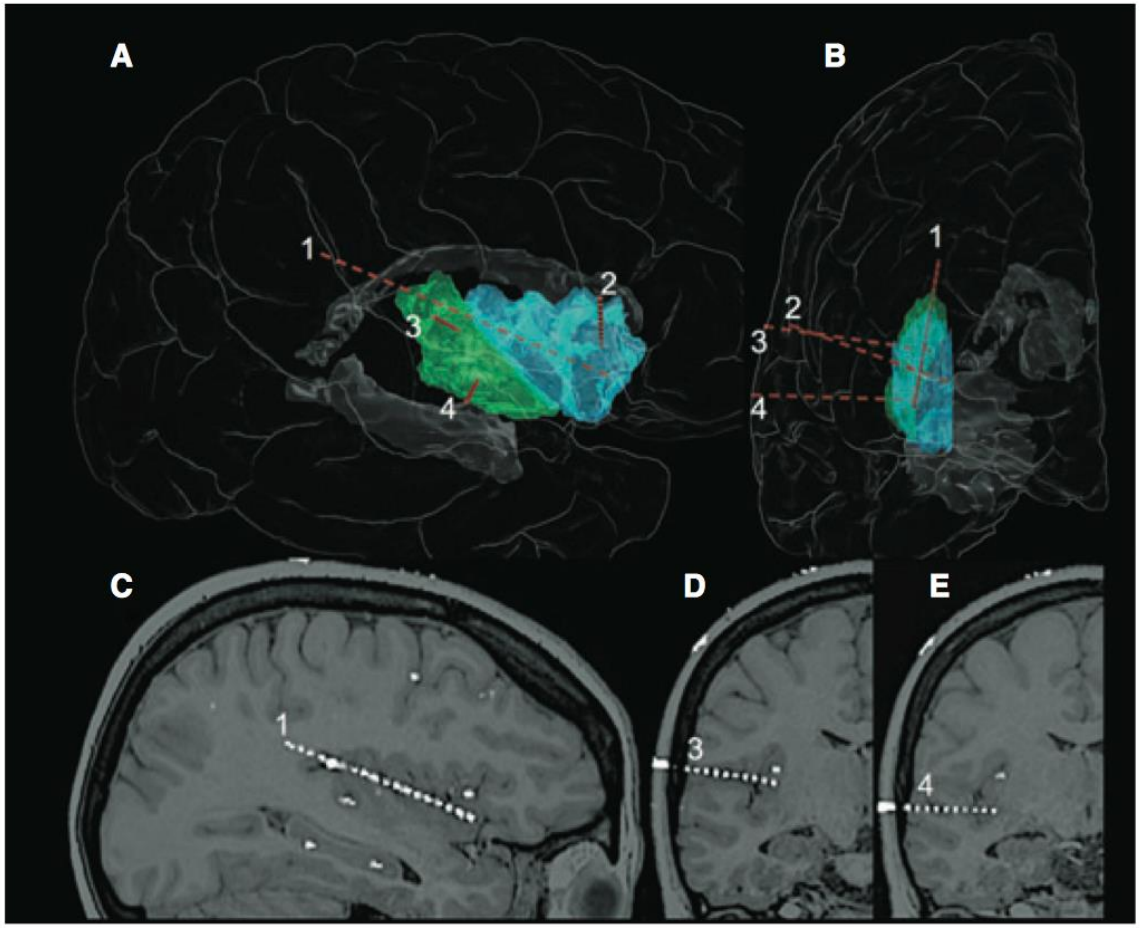

Figure 3.

(**A**–**B**) Lateral and frontal 3D views of the insular coverage by intracerebral electrodes in Patient 6. In green the long insular gyri and in light blue the short insular gyri. Dotted red lines correspond to the four electrodes (dots represent recording contacts) sampling the insula through a parasagittal transinsular approach (electrode 1) and transopercular-transsylvian trajectories (electrodes 2, 3, and 4). Lateral ventricle and hippocampus are shadowed in black. (**C**–**E**) Reformatted slices of T_1-weighted 3D MRI blended to a co-registered CT scan obtained after electrode implantation in the same patient. The exact intracerebral position of single recording contacts of electrodes 1, 3, and 4 is easily identifiable. Postprocessing of neuroimages by: FMRIB Software Library (FSL, http://www.fmrib.ox.ac.uk/fsl/); Freesurfer (http://surfer.nmr.mgh.harvard.edu/); 3D Slicer (http://www.slicer.org/). Artistic rendering by Cinema 4D (Maxon Computer GmbH, Friedrichsdorf, Germany).

SEEG-Guided Radiofrequency Thermo-coagualation and Laser Ablation

FULL-LENGTH ORIGINAL RESEARCH

Better object recognition and naming outcome with MRI-guided stereotactic laser amygdalohippocampotomy for temporal lobe epilepsy

*†‡Daniel L. Drane, *†David W. Loring, §Natalie L. Voets, *Michele Price, ¶Jeffrey G. Ojemann, *#Jon T. Willie, **Amit M. Saindane, ‡Vaishali Phatak, *Mirjana Ivanisevic, ††Scott Millis, *†Sandra L. Helmers, ‡¶John W. Miller, *†Kimford J. Meador, and *#Robert E. Gross

Epilepsia, 56(1):101–113, 2015
doi: 10.1111/epi.12860

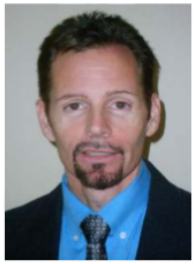

Dr. Daniel L. Drane is Assistant Professor of Neurology and Pediatrics at Emory University School of Medicine.

Summary

Objectives: Patients with temporal lobe epilepsy (TLE) experience significant deficits in category-related object recognition and naming following standard surgical approaches. These deficits may result from a decoupling of core processing modules (e.g., language, visual processing, and semantic memory), due to "collateral damage" to temporal regions outside the hippocampus following open surgical approaches. We predicted that stereotactic laser amygdalohippocampotomy (SLAH) would minimize such deficits because it preserves white matter pathways and neocortical regions that are critical for these cognitive processes.

Methods: Tests of naming and recognition of common nouns (Boston Naming Test) and famous persons were compared with nonparametric analyses using exact tests between a group of 19 patients with medically intractable mesial TLE undergoing SLAH (10 dominant, 9 nondominant), and a comparable series of TLE patients undergoing standard surgical approaches ($n = 39$) using a prospective, nonrandomized, nonblinded, parallel-group design.

Results: Performance declines were significantly greater for the patients with dominant TLE who were undergoing open resection versus SLAH for naming famous faces and common nouns ($F = 24.3$, $p < 0.0001$, $\eta^2 = 0.57$, and $F = 11.2$, $p < 0.001$, $\eta^2 = 0.39$, respectively), and for the patients with nondominant TLE undergoing open resection versus SLAH for recognizing famous faces ($F = 3.9$, $p < 0.02$, $\eta^2 = 0.19$). When examined on an individual subject basis, no SLAH patients experienced any performance declines on these measures. In contrast, 32 of the 39 patients undergoing standard surgical approaches declined on one or more measures for both object types ($p < 0.001$, Fisher's exact test). Twenty-one of 22 left (dominant) TLE patients declined on one or both naming tasks after open resection, while 11 of 17 right (nondominant) TLE patients declined on face recognition.

Significance: Preliminary results suggest (1) naming and recognition functions can be spared in TLE patients undergoing SLAH, and (2) the hippocampus does not appear to be an essential component of neural networks underlying name retrieval or recognition of common objects or famous faces.

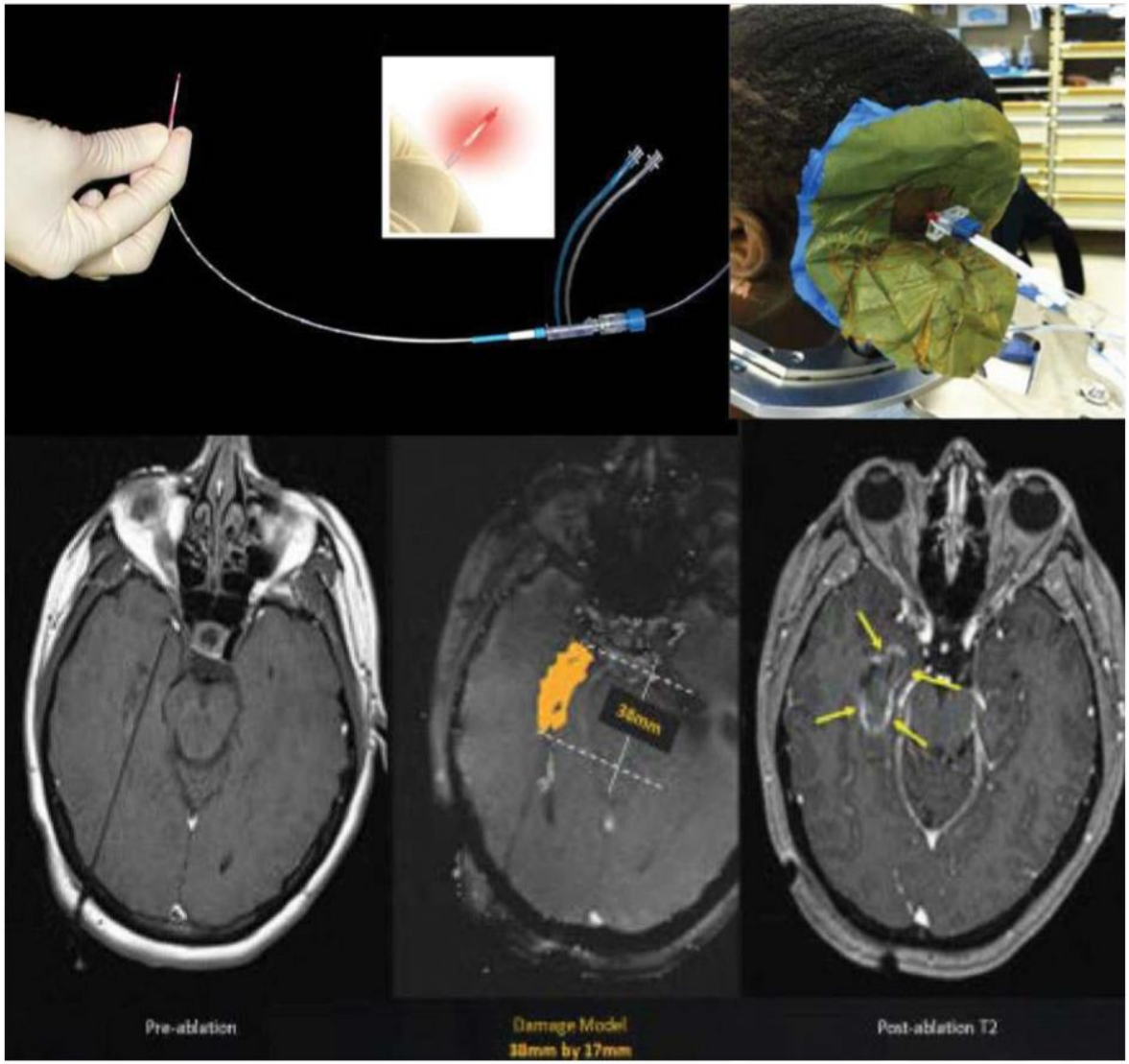

Figure 1.
Depiction of the optical fiber, the ablation process, and pre- and postablation MRI images in an axial plane.
Epilepsia © ILAE

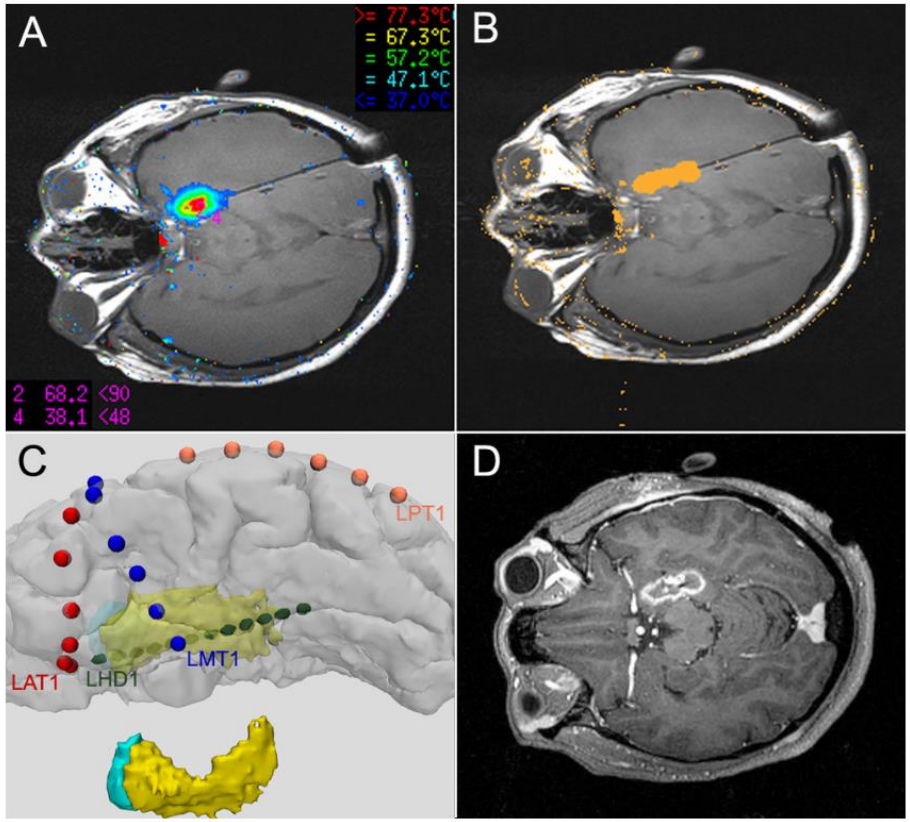

Figure 1 Ablation of mesial temporal lobe using stereotactic MRI-guided LITT: temperature measurement with MRI thermometry during the ablation with optimal temperature between 60°C and 80°C (A). Depiction of irreversible lesion zone at the completion of ablation in the axial (B) and postablation axial T1 image with gadolinium contrast enhancement of lesion zone (D). A basolateral view of coregistration of intracranial depth and subdural electrodes with preimplantation brain MRI and postimplantation CT images (C). LAT1, the first contact on the left anterior temporal 1×6 subdural electrode strip; LHD1, the first contact of the left 1×12 hippocampal depth electrode; LITT, laser interstitial thermal therapy; LMT1, the first contact on the left middle temporal 1×6 subdural electrode strip; LPT1, the first contact on the left posterior temporal 1×6 subdural electrode strip.

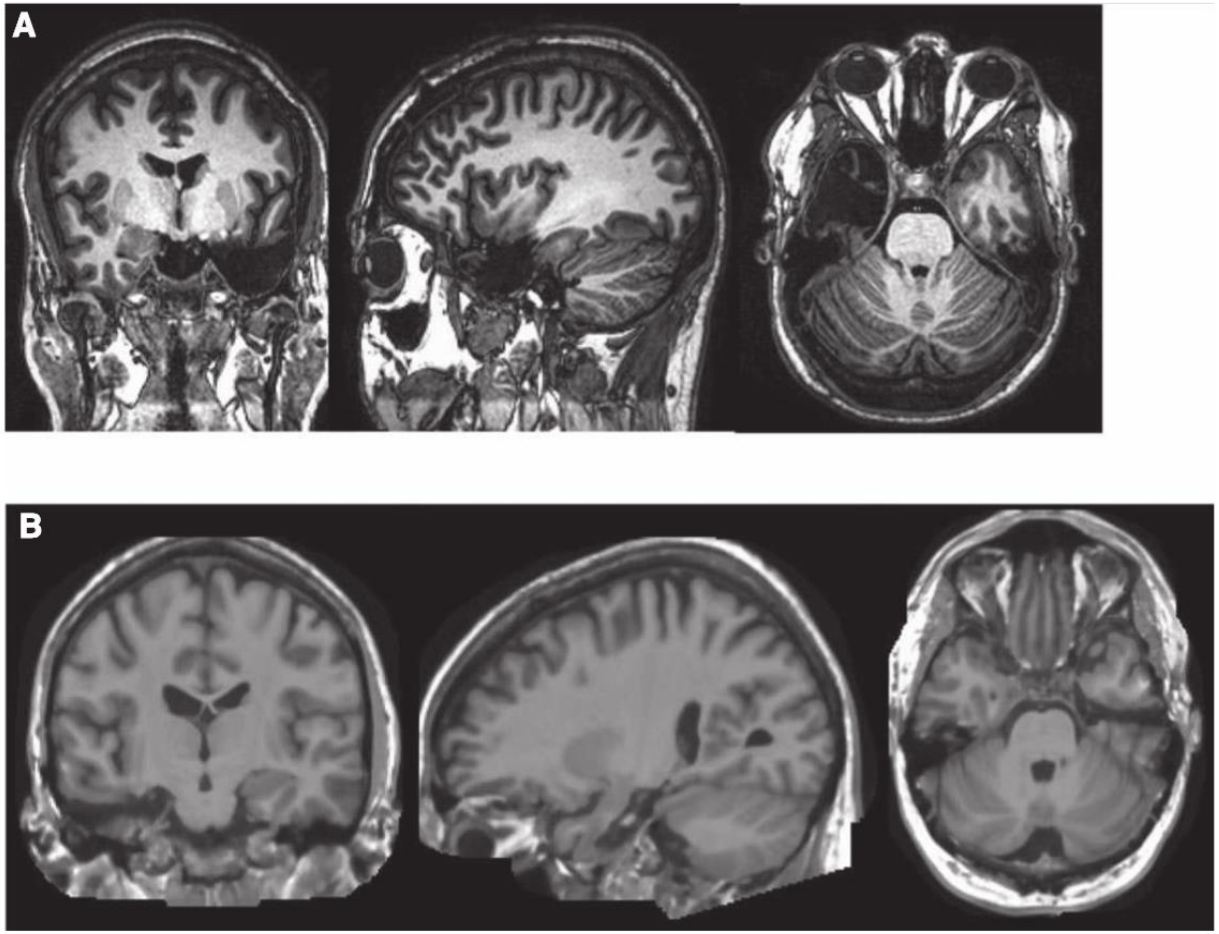

Figure 2.
MRI scans demonstrating surgical resections: (**A**) Tailored anterior temporal lobectomy (ATL) performed at the University of Washington—representative coronal, sagittal, and axial slices in a patient undergoing left ATL; (**B**) selective amygdalohippocampectomy performed at Emory University—representative coronal, sagittal, and axial slices in a patient undergoing a right temporal lobe resection.

Epilepsy Research 142 (2018) 131–134

Contents lists available at ScienceDirect

Epilepsy Research

journal homepage: www.elsevier.com/locate/epilepsyres

MR-guided laser ablation for the treatment of hypothalamic hamartomas

Daniel J. Curry[a,b,*], Jeffery Raskin[a,b], Irfan Ali[c,d], Angus A. Wilfong[e]

[a] Section of Pediatric Neurosurgery, Texas Children's Hospital, Houston, TX, United States
[b] Department of Neurosurgery, Baylor College of Medicine, Houston, TX, United States
[c] Section of Neurology, Texas Children's Hospital, Houston, TX, United States
[d] Section of Pediatric Neurology and Developmental Neuroscience, Baylor College of Medicine, United States
[e] Division of Pediatric Neurology, Phoenix Children's Hospital, Barrow Neurological Institute, Phoenix, AZ, United States

ARTICLE INFO

Keywords:
Hypothalamic hamartoma
Stereotactic laser ablation
MRgLITT
Gelastic epilepsy

ABSTRACT

Hypothalamic hamartoma is an archetypal example of subcortical epilepsy that can be associated with intractable gelastic epilepsy, secondary epilepsy, and epileptic encephalopathy. The history of its surgical treatment is fraught with mislocalization of the seizure focus, modest efficacy and a high complication rate. Many minimally invasive techniques have been described to mitigate this high complication profile of which MR-guided laser ablation is one. The technology combines instant effect of thermal coagulation with stereotactic precision and guidance with real time MR thermography. This article presents a series of 71 hypothalamic hamartoma patients operated with laser ablation. Ninety-three percent (93%) were free of gelastic seizures at one year with 23% of the patients requiring more than one ablation. One patient experienced a significant memory deficit and one patient experienced worsening diabetes insipidus. Stereotactic laser ablation appears to be a safe and effective surgical option in the treatment of hypothalamic hamartoma.

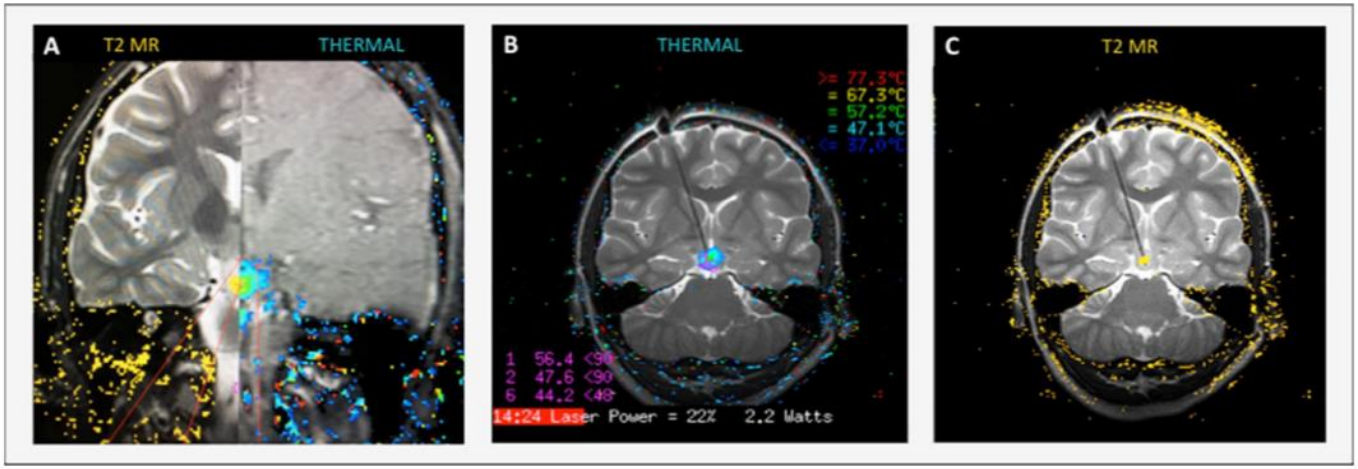

Fig. 1. Real-Time LITT of Hypothalamic Hamartomas.
(A) Split-screen, (B) thermal, and (C) T2 background images of the stereotactic laser ablation of a HH showing the real-time MR thermogram (right of spilt on A; B) overlayed onto the background images exhibiting the irreversible damage map (left of spilt on A; C).

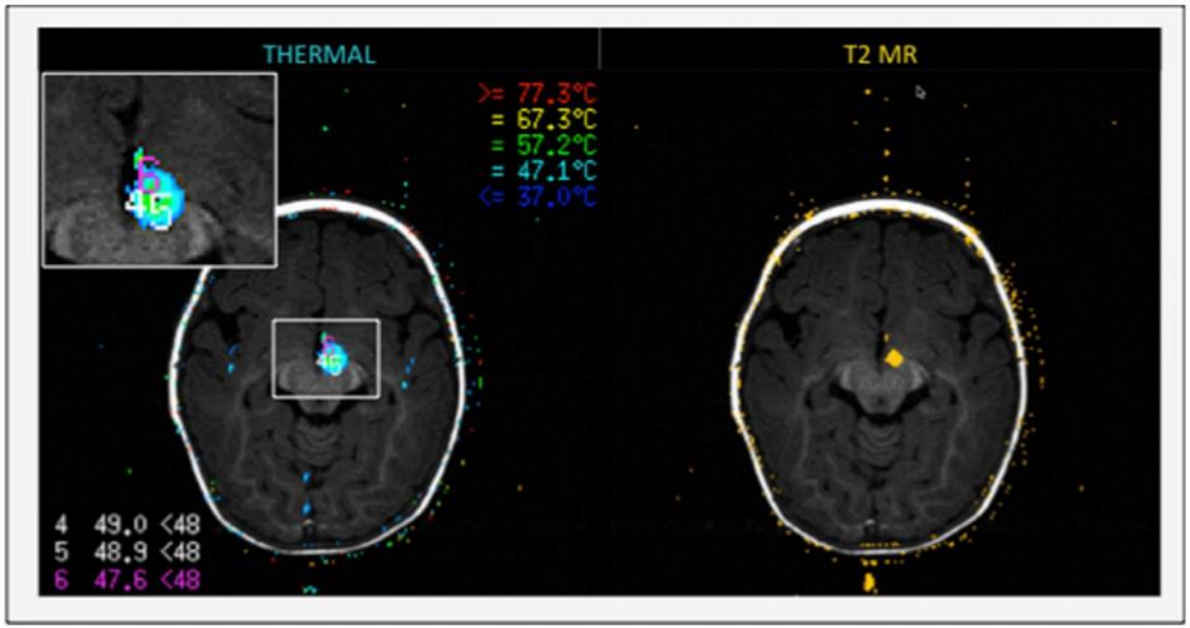

Fig. 2. Use of Low-Limit Thresholds.
Low-limit thresholds, set at 48 °C, are placed on the [4] mammillothalamic tract, [5] cerebral peduncle, and [6] fornix, on the MR thermogram (left; insert shown), and provide automatic laser shut-off when these structures reach the set threshold. These structures were not included in the irreversible damage map (right).

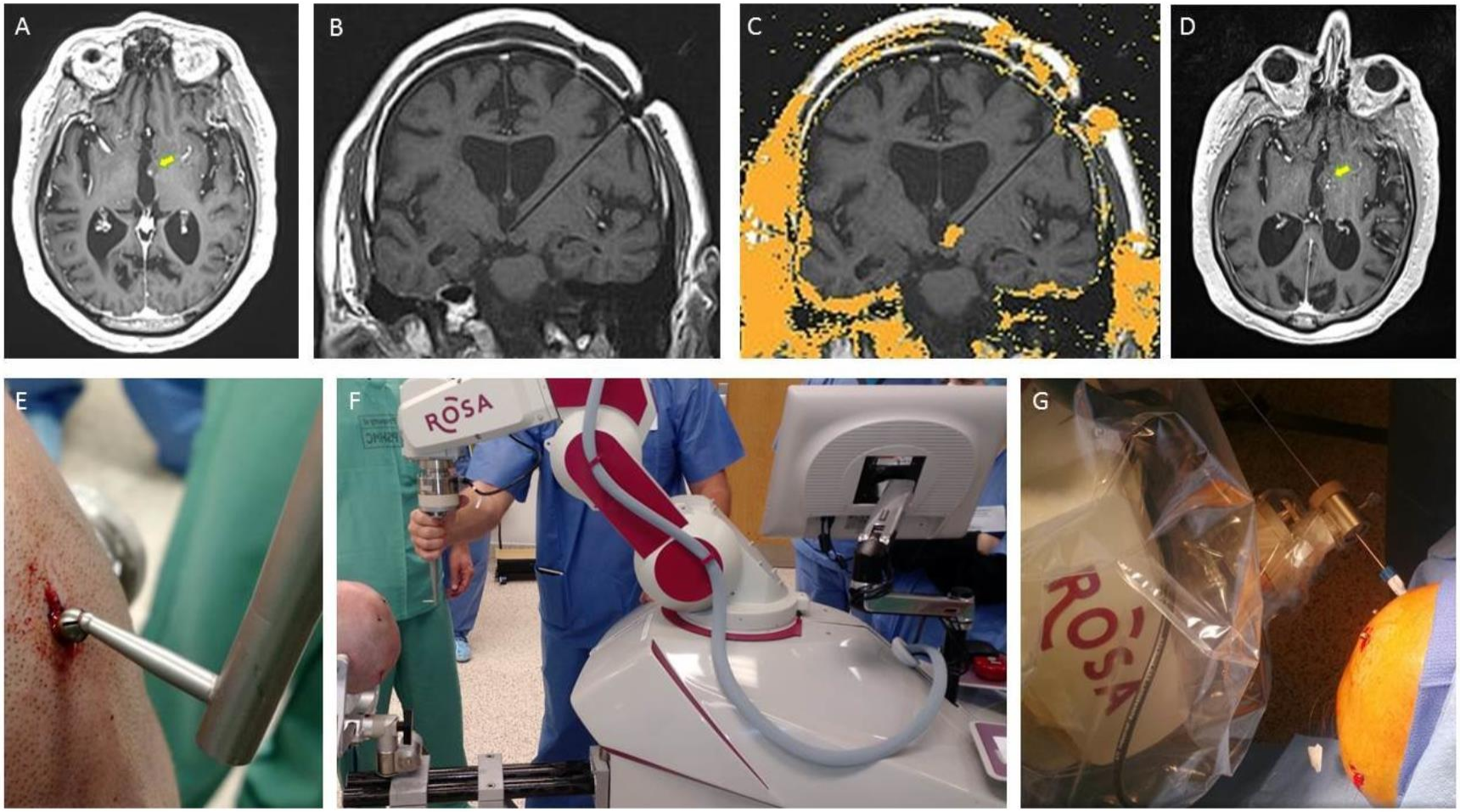
A
B
C
D
E
F
ROSA
G
ROSA

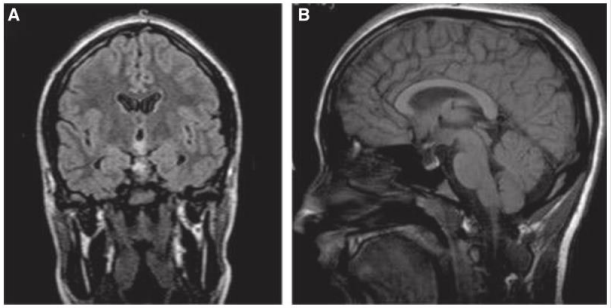

Figure 1.
MRI of the hamartoma. (**A**) Sagittal T_1 image shows its connection at the third ventricle. (**B**) Coronal FLAIR image shows that the hamartoma has more hyperintense signal, and shows greater attachment to one side.
Epilepsia © ILAE

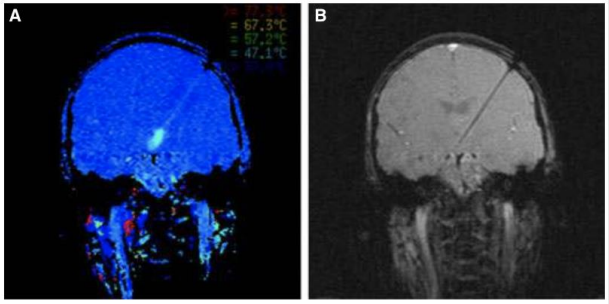

Figure 2.
(**A**) The entire length of laser catheter and target is captured with an oblique coronal image. (**B**) Then, a test dose of 3 W for 30 s is used to confirm location of fiber.
Epilepsia © ILAE

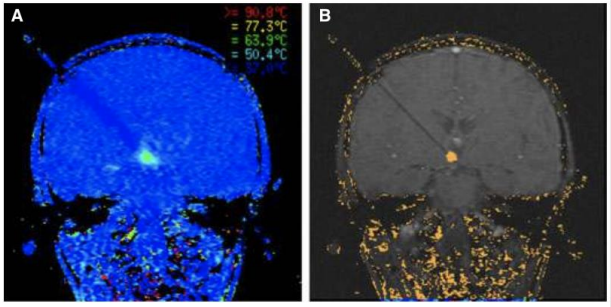

Figure 3.
(**A**) Real-time temperature monitoring is shown with a laser exposure of 6 W for 40 s. (**B**) Arrhenius-based damage estimation in orange enables the surgeon to evaluate coverage of targeted hamartoma.
Epilepsia © ILAE

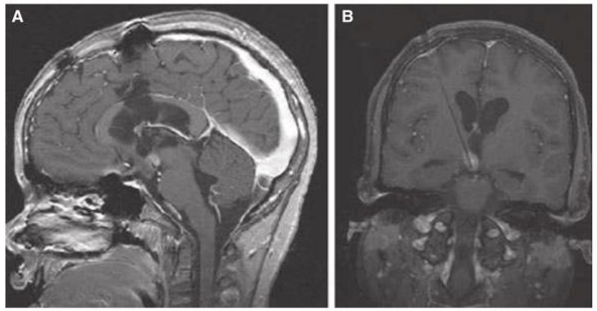

Figure 4.
Acute confirmation of ablation coverage is done with postcontrast T_1 images, as seen in the coronal (**A**) and sagittal (**B**) images.
Epilepsia © ILAE

Stereotactic and Functional Neurosurgery

Case Report

Stereotact Funct Neurosurg 2014;92:397–404
DOI: 10.1159/000366001

Received: January 22, 2014
Accepted after revision: July 14, 2014
Published online: October 29, 2014

Laser Ablation as Treatment Strategy for Medically Refractory Dominant Insular Epilepsy: Therapeutic and Functional Considerations

Ammar H. Hawasli[a] S. Kathleen Bandt[a] R. Edward Hogan[b] Nicole Werner[b]
Eric C. Leuthardt[a, c, d]

Departments of [a]Neurosurgery, [b]Neurology and [c]Biomedical Engineering, and [d]Center for Innovation in Neuroscience and Technology, Washington University School of Medicine, St. Louis, Mo., USA

Abstract

Since its introduction to neurosurgery in 2008, laser ablative techniques have been largely confined to the management of unresectable tumors. Application of this technology for the management of focal epilepsy in the adult population has not been fully explored. Given that nearly 1,000,000 Americans live with medically refractory epilepsy and current surgical techniques only address a fraction of epileptic pathologies, additional therapeutic options are needed. We report the successful treatment of dominant insular epilepsy in a 53-year-old male with minimally invasive laser ablation complicated by mild verbal and memory deficits. We also report neuropsychological test data on this patient before surgery and at 8 months after the ablation procedure. This account represents the first reported successful patient outcome of laser ablation as an effective treatment option for medically refractory post-stroke epilepsy in an adult.

50% seizure freedom
No permanent neurologic deficits

JNS PEDIATRICS

CLINICAL ARTICLE

J Neurosurg Pediatr 20:575–582, 2017

Magnetic resonance imaging–guided laser interstitial thermal therapy as treatment for intractable insular epilepsy in children

M. Scott Perry, MD,[1] David J. Donahue, MD,[1] Saleem I. Malik, MD,[1] Cynthia G. Keator, MD,[1] Angel Hernandez, MD,[1] Rohit K. Reddy, MD,[2] Freedom F. Perkins Jr., MD,[2] Mark R. Lee, MD, PhD,[2,4] and Dave F. Clarke, MD[2,3]

[1]Comprehensive Epilepsy Program, Jane and John Justin Neuroscience Center, Cook Children's Medical Center, Fort Worth; [2]Comprehensive Epilepsy Program, Dell Children's Hospital, Austin; and Departments of [3]Pediatrics and [4]Surgery and Perioperative Services, Dell Medical School, University of Texas, Austin, Texas

OBJECTIVE Seizure onset within the insula is increasingly recognized as a cause of intractable epilepsy. Surgery within the insula is difficult, with considerable risks, given the rich vascular supply and location near critical cortex. MRI-guided laser interstitial thermal therapy (LiTT) provides an attractive treatment option for insular epilepsy, allowing direct ablation of abnormal tissue while sparing nearby normal cortex. Herein, the authors describe their experience using this technique in a large cohort of children undergoing treatment of intractable localization-related epilepsy of insular onset.

METHODS The combined epilepsy surgery database of Cook Children's Medical Center and Dell Children's Hospital was queried for all cases of insular onset epilepsy treated with LiTT. Patients without at least 6 months of follow-up data and cases preoperatively designated as palliative were excluded. Patient demographics, presurgical evaluation, surgical plan, and outcome were collected from patient charts and described.

RESULTS Twenty patients (mean age 12.8 years, range 6.1–18.6 years) underwent a total of 24 LiTT procedures; 70% of these patients had normal findings on MRI. Patients underwent a mean follow-up of 20.4 months after their last surgery (range 7–39 months), with 10 (50%) in Engel Class I, 1 (5%) in Engel Class II, 5 (25%) in Engel Class III, and 4 (20%) in Engel Class IV at last follow-up. Patients were discharged within 24 hours of the procedure in 15 (63%) cases, in 48 hours in 6 (24%) cases, and in more than 48 hours in the remaining cases. Adverse functional effects were experienced following 7 (29%) of the procedures: mild hemiparesis after 6 procedures (all patients experienced complete resolution or had minimal residual dysfunction by 6 months), and expressive language dysfunction after 1 procedure (resolved by 3 months).

CONCLUSIONS To their knowledge, the authors present the largest cohort of pediatric patients undergoing insular surgery for treatment of intractable epilepsy. The patient outcomes suggest that LiTT can successfully treat intractable seizures originating within the insula and offers an attractive alternative to open resection. This is the first description of LiTT applied to insular epilepsy and represents one of only a few series describing the use of LiTT in children. The results indicate that seizure reduction after LiTT compares favorably to that after conventional open surgical techniques.

https://thejns.org/doi/abs/10.3171/2017.6.PEDS17158

KEY WORDS insular epilepsy; laser interstitial thermal therapy; epilepsy surgery

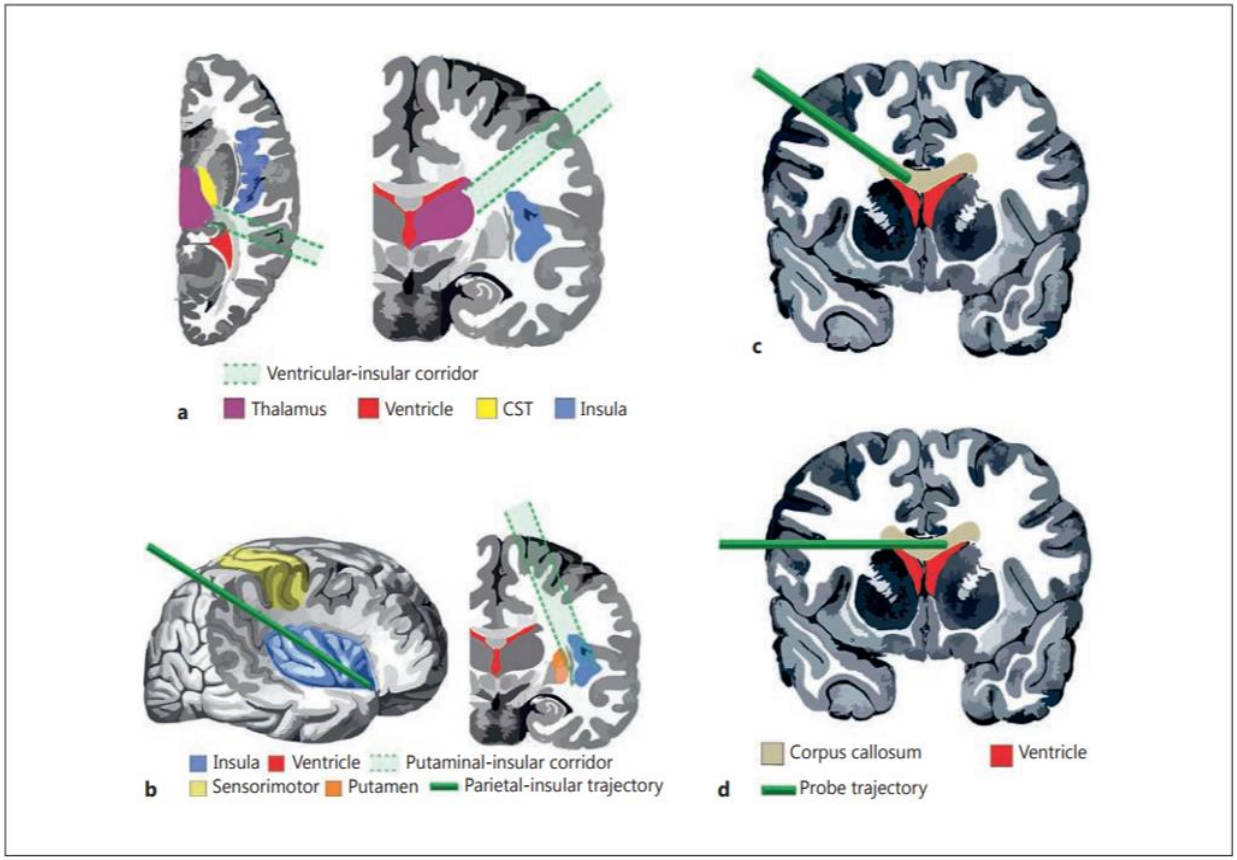

Fig. 3. a Thalamic lesion, showing a common interstitial laser ablation (ILA) trajectory to the thalamus. The approach involved a mid- to high-parietal cortical entry posterior to the sensory cortex. There tended to be a narrow (1–1.5 cm) region between the anterior portion of trigone of the lateral ventricle and the high posterior aspect of the insula. This entry zone is called the ventricular-insular corridor, which afforded the best access to the thalamus while avoiding the corticospinal tract Left, axial view; right, coronal view. **b** Insular lesion, showing a common ILA trajectory to the insula. The insula has an oval-discoid (i.e., a "flattened football") shape that is angled downward from posterior to anterior in the sagittal plane and leans medial to lateral in the coronal plane. To best access the entirety of the insula (if required), a trajectory with a high medial parietal entry, posterior to the sensory cortex, in the plane between the putamen medially and the insula laterally was used. This corridor we putatively term the putaminal-insular corridor. Left, side view; right, coronal view. **c**, **d** Common ILA trajectories to the corpus callosum. **c** Unilateral corpus callosum lesion. **d** Bilateral corpus callosum lesion. There were several considerations, depending on the location of the lesion in the corpus callosum and whether the lesion was unilateral or bilateral. If the lesion was more unilateral in nature a higher frontal or parietal trajectory was taken (**c**). If more bilateral in distribution, a lower trajectory was taken to more fully cross the corpus callosum (**d**).

Stereotact Funct Neurosurg 2017;95:417–428
DOI: 10.1159/000485387

Epilepsia, 52(9):e101–e105, 2011
doi: 10.1111/j.1528-1167.2011.03116.x

BRIEF COMMUNICATION

Radiofrequency lesioning for epileptogenic periventricular nodular heterotopia: A rational approach

*[1]Friedhelm C. Schmitt, †[1]Juergen Voges, †Lars Buentjen, ‡Friedrich Woermann, ‡Heinz W. Pannek, §Martin Skalej, *Hans-Jochen Heinze, and ‡Alois Ebner

Departments of *Neurology and †Stereotactic Neurosurgery, University of Magdeburg, Magdeburg, Germany; ‡Department of Presurgical Evaluation, Bethel Epilepsy Centre, Bielefeld, Germany; and §Institute for Neuroradiology, University of Magdeburg, Magdeburg, Germany

Summary

Periventricular nodular heterotopias (PNHs) are frequently associated with pharmacoresistant epilepsy. They are considered part of a dysfunctional network, connected to the overlying cortex. Therefore, removal of the PNHs and additional cortectomy or lobectomy seem to be essential for significant and long-lasting seizure reduction. These procedures, however, can have considerable limitations, especially in patients with functional eloquent cortex adjacent to the PNH. Alternatively, stereotactic neurosurgery can reduce the surgical trauma. Presented is a 56-year-old man who became seizure-free after stereotactically guided radiofrequency lesioning of a solitary PNH.

KEY WORDS: Epileptogenity, Epilepsy surgery, Network, Stereotaxy, Thermoablation, Thermocoagulation.

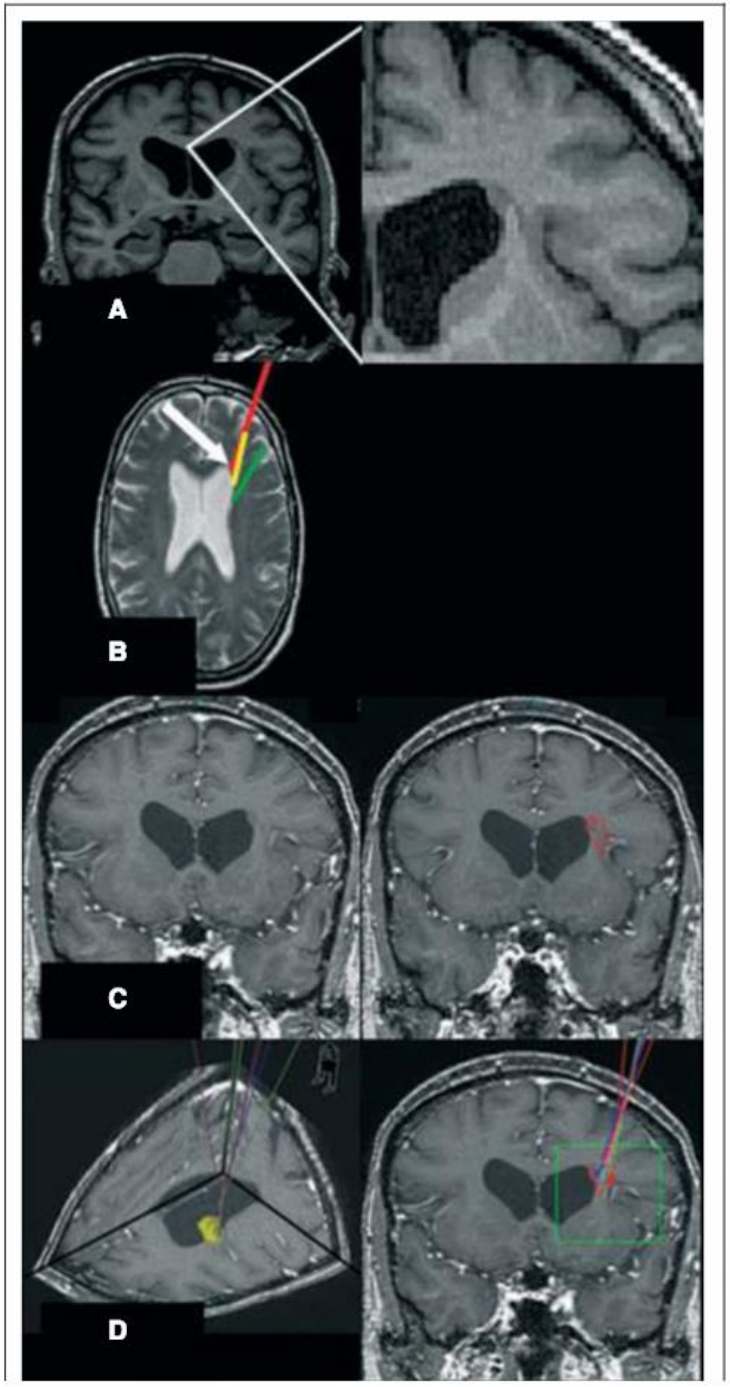

Figure 1.

(**A**) T_1-weighted MRI illustrating the preoperative status with the PNH near the ventricular wall and its connection to the insular cortex. (**B**) T_1-weighted MRI illustrating individual electrode position in relation to the PNH (white arrow). Locations of electrode A (green), electrode B (yellow), and electrode C (red). Note the proximity of electrode B and C to the PNH. (**C**) Definition of the tissue volume for RFL (red) on coronal T_1-weighted MRI coregistered in the stereotactic coordinate system. (**D**) T_1-weighted MRI illustrating surgical approaches for stereotactically guided RFL at different target points in projection onto the volume of interest (yellow) containing the PNH. (**E**) T_1-weighted MRI illustrating the result 6 months after RFL. A small area of the heterotopia has deliberately not been coagulated in order to not disrupt the ventricular wall by the RFL procedure.

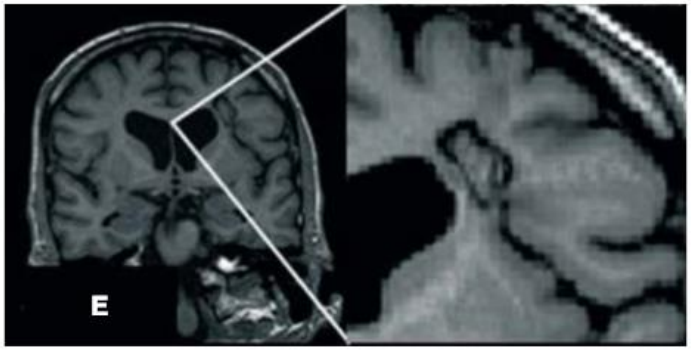

Seizures Outcome After Stereoelectroencephalography-Guided Thermocoagulations in Malformations of Cortical Development Poorly Accessible to Surgical Resection

Hélène Catenoix, MD*‡
François Mauguière, MD, PhD*‡
Alexandra Montavont, MD*‡
Philippe Ryvlin, MD, PhD*‡
Marc Guénot, MD, PhD‡§
Jean Isnard, MD, PhD*‡

*Service de Neurologie Fonctionnelle et d'Epileptologie, Hôpital Neurologique Pierre Wertheimer, Hospices Civils de Lyon, Bron, France; ‡Centre de Recherche en Neurosciences, INSERM U1028, CNRS 5292, UCBL-1, Lyon, France; §Service de Neurochirurgie Fonctionnelle, Hôpital Neurologique Pierre Wertheimer, Hospices Civils de Lyon, Bron, France

Correspondence:
Hélène Catenoix, MD,
Service de Neurologie Fonctionnelle et d'Epileptologie,
Hôpital Neurologique Pierre Wertheimer,
59 Boulevard Pinel,
69677 Bron Cedex, France.
E-mail: helene.catenoix@chu-lyon.fr

Received, September 5, 2014.
Accepted, February 1, 2015.
Published Online, March 16, 2015.

BACKGROUND: Radiofrequency thermocoagulation (RFTC) guided by stereoelectroencephalography (SEEG) has proved to be a safe palliative method to reduce seizure frequency in patients with drug-resistant partial epilepsy. In malformation of cortical development (MCD), increasing the number of implanted electrodes over that needed for mapping of the epileptogenic zone could help to maximize RFTC efficiency.
OBJECTIVE: To evaluate the benefit of SEEG-guided RFTC in 14 patients suffering from drug-resistant epilepsy related to MCD located in functional cortical areas or in regions poorly accessible to surgery.
METHODS: Ten men and 4 women were treated by RFTC. Thermolesions were produced by applying a 50-V, 120-mA current for 10 to 30 seconds within the epileptogenic zone as identified by the SEEG investigation.
RESULTS: An average of 25.8 $\pm$ 17.5 thermolesions were made per procedure. The median follow-up after the procedure was 41.7 months. Sixty-four percent of the patients experienced a long-term decrease in seizure frequency of $>$50%, of whom 6 (43%) presented long-lasting freedom from seizure. When a focal low-voltage fast activity was present at seizure onset on SEEG recordings, 87.5% of patients were responders or seizure free. All of the patients in whom electric stimulation reproduced spontaneous seizures were responders.
CONCLUSION: Our results show the good benefit-risk ratio of the SEEG-guided procedure for patients suffering from MCD in whom surgery is risky. This study identifies 2 factors, focal low-voltage, high-frequency activity at seizure onset and lowered epileptogenic threshold in the coagulated area, that could be predictive of a favorable seizure outcome after RFTC.

KEY WORDS: Epilepsy, Epilepsy surgery, Malformation cortical of development, Radiofrequency thermocoagulations, SEEG

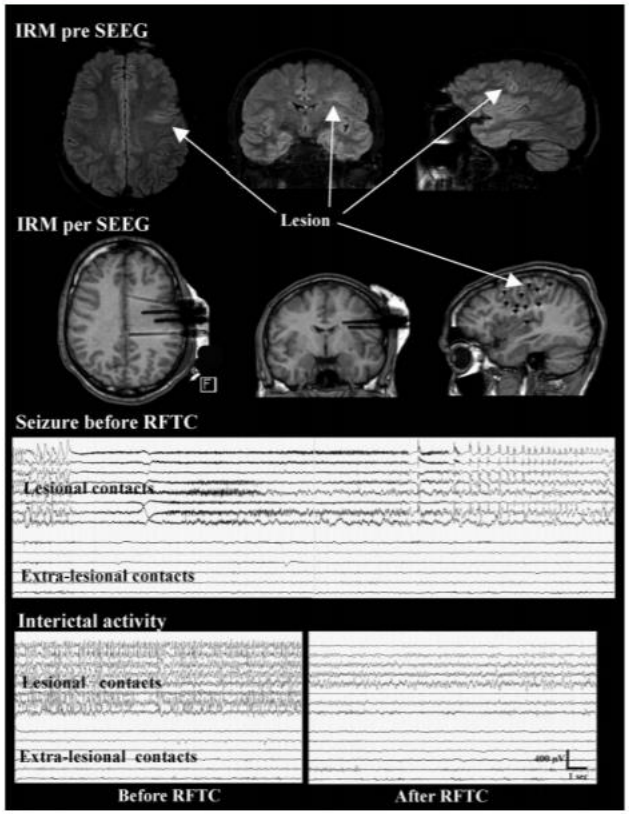

FIGURE 1. *Illustration in a seizure-free patient (patient 3). Magnetic resonance imaging (MRI) before stereoelectroencephalography (SEEG): axial, coronal, and sagittal fluid-attenuated inversion-recovery MRI slices showing a left central focal cortical dysplasia (arrows). MRI per SEEG: localization of depth electrodes on T1 MRI slices. Black dots correspond to the artifact created by the electrode leads. All depth electrodes are visible on the sagittal slice with lesional contacts (arrow). Seizure before radiofrequency thermocoagulation (RFTC): SEEG recording of a seizure at lesional and extralesional contacts. The low-voltage fast discharge at seizure onset is restricted to the malformation for 20 seconds. Interictal activity: SEEG recordings of interictal activity before and after RFTC. The continuous spike and polyspike interictal activity in the lesional contacts disappeared after RFTC was performed in the lesion.*

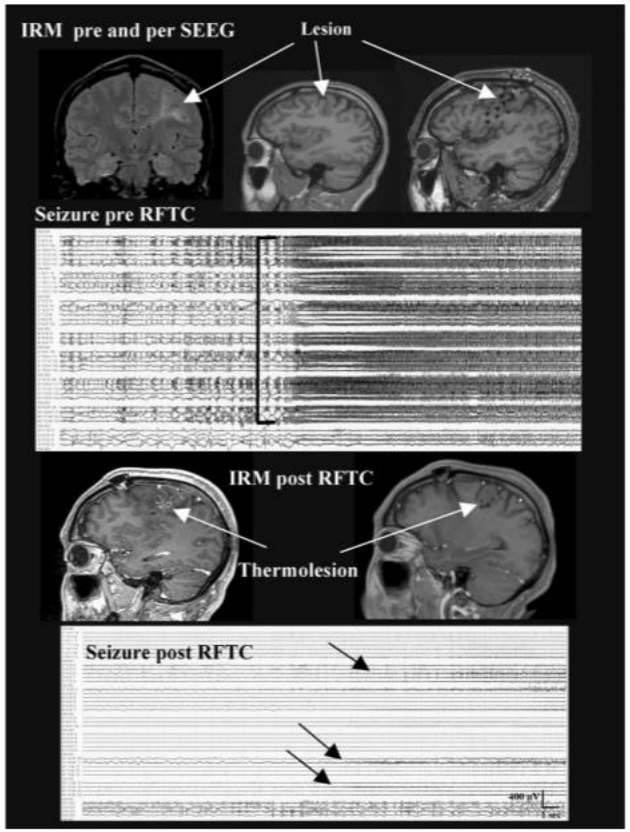

FIGURE 2. *Illustration in a responder patient (patient 5). Magnetic resonance imaging (MRI) before and per stereoelectroencephalography (SEEG): coronal fluid-attenuated inversion-recovery slice (left) and sagittal T1 MRI slice (middle) showing a left central focal cortical dysplasia (arrows). Localization of depth electrodes on T1 sagittal MRI slices (right) with lesional contacts (arrow). Black dots correspond to the artifact created by the electrode leads. Seizure before radiofrequency thermocoagulation (RFTC): SEEG recording of interictal and ictal activity at lesional contacts before RFTC. See the continuous spikes of interictal activity and the extended fast discharge at seizure onset (bracket). MRI after RFTC: thermolesion (arrow) on T1 sagittal MRI slices immediately after the coagulations with gadolinium enhancement (left), and 1 year later (right). Seizure after RFTC: SEEG recording of interictal and ictal activity after RFTC. The spiking interictal activity and the recruitment of the discharge at seizure onset were much decreased (arrows).*

Stereoelectroencephalography-Guided Laser Ablations in Patients With Neocortical Pharmacoresistant Focal Epilepsy: Concept and Operative Technique

Louis Ross, MD*
Ahsan M. Naduvil, MD‡
Juan C. Bulacio, MD‡
Imad M. Najm, MD‡
Jorge A. Gonzalez-Martinez, MD, PhD*‡

*Department of Neurosurgery, Cleveland Clinic, Ohio; ‡Epilepsy Center, Cleveland Clinic, Cleveland, Ohio

Correspondence:
Jorge Gonzalez-Martinez, MD, PhD,
9500 Euclid Ave,
Cleveland, OH 44195.
E-mail: gonzalj1@ccf.org

Received, June 24, 2017.
Accepted, January 23, 2018.

BACKGROUND: Laser ablation surgery has had encouraging results in the treatment of multiple intracranial diseases including primary and metastatic brain tumors, radiation necrosis, and epilepsy. The use of the stereoelectroencephalography (SEEG) method in combination with laser thermocoagulation therapy with the goal of modulating epileptic networks in patients with neocortical nonlesional phamacoresistant epilepsy has not been previously described.

OBJECTIVE: To describe the novel methodological and conceptual aspects related to SEEG-guided laser ablations in patients with magnetic resonance imaging (MRI)-negative pharmacoresistant neocortical focal epilepsy.

METHODS: Guided by previous SEEG intracranial data, a laser ablation probe was inserted by using a robotic guidance device in a 17-yr-old medically refractory epilepsy patient with difficult to localize seizures and nonlesional MRI. The laser applicator position was confirmed by MRI, targeting the left mesial rostral superior frontal gyrus. The ablation was performed under multiplanar digital imaging views and real-time thermal imaging and treatment estimates in each plane. A postablation MRI (contrasted T1 sequence) confirmed the ablation's location and size.

RESULTS: The entire procedure was achieved in approximately 100 min. The actual ablation was performed in less than 3 min. Approximately, additional 30 min preoperatively were used for positioning and robot registration. Precise placement of laser application (in comparison with preplanned trajectories) was achieved using the robotic guidance and confirmed by the intraoperative magnetic resonance images. No complications were reported. The patient has been seizure-free since surgery. The follow-up period is 20 mo. Two additional patients, treated with similar methodology, are also described.

CONCLUSION: The preliminary experience with the described method shows the feasibility of a unique combination of the SEEG methodology with laser thermocoagulation in patients with neocortical MRI-negative pharmacoresistant focal epilepsy.

KEY WORDS: Epilepsy surgery, Stereoelectroencephalography, Robotics, Laser ablation, Treatment

Operative Neurosurgery 0:1–8, 2018 DOI: 10.1093/ons/opy022

CONCLUSION: The preliminary experience with the described method shows the feasibility of a unique combination of the SEEG methodology with laser thermocoagulation in patients with **neocortical MRI-negative pharmacoresistant focal epilepsy**.

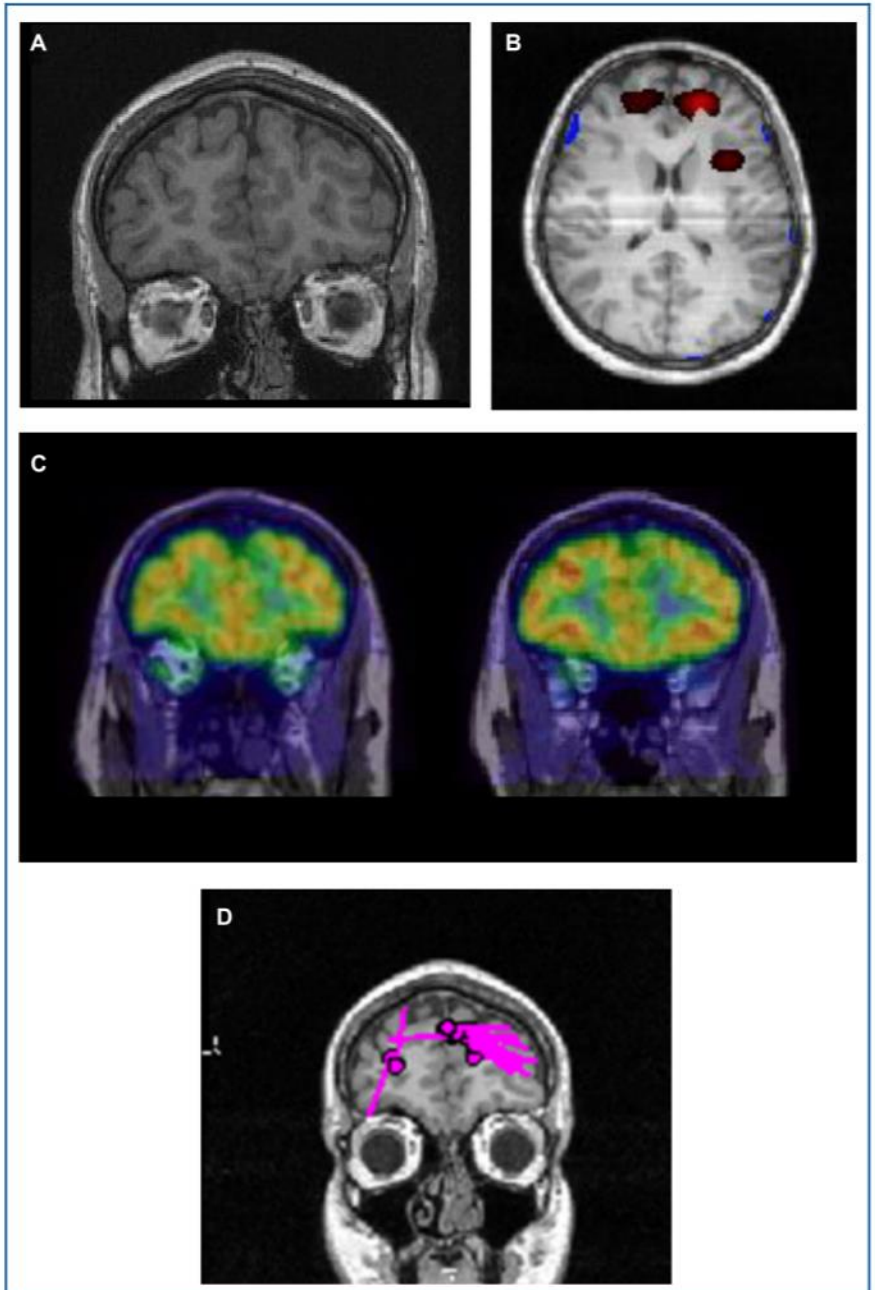

FIGURE 1. *Left rostral frontal seizure localization supported by non-invasive testing.* **A**, *MR image (Coronal T1, rostral slice) demonstrating the absence of an identifiable lesion.* **B**, *Ictal-SPECT image depicting focal hyper-perfusion in the left frontal rostral region.* **C**, *FDG-PET showing focal hypometabolism in the left frontal region.* **D**, *MEG scan showing focal discharges in the left frontal rostral region, in corresponding topography with the ictal-SPECT and PET scans.*

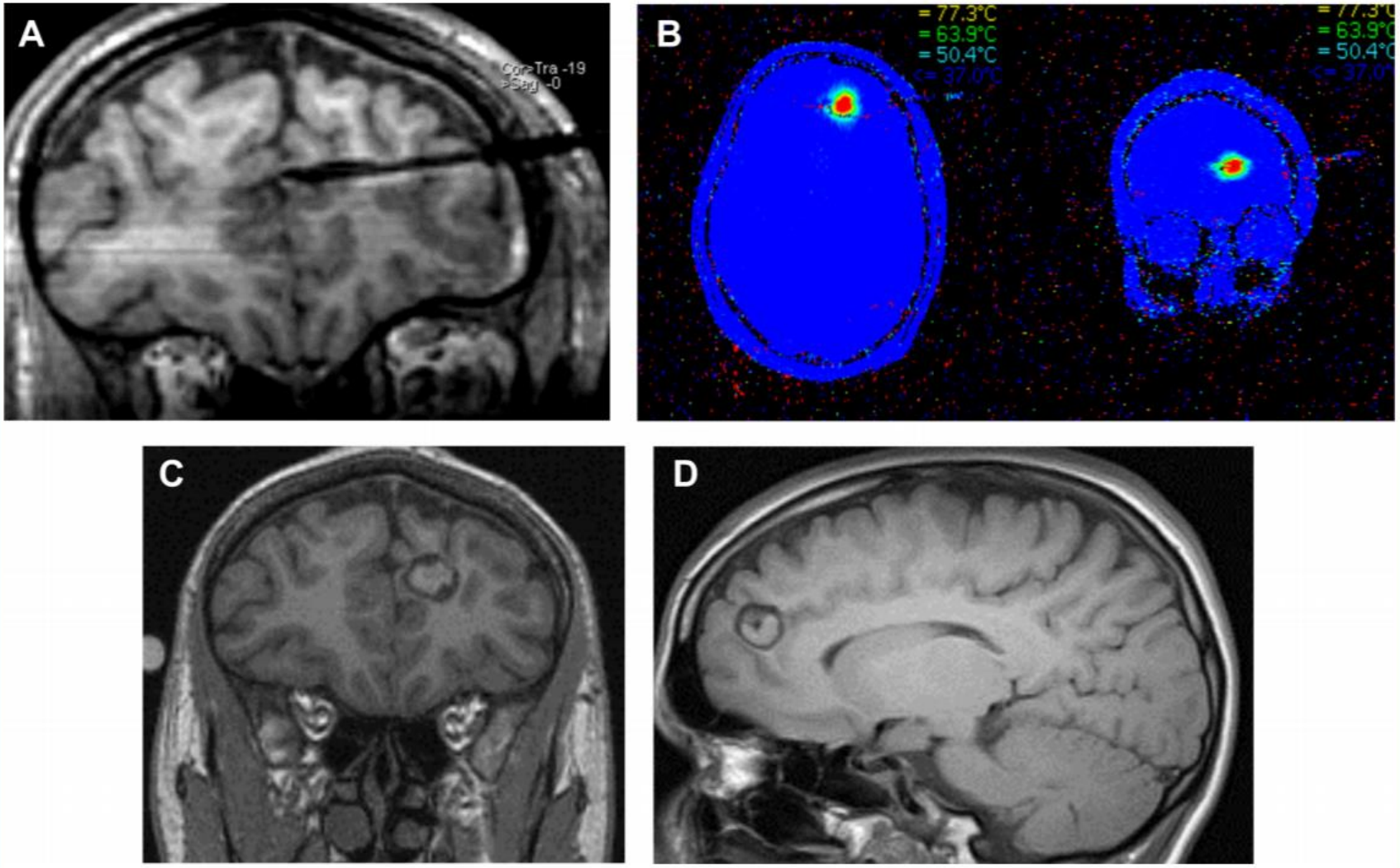

FIGURE 3. *Laser procedure and postoperative MRI.* **A**, *Intraoperative MRI image (coronal T1) showing the final laser probe position, following the previous L′ SEEG electrode trajectory.* **B**, *Real-time thermography images showing the focal rise in temperature during the ablation of the mesial frontal area that corresponded to the mesial contacts of electrode L′.* **C** *and* **D**, *Coronal and sagittal MR images depicting the final ablation results, with focal lesion located in the mesial rostral frontal cortex.*

SEEG Interpretation

DECISIONAL TREE IN NLE

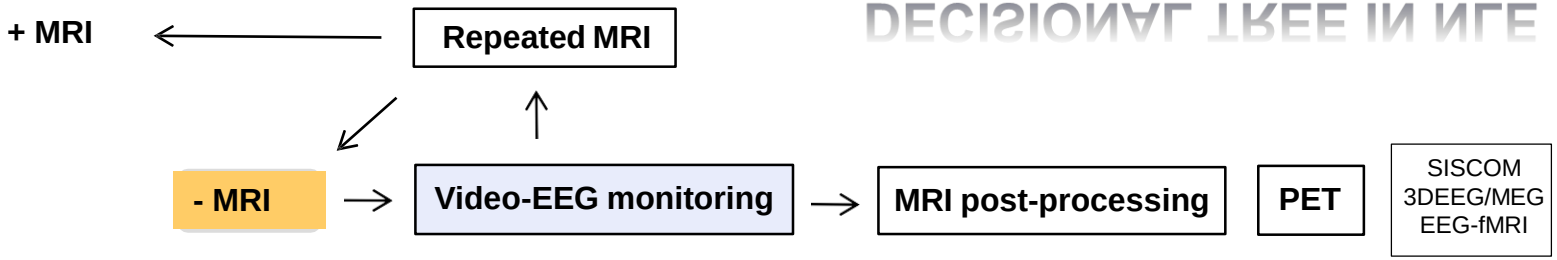

Usefulness of focal rhythmic discharges on scalp EEG of patients with focal cortical dysplasia and intractable epilepsy [1]

Antonio Gambardella [a,2], André Palmini [b], Frederick Andermann [a,*], François Dubeau [a], Jaderson C. Da Costa [b], L. Felipe Quesney [a], Eva Andermann [a], André Olivier [a]

Table 2
Comparison of the spatial distribution of interictal epileptiform abnormalities on scalp EEGs with the location of the structural lesion

	Rhythmic epileptiform discharges (REDs)			Interictal spiking		
	Focal/regional	Multiregional	Absent	Focal/regional	Multiregional	Absent
FCDLs [a]						
Focal/lobar	7	0	9	3	12	1
Multilobar	3	5	10	7	11	0
Non-FCDLs [b]						
Focal/lobar	0	0	36	10	7	19
Multilobar	0	0	4	0	4	0

FCDLs = focal cortical dysplastic lesions.
[a] Patients with cortical dysplasia (n = 34).
[b] Patients with other structural cortical lesions (n = 40).

Electroenceph clin Neurophysiol 1996; 98: 243-249

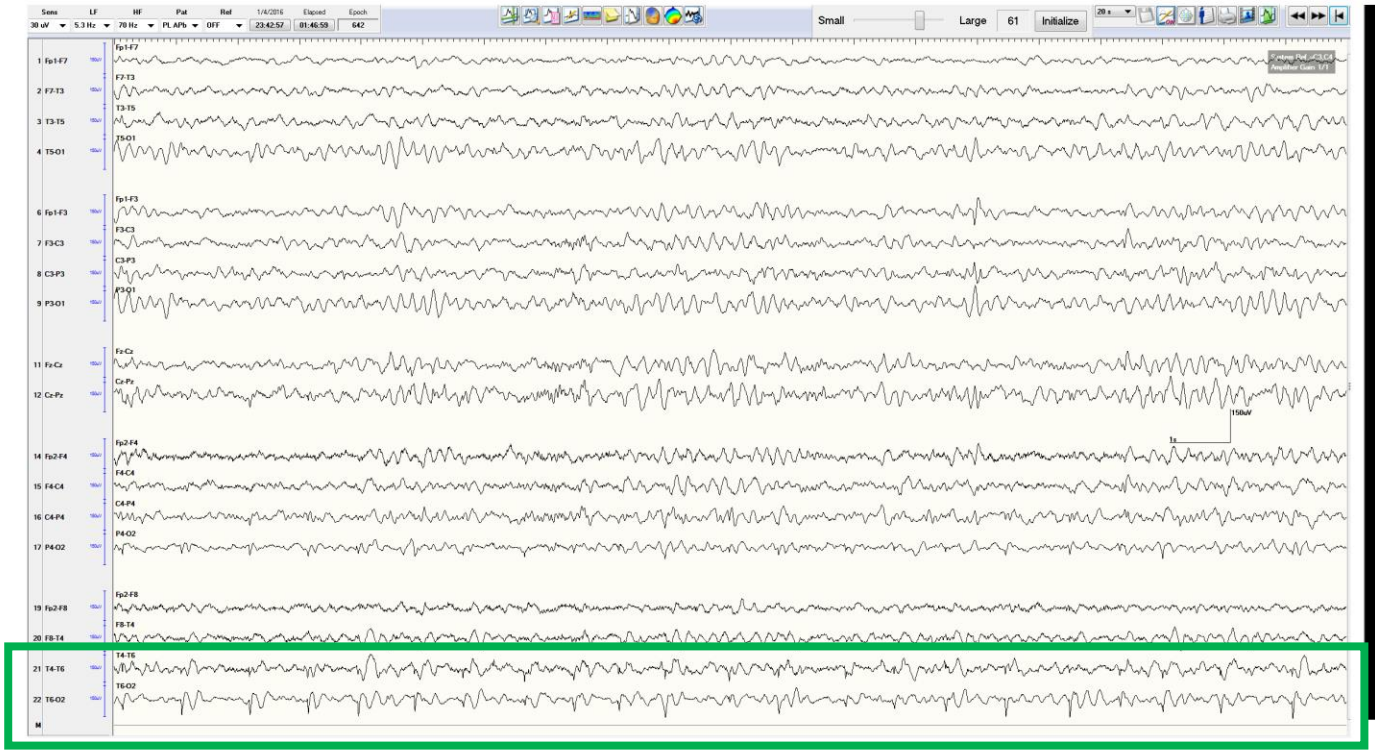
Small
Large
61
Initialize
Fp1-F7
F7-T3
T3-T5
T5-O1
Fp1-F3
F3-C3
C3-P3
P3-O1
Fz-Cz
Cz-Pz
Fp2-F4
F4-C4
C4-P4
P4-O2
Fp2-F8
F8-T4
T4-T6
T6-O2

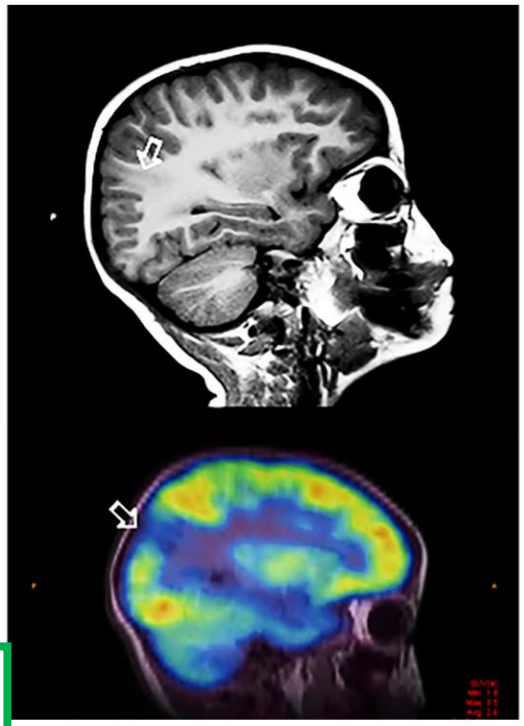

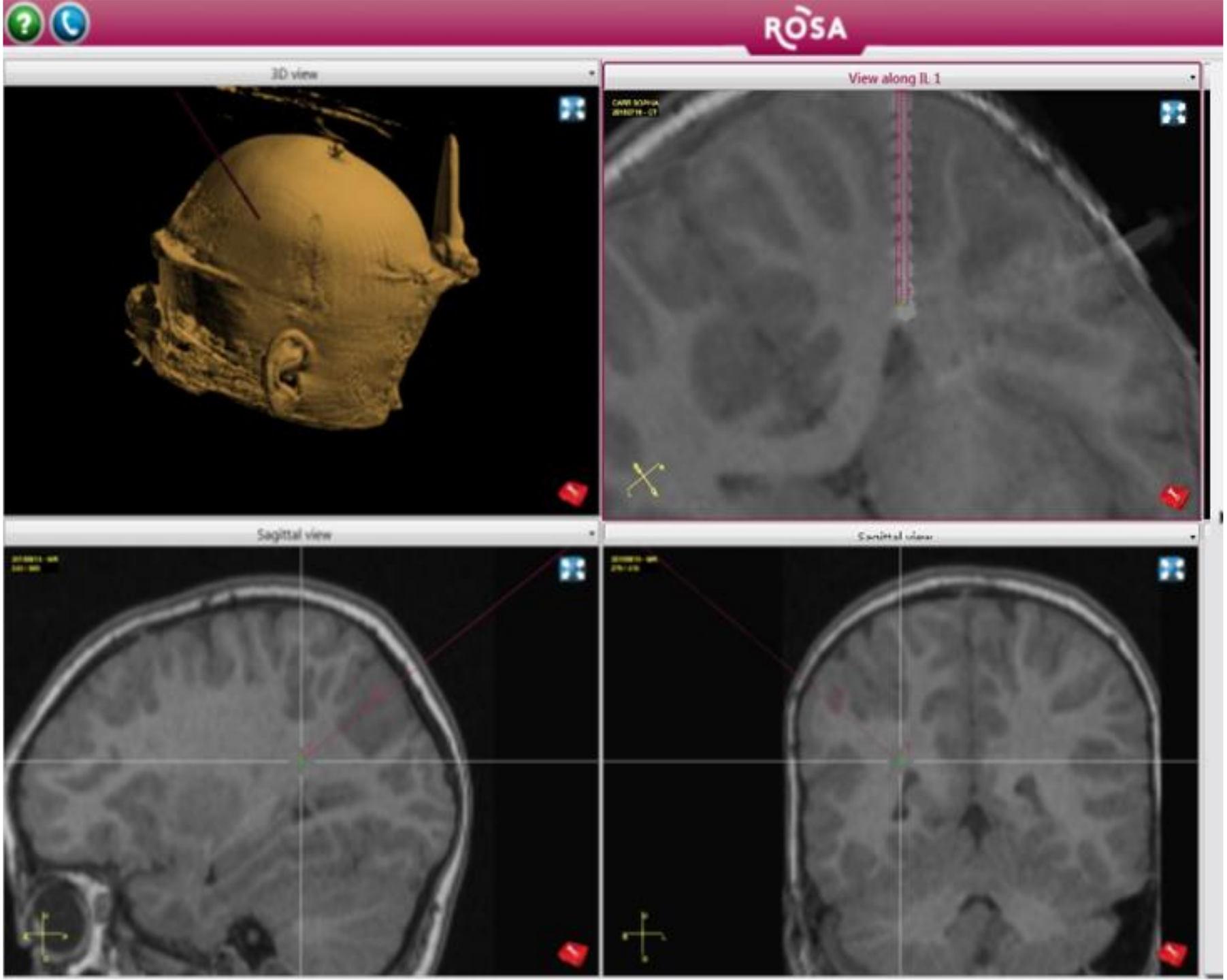
ROSA
3D view
View along IL 1
Sagittal view

Recognize the relevant (dysplastic) spikes

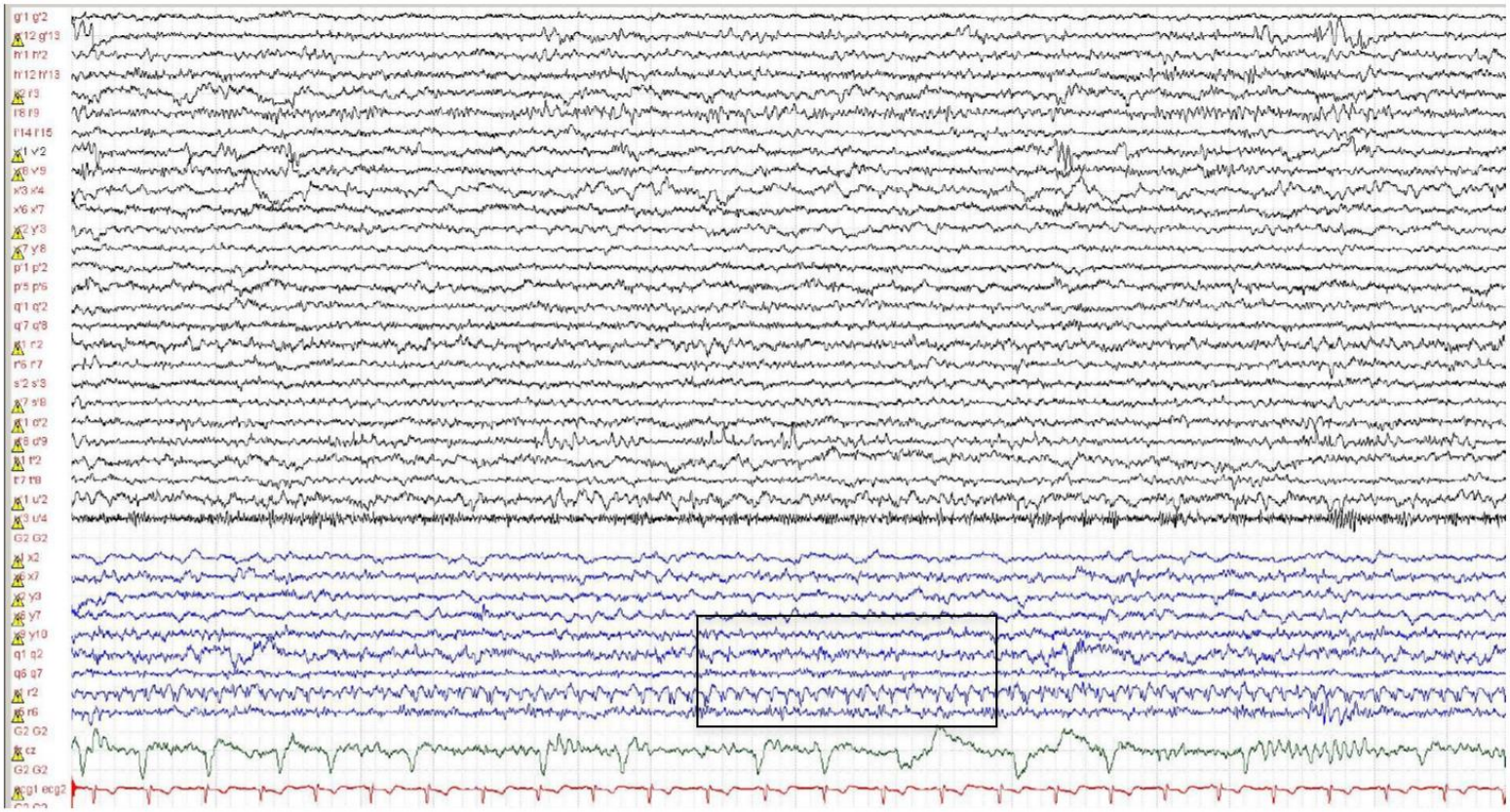

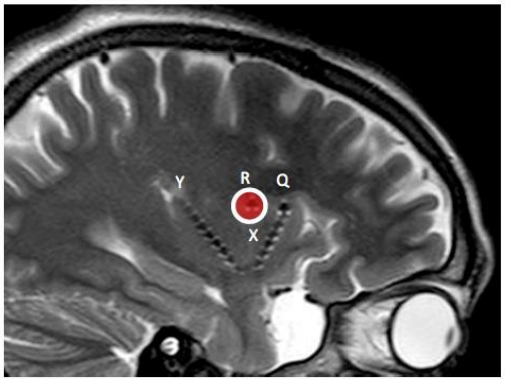

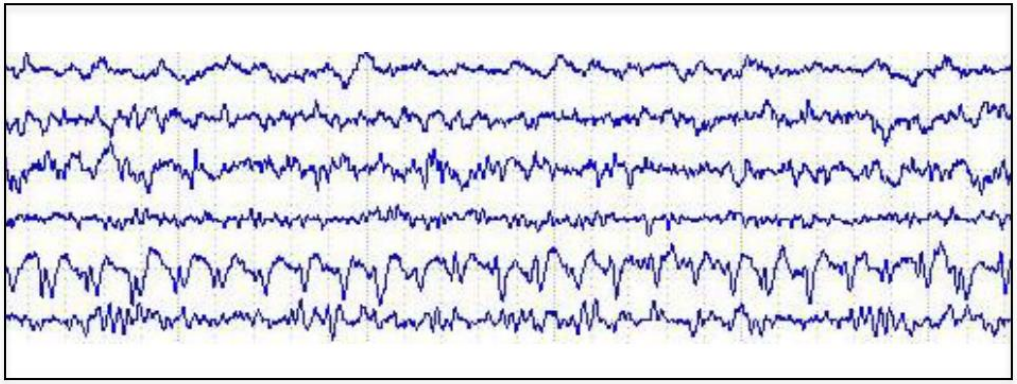

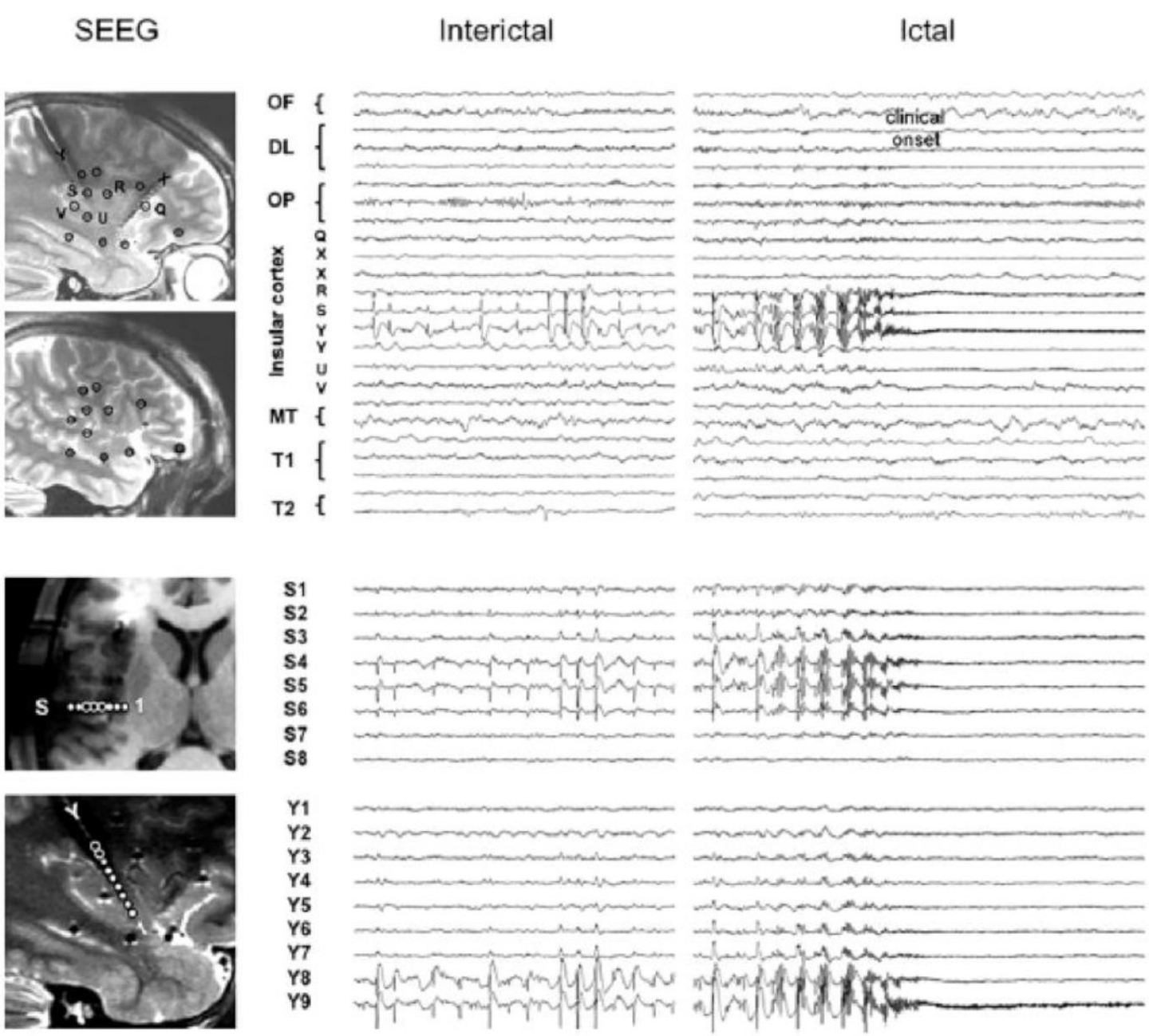

Dimova et al. 2017

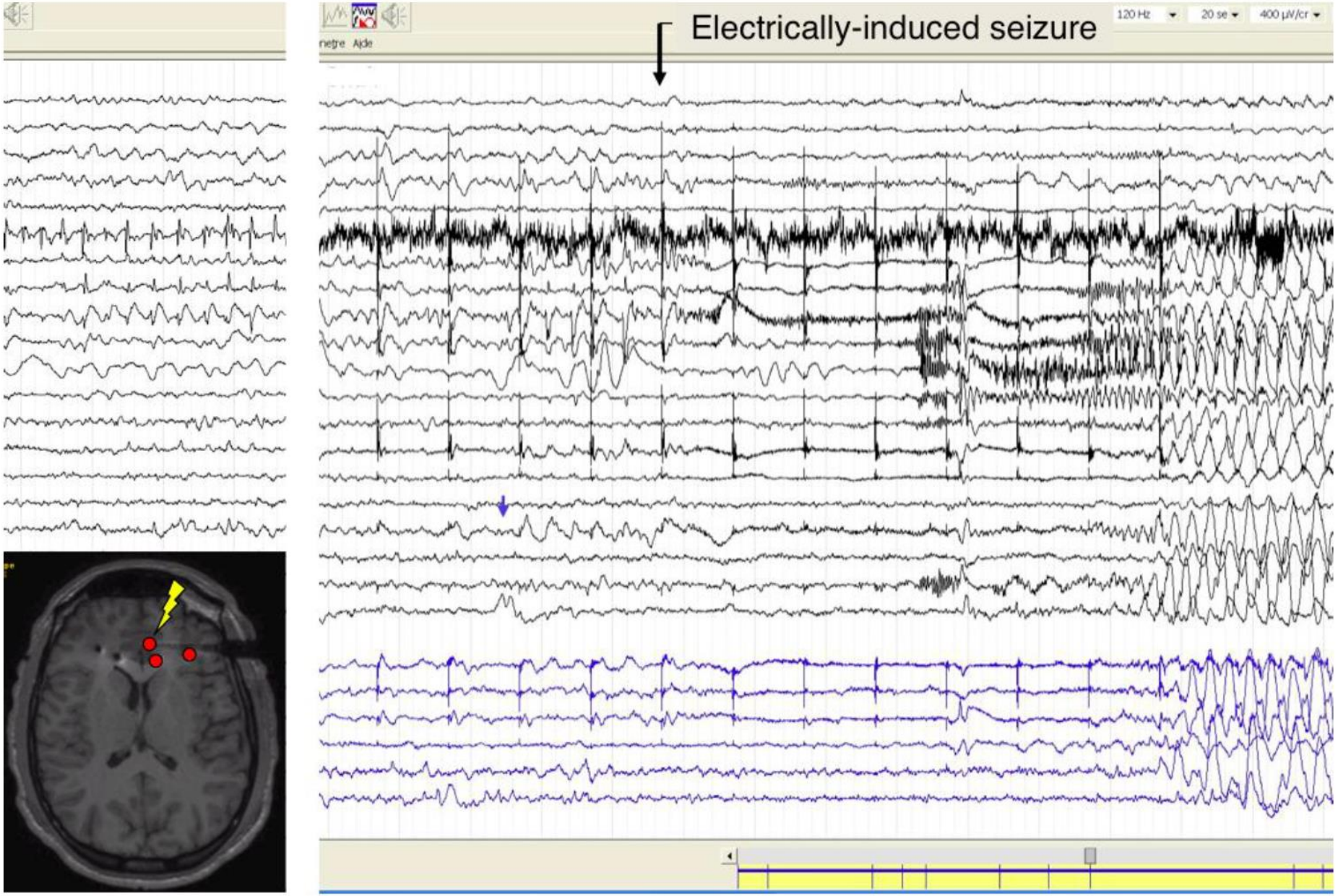
Electrically-induced seizure
120 Hz
20 se
400 µV/cr
netre Aide

The good, the bad and the ugly

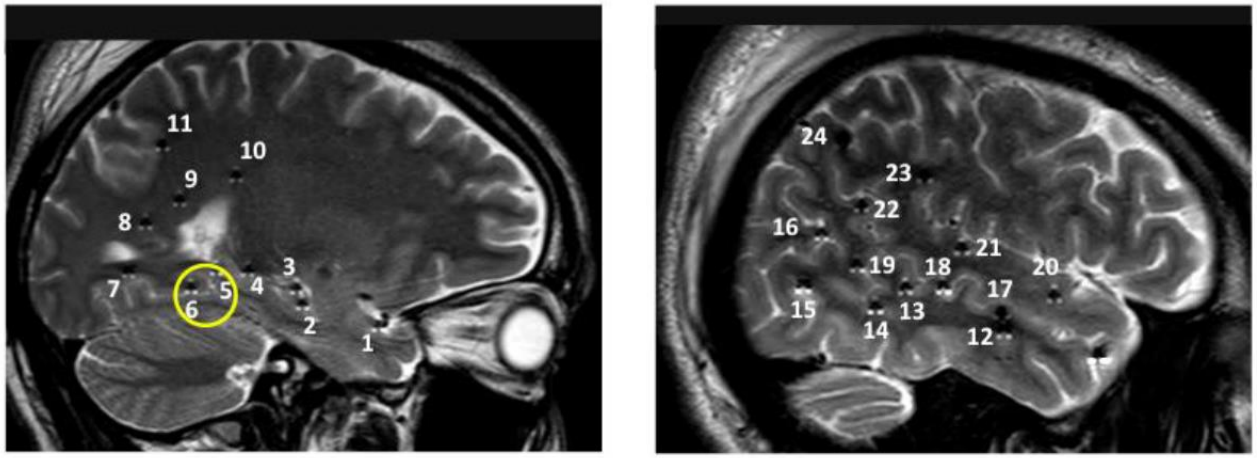

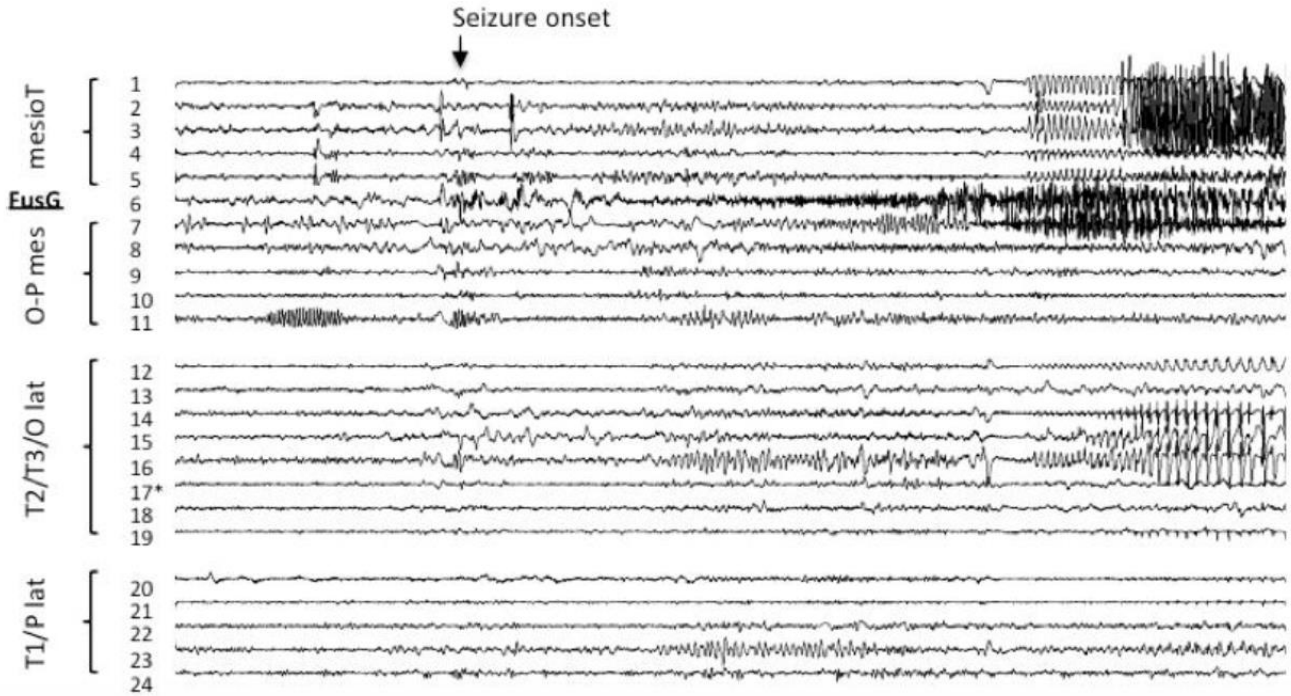

The good, the bad and the ugly

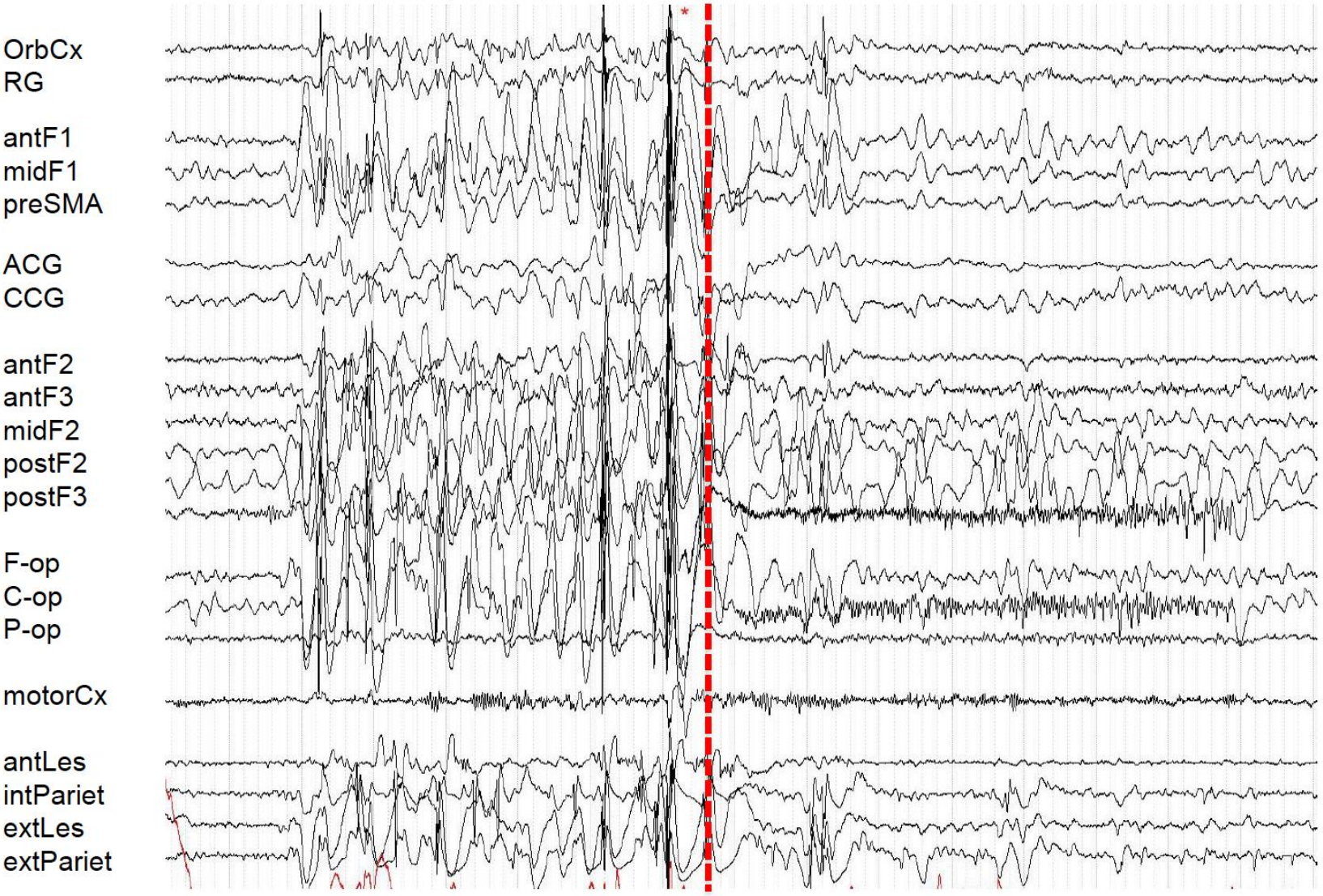

The good, the bad and the ugly

1st SEEG investigation

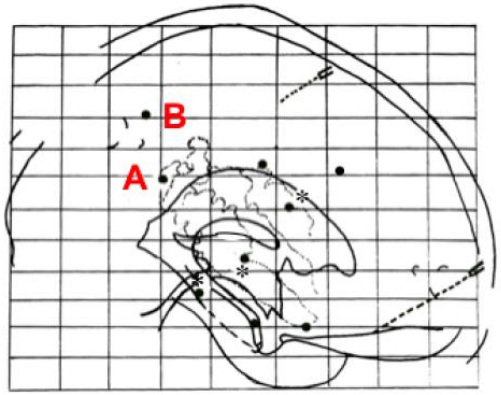

● right electrodes ◀ left electrodes

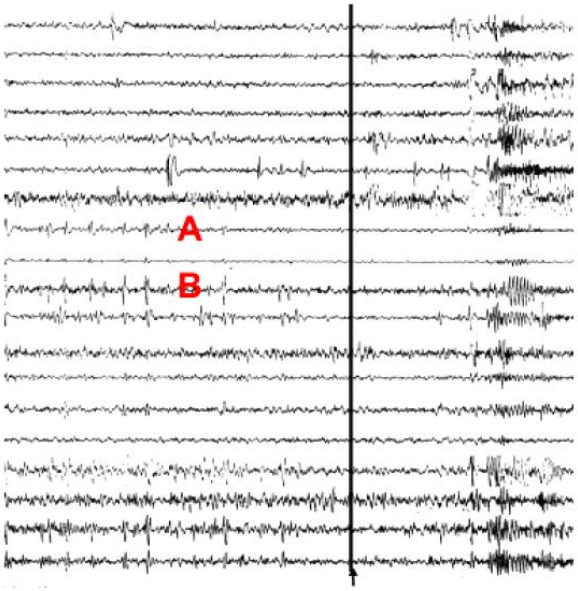

clinical onset

2d SEEG investigation

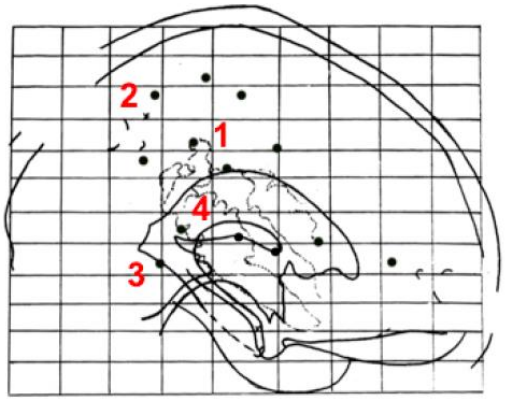

● right electrodes

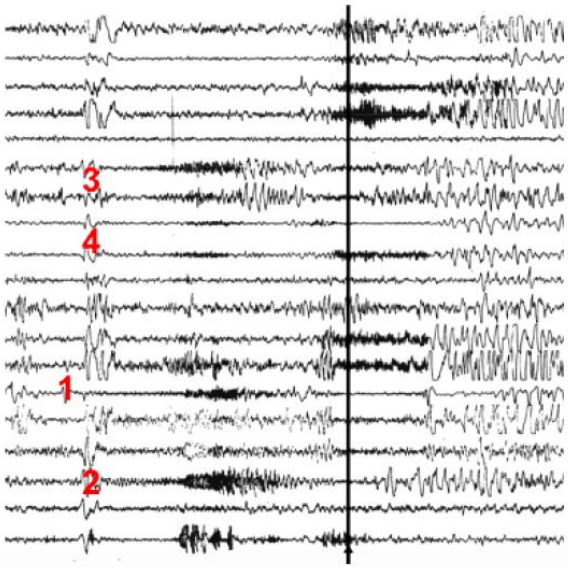

The good, the bad and the ugly

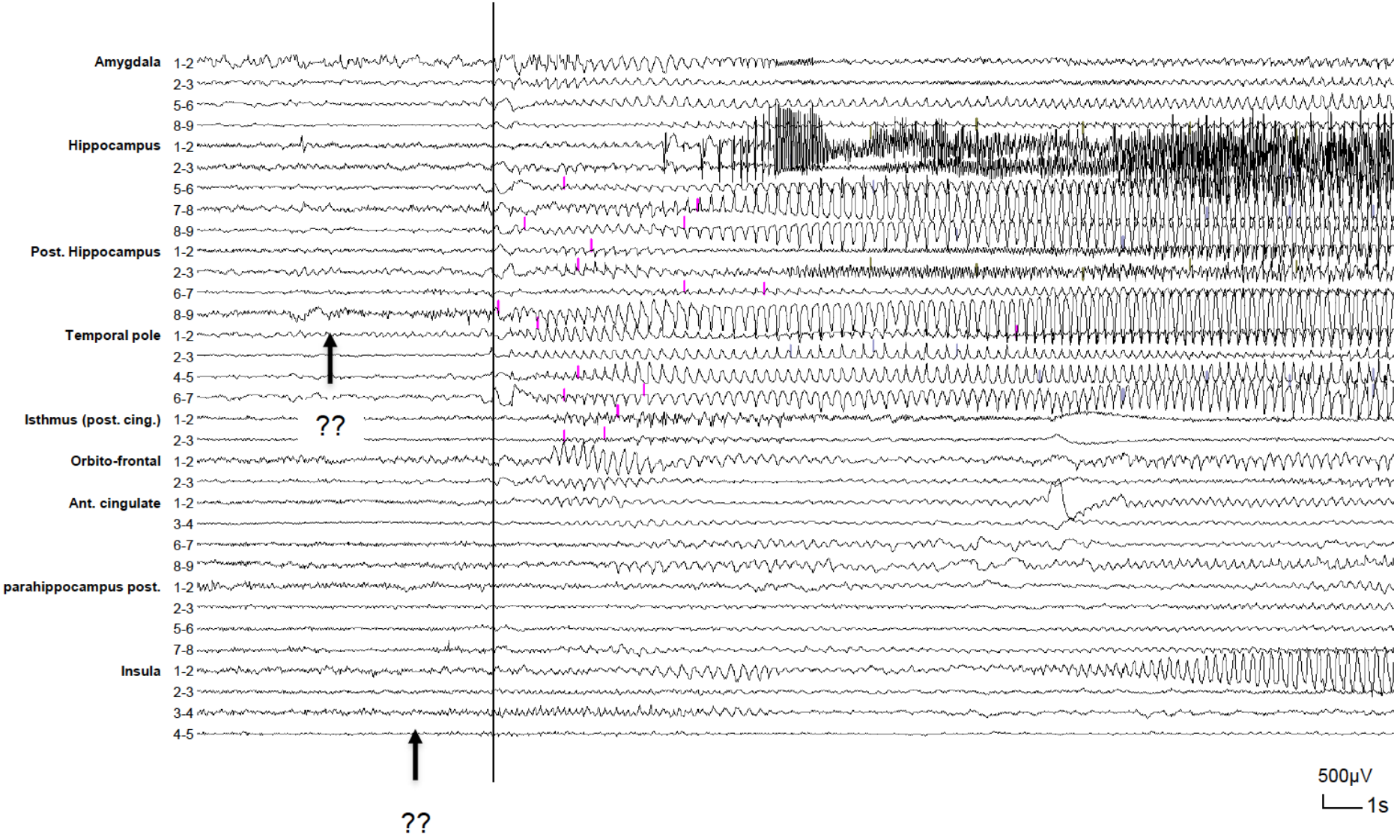

The good, the bad and the ugly

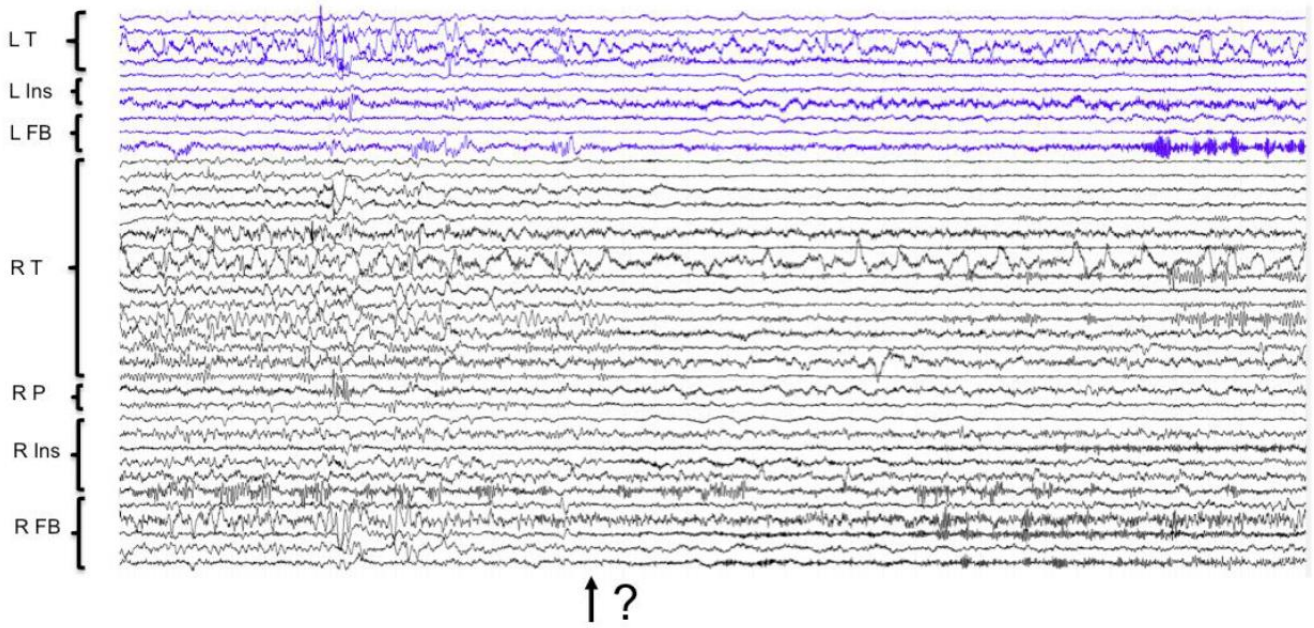

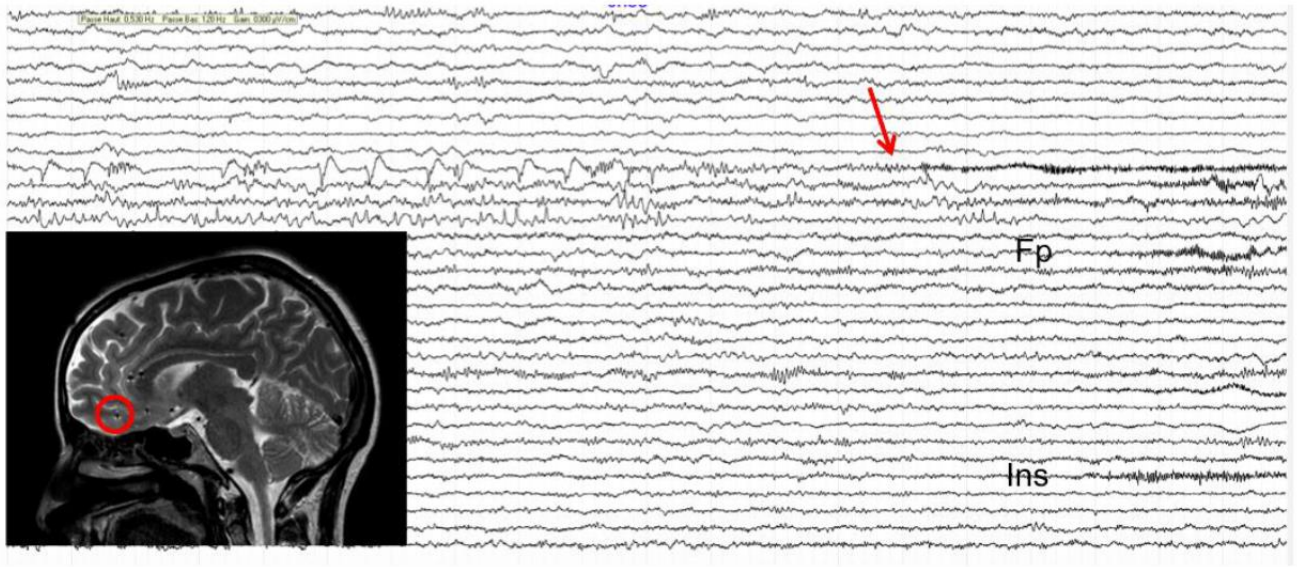

The good, the bad and the ugly

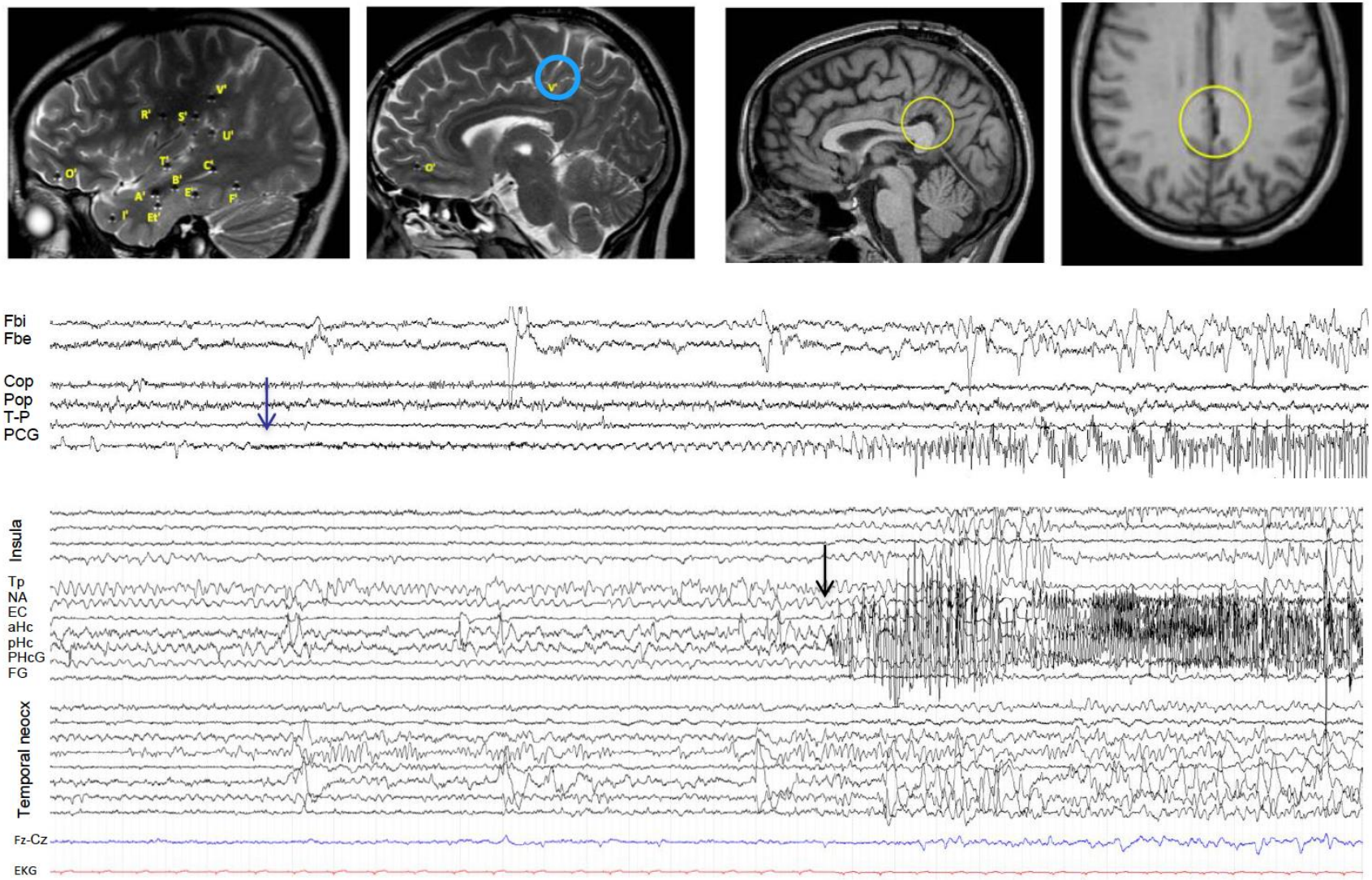

The issue of early versus late spread

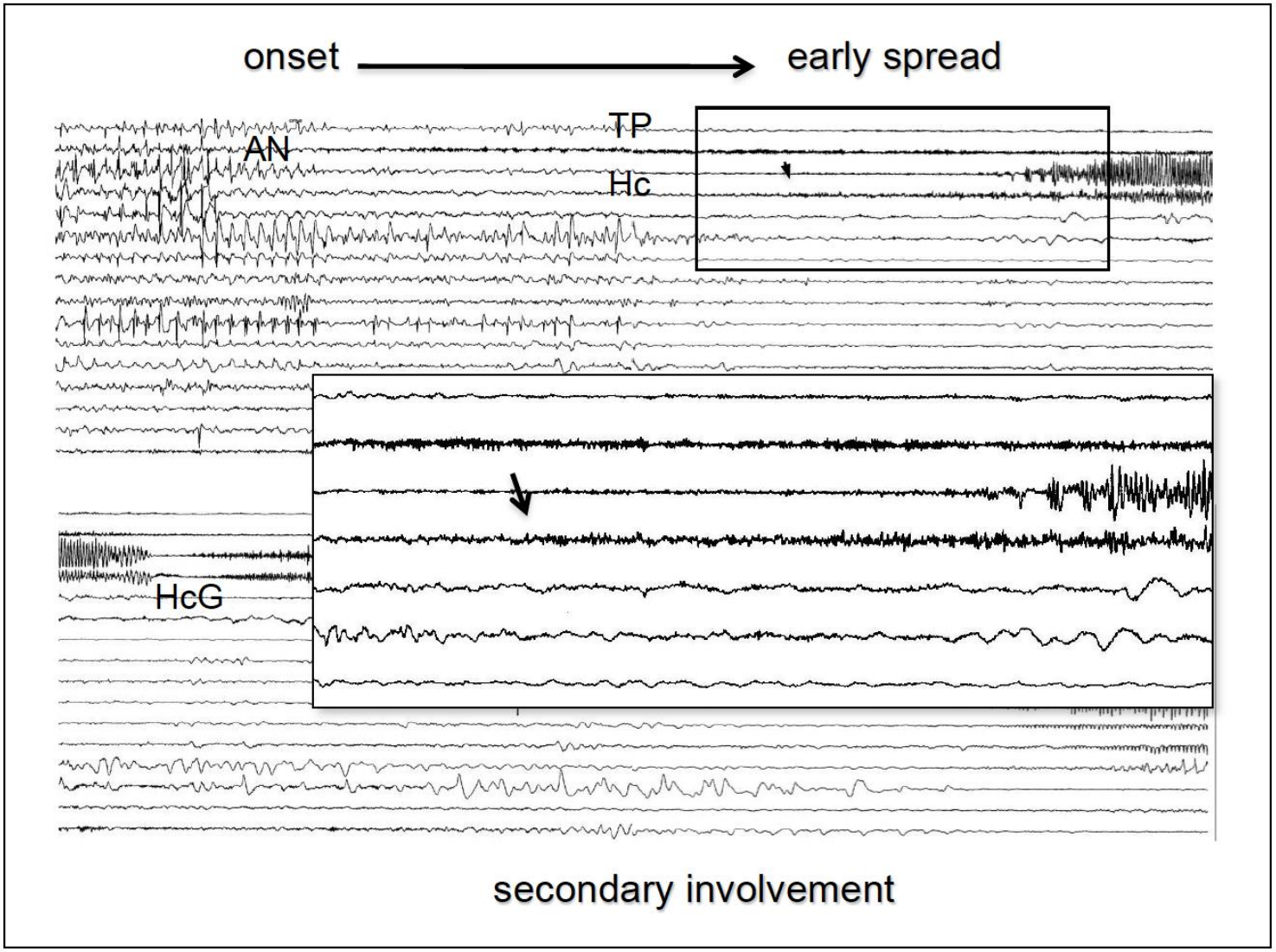

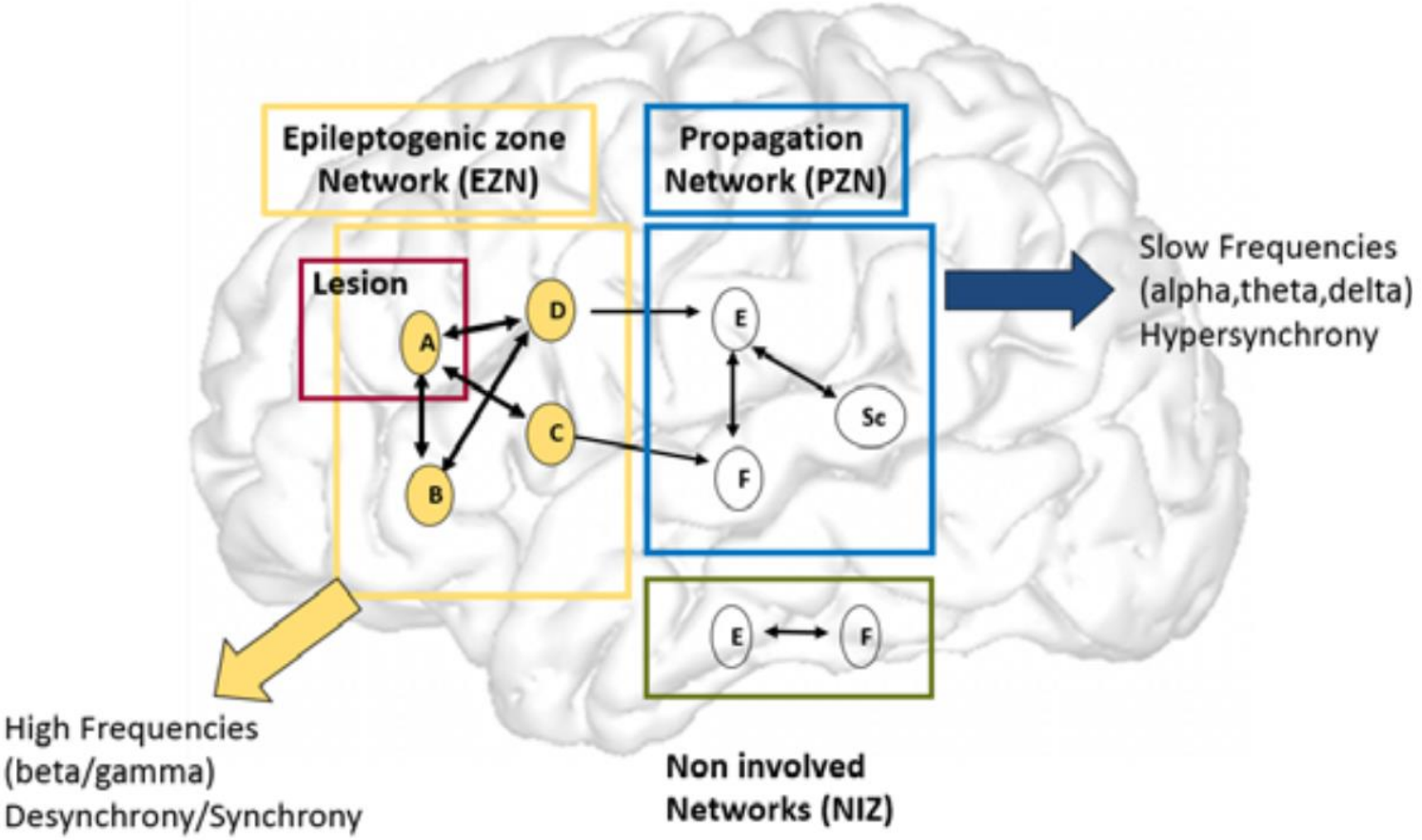

The concept of epileptogenic networks in focal epilepsies is illustrated. The cerebral regions are represented by letters (A, B, etc). The scheme proposes a hierarchical organization in terms of epileptogenicity in the epileptic brain. The EZ includes different brain regions that are able to generate seizures, in particular, fast activities, defining the EZ Network (labeled A, B, C, and D). A represents a region with putative (visible or not) lesion. The EZ Net- work is also characterized by a pattern of synchrony–desynchrony. A second set of regions are less epileptogenic, are triggered in seizures by the EZ, and are within the “propagation zone network” (E, F, SC, and H). SC schematizes the involvement of subcortical (thalamus for instance) regions. Activity recorded in these regions is generally of lower frequency and more synchronized than in the EZ. Some regions are not involved during seizure propagation (NIN, noninvolved network, G, H).

You only see what you look at

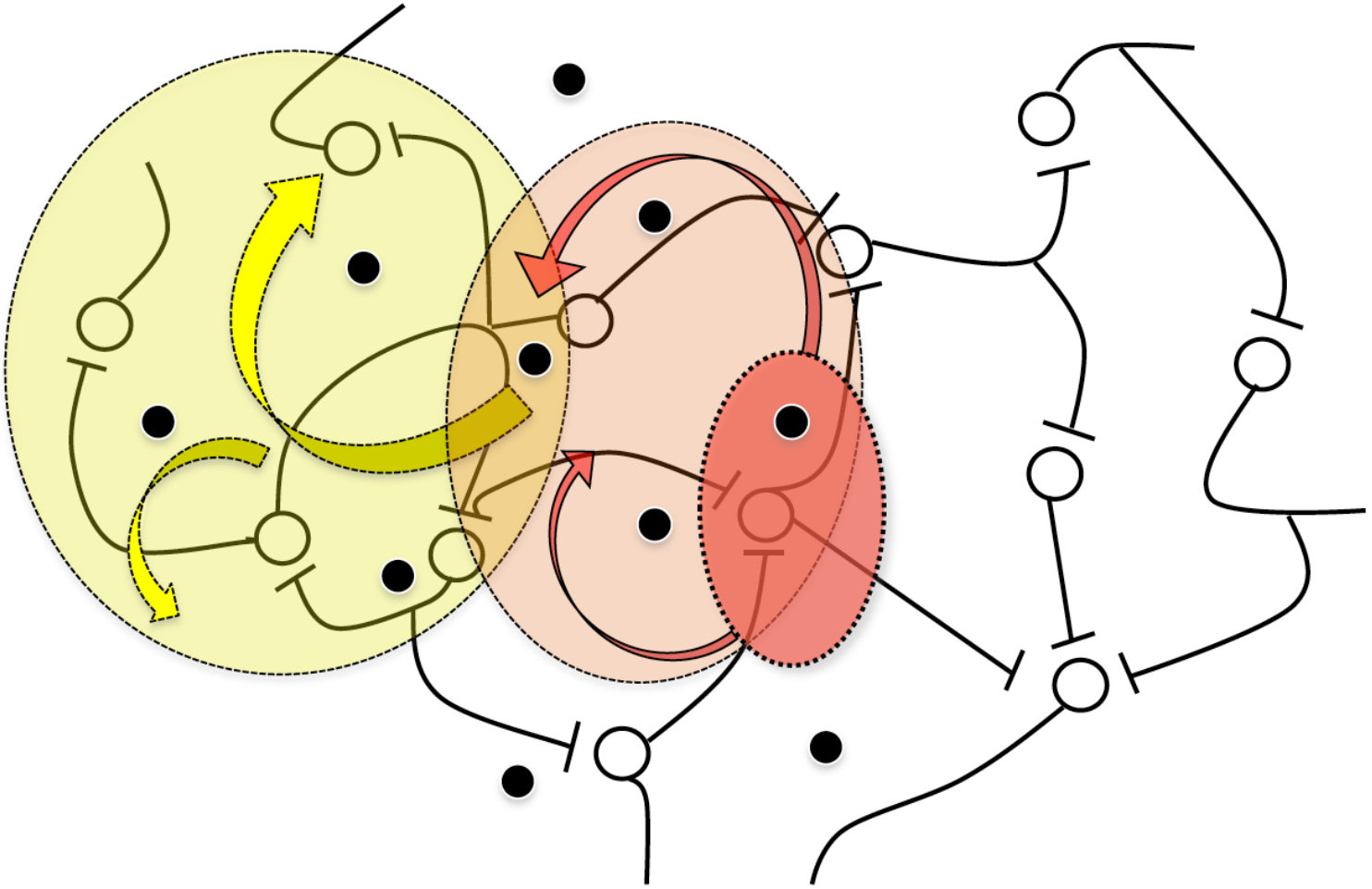

You only see what you look at

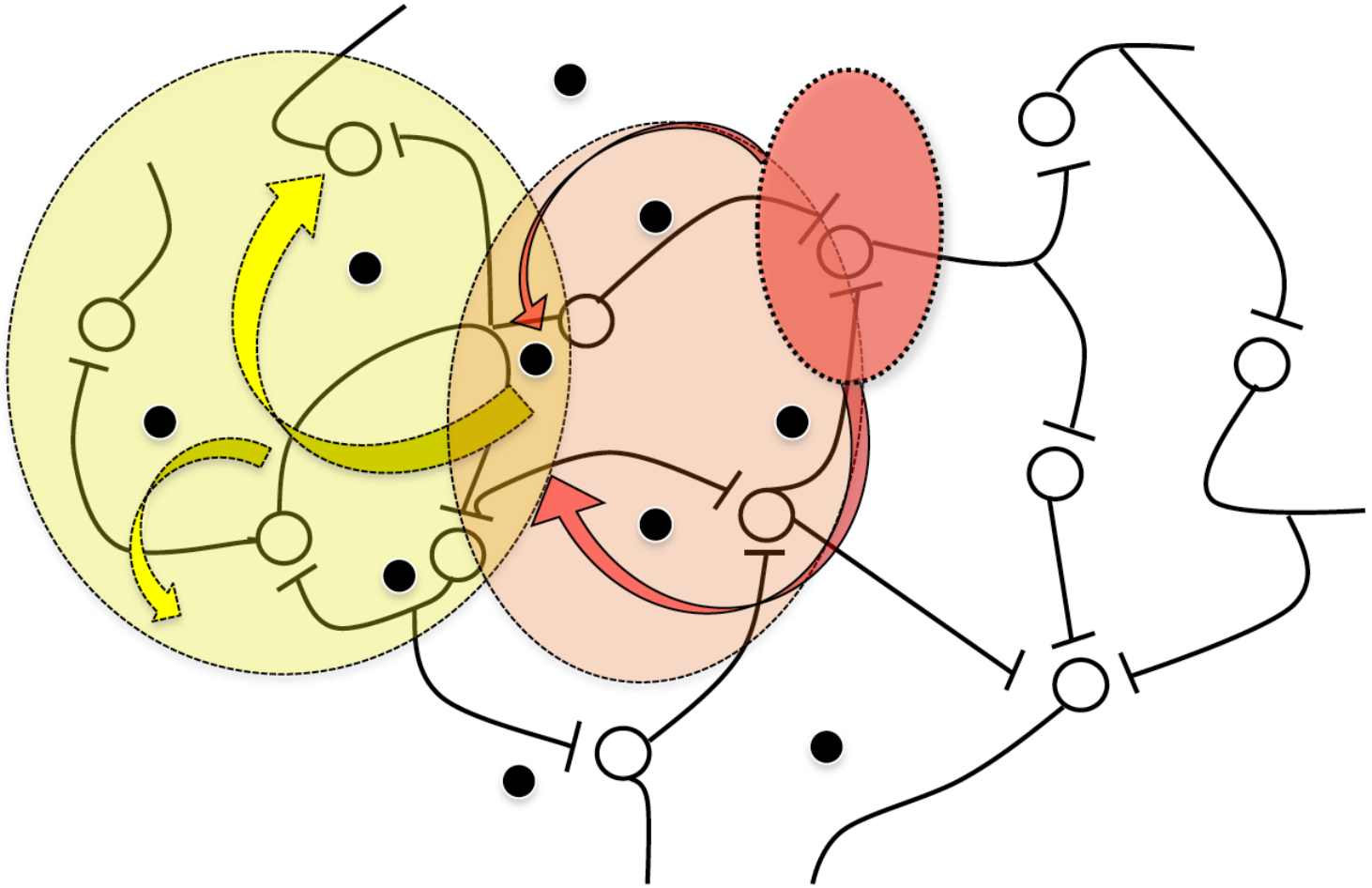

You only see what you look at

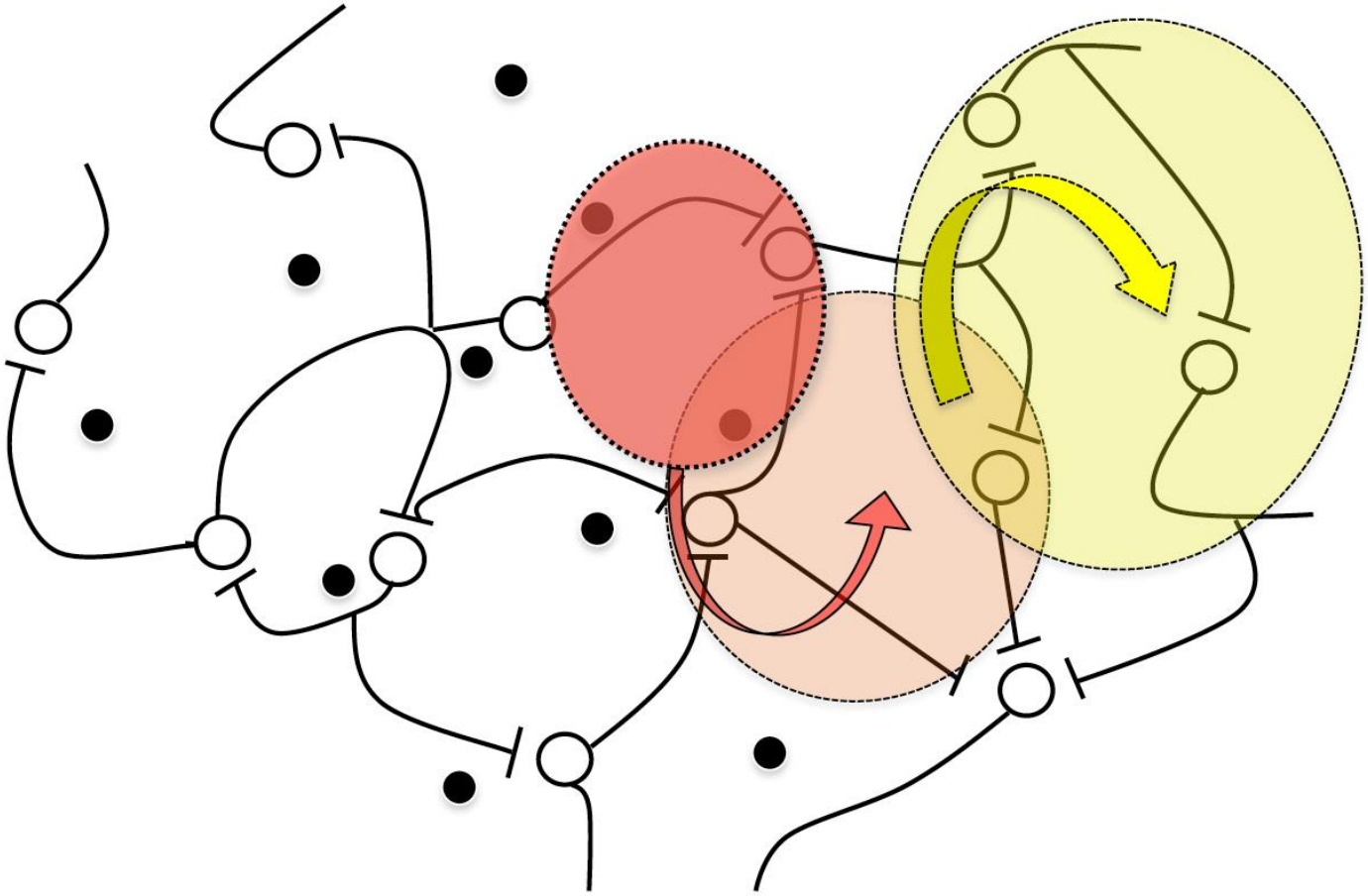

Biomarker of Epileptogenic Zone (EZ)

EZ is characterized by combination of 3 biomarkers observed at seizure onset:

- Fast activity at 80–120 Hz or higher
- Slow DC shift (Very slow transient polarizing shift)
- Voltage depression (flattening).

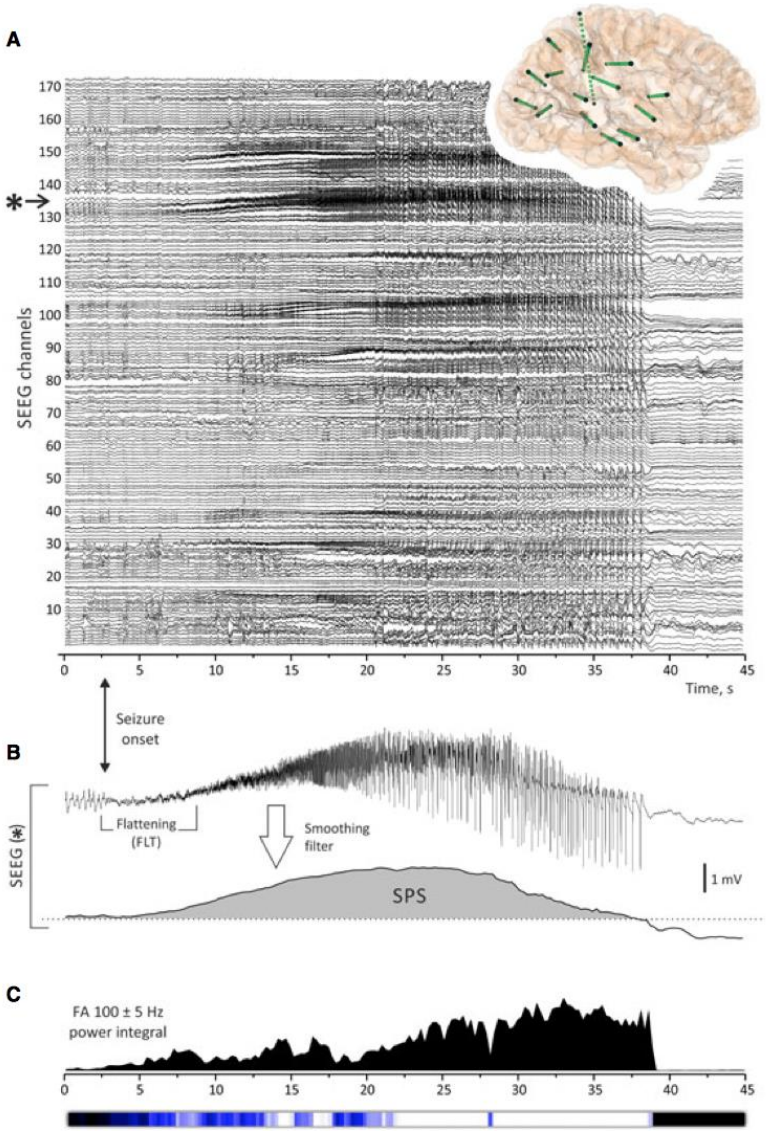

Figure 1.

SEEG patterns during ictal event. (**A**) Complete profile of presurgical SEEG recordings (172 channels) during a seizure in patient rPt8. The 3D scheme of the intracranial electrodes implanted with Talairach reference frame is shown in the upper right inset. The onset of the partial seizure is marked by the bidirectional arrow at the bottom. (**B**) Amplification of the trace marked by the asterisk (**A**). SEEG flattening pattern at seizure onset is indicated. After a smoothing filter is applied to the upper SEEG trace, a slow polarizing shift (SPS) marked by the gray-shaded area is isolated (lower trace). (**C**) Method to assess the power distribution of the fast activity (FA). Following the procedure detailed in Gnatkovsky et al.,[8] a dominant FA at 110 ± 5 Hz was observed at seizure onset. Changes of the 110 ± 5 Hz FA power integral of the single trace shown in (**B**) are represented both as a continuous graph (upper graph) and as an intensity strip (lower strip). Time calibration is the same in (**A**–**C**).

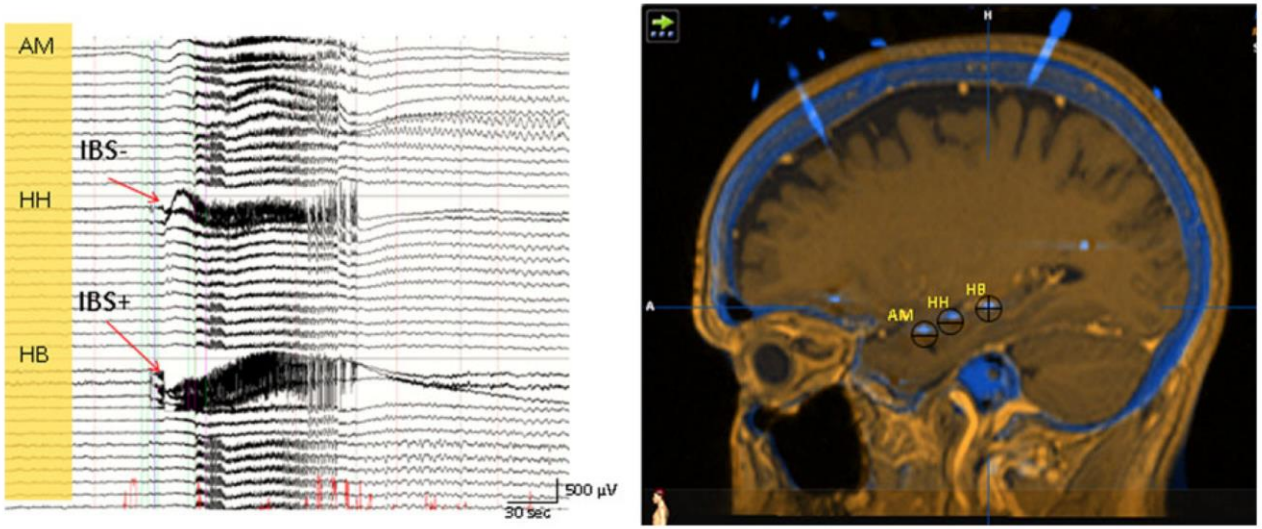

Figure 5.

Illustration of a dipole of IBS along the longitudinal axis to amygdala/hippocampus complex (A-H complex). A negative pole is seen at the anterior segment of the A-H complex (AM1-2, HH1-2) and a positive pole seen at the posterior of portion of the A-H complex (HB1-3) (**A**). The sagittal view of the MRI brain showing the location of AM, HH, and HB electrodes and the location of the dipole (**B**). A similar dipole distribution of the IBS is illustrated in Fig. 1. IBS are observed with input filter of 0.016–30 Hz, 5 min/page timescale, and sensitivity of 100 µV/mm. IBS, ictal baseline shifts; AM, amygdala; HH, hippocampal head; HB, hippocampal body.

doi:10.1093/brain/awx306 BRAIN 2018: 141; 117–131 | 117

BRAIN
A JOURNAL OF NEUROLOGY

A fingerprint of the epileptogenic zone in human epilepsies

Olesya Grinenko,[1,*] Jian Li,[2,*] John C. Mosher,[1] Irene Z. Wang,[1] Juan C. Bulacio,[1] Jorge Gonzalez-Martinez,[1] Dileep Nair,[1] Imad Najm,[1] Richard M. Leahy[2] and Patrick Chauvel[1]

*These authors contributed equally to this work.

Defining a bio-electrical marker for the brain area responsible for initiating a seizure remains an unsolved problem. Fast gamma activity has been identified as the most specific marker for seizure onset, but conflicting results have been reported. In this study, we describe an alternative marker, based on an objective description of interictal to ictal transition, with the aim of identifying a time-frequency pattern or 'fingerprint' that can differentiate the epileptogenic zone from areas of propagation. Seventeen patients who underwent stereoelectroencephalography were included in the study. Each had seizure onset characterized by sustained gamma activity and were seizure-free after tailored resection or laser ablation. We postulated that the epileptogenic zone was always located inside the resection region based on seizure freedom following surgery. To characterize the ictal frequency pattern, we applied the Morlet wavelet transform to data from each pair of adjacent intracerebral electrode contacts. Based on a visual assessment of the time-frequency plots, we hypothesized that a specific time-frequency pattern in the epileptogenic zone should include a combination of (i) sharp transients or spikes; preceding (ii) multiband fast activity concurrent; with (iii) suppression of lower frequencies. To test this hypothesis, we developed software that automatically extracted each of these features from the time-frequency data. We then used a support vector machine to classify each contact-pair as being within epileptogenic zone or not, based on these features. Our machine learning system identified this pattern in 15 of 17 patients. The total number of identified contacts across all patients was 64, with 58 localized inside the resected area. Subsequent quantitative analysis showed strong correlation between maximum frequency of fast activity and suppression inside the resection but not outside. We did not observe significant discrimination power using only the maximum frequency or the timing of fast activity to differentiate contacts either between resected and non-resected regions or between contacts identified as epileptogenic versus non-epileptogenic. Instead of identifying a single frequency or a single timing trait, we observed the more complex pattern described above that distinguishes the epileptogenic zone. This pattern encompasses interictal to ictal transition and may extend until seizure end. Its time-frequency characteristics can be explained in light of recent models emphasizing the role of fast inhibitory interneurons acting on pyramidal cells as a prominent mechanism in seizure triggering. The pattern clearly differentiates the epileptogenic zone from areas of propagation and, as such, represents an epileptogenic zone 'fingerprint'.

The pre-ictal spike(s) would correspond to a progressive synchronization of pyramidal cells (slow component) activating disinhibited fast somatic inhibitory interneurons **(fast component).** Successive bursts of fast interneuron activities would then merge into a sustained discharge **(multiband fast activity)** leading to pyramidal silencing **(suppression).** The last part of the seizure **(end of suppression coinciding with fast activity decrease)** could be due to local and remote post-inhibitory rebound bursting pyramidal neurons activity

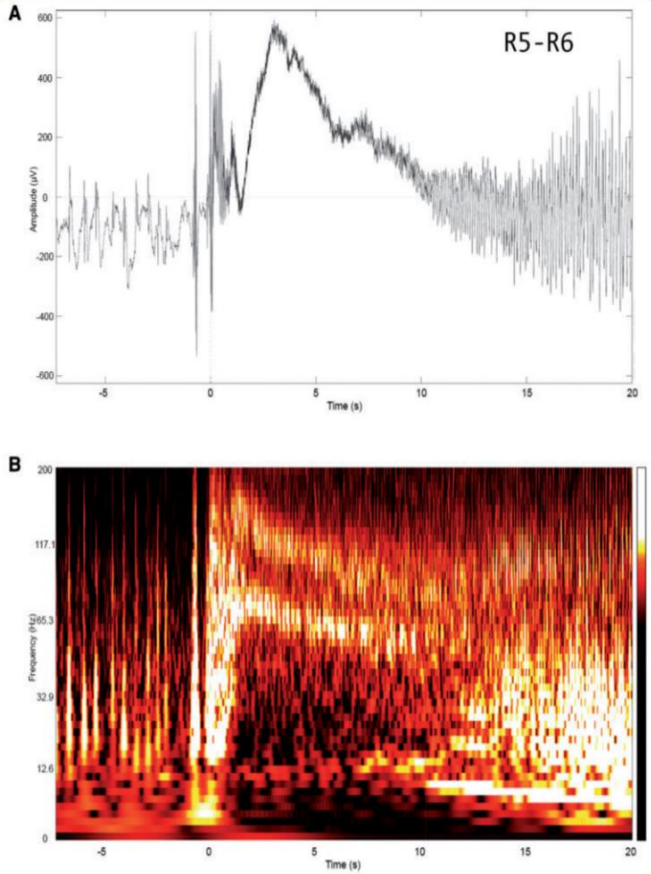

Figure 2 Example of pre-ictal to ictal transitions in the epileptogenic zone. Channel R5-R6 from Fig. 1A from 5 s before to 20 s after the ictal onset is shown in (**A**) and the corresponding time frequency plot (logarithmic scale) is shown in **B**. The time frequency plot shows the proposed 'fingerprint': a combination of pre-ictal spikes, multi-band fast activity and simultaneous suppression of slower background frequencies. Note that fast activity is characterized by multiple bands that are not harmonically related, chirp at different frequency rates, and whose amplitudes vary independently across bands.

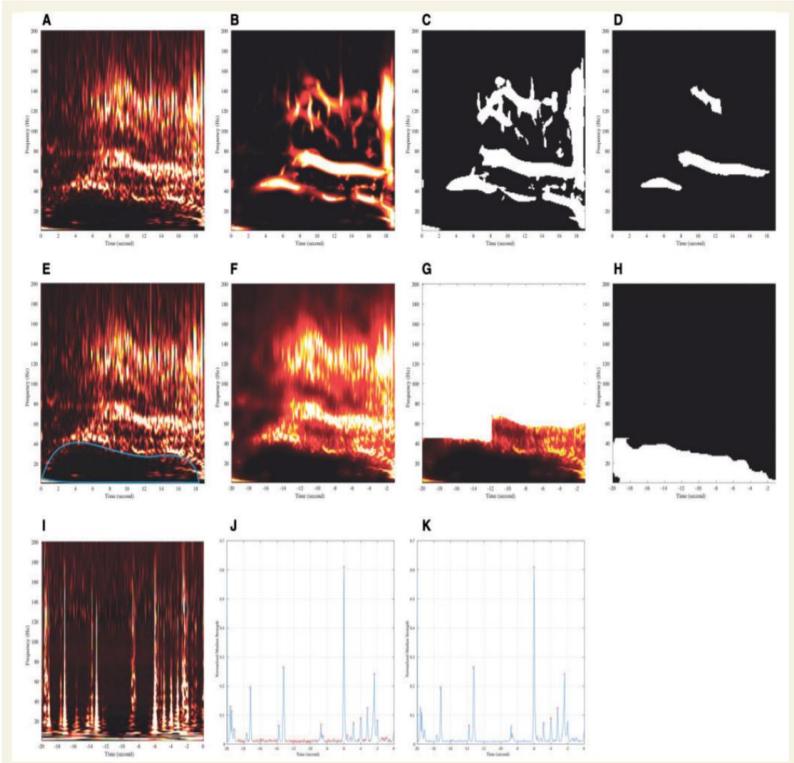

Figure 3 Illustration of feature extraction procedure. (**A–D**) Fast activity extraction. (**A**) Original post-onset time-frequency plot. (**B**) Frangi filtering result. (**C**) Thresholding result. (**D**) Final morphological cleaning result. (**E–H**) Suppression extraction. (**E**) Original post-onset time-frequency plot with ideal suppression region. (**F**) Guided filtering result. (**G**) Fast activity-based spatial constraint. (**H**) Final thresholding result. (**I–K**) Preictal spikes extraction. (**I**) Original pre-onset time-frequency plot. (**J**) Median statistics for each time point. (**K**) Small circles indicate major local maxima as the spike candidates.

Message to take home

Have a strong hypothesis and a clear objective :

- Left temporal : can I spare the mesiotemporal region ?
- T+ : what is the extent of the epileptogenic zone ?
- Extra-temporal : where is the MRI-occult lesion (FCD++) ?

Strongly rely your localizing hypothesis on :

- Electroclinical correlations +++
- Scalp-EEG marker of FCD
- Validated MRI post-processing (MAP) and FDG-PET
- HD-EEG and/or MEG and/or fMRI spikes

Avoid fishing expeditions : it never works !

Recognize relevant / unrelevant IEEG patterns